

Utah State University

DigitalCommons@USU

All Graduate Theses and Dissertations, Fall
2023 to Present

Graduate Studies


12-2023

Controls on Sediment Connectivity in Fluvial Networks Impacted by Wildfire Across Utah

Alec Arditti

Utah State University, alec.arditti@usu.edu

Follow this and additional works at: <https://digitalcommons.usu.edu/etd2023>

 Part of the [Hydrology Commons](#), and the [Water Resource Management Commons](#)

Recommended Citation

Arditti, Alec, "Controls on Sediment Connectivity in Fluvial Networks Impacted by Wildfire Across Utah" (2023). *All Graduate Theses and Dissertations, Fall 2023 to Present*. 17.

<https://digitalcommons.usu.edu/etd2023/17>

This Thesis is brought to you for free and open access by the Graduate Studies at DigitalCommons@USU. It has been accepted for inclusion in All Graduate Theses and Dissertations, Fall 2023 to Present by an authorized administrator of DigitalCommons@USU. For more information, please contact digitalcommons@usu.edu.



CONTROLS ON SEDIMENT CONNECTIVITY IN FLUVIAL NETWORKS
IMPACTED BY WILDFIRE ACROSS UTAH

by

Alec Arditti

A thesis submitted in partial fulfillment
of the requirements for the degree

of

MASTER OF SCIENCE

in

Watershed Science

Approved:

Patrick Belmont, Ph.D.
Major Professor

Brendan Murphy, Ph.D.
Major Professor

Larissa Yocom, Ph.D.
Committee Member

Jon Czuba, Ph.D.
Committee Member

D. Richard Cutler, Ph.D.
Vice Provost of Graduate Studies

UTAH STATE UNIVERSITY
Logan, Utah

2023

Copyright © Alec Justin Arditti 2023

All Rights Reserved

ABSTRACT

Sediment Connectivity in Fluvial Networks Impacted by Wildfire Across Utah

by

Alec Arditti, Master of Science

Utah State University, 2023

Major Professors: Dr. Patrick Belmont and Dr. Brendan Murphy
Department: Watershed Sciences

Wildfire-induced flooding and sedimentation are among the greatest disturbances to watersheds, fish populations and reservoirs in the western US. Burned landscapes are highly susceptible to runoff and erosion and have the potential to produce large, episodic pulses of sediment that put downstream resources at risk; however, the spatial distribution and distance downstream where impacts occur depend on the connectivity of the watershed. Sediment bottlenecks are locations within the riverscape where local conditions produce a persistent decrease in downstream connectivity of sediment, resulting in measurable deposition of fluvial sediment and potentially a substantial modification of local channel and valley bottom morphology. The primary objective of this research is to evaluate controls on the volume, location, and prevalence of sediment bottlenecks in fluvial networks after wildfire. We identified and surveyed 86 sediment bottlenecks associated with 15 wildfires throughout Utah. The mechanisms responsible for these sediment bottlenecks were attributed to either valley bottom morphology or structural factors, including large in-stream wood, beaver dams, debris flow deposits, and

human infrastructure. We developed a suite of geomorphic and landscape-based reach metrics, which we then analyzed as predictor variables on the volume and location of these sediment bottlenecks. Additionally, we digitized large wood and debris Flow Deposits at each site from aerial imagery, as both often increase considerably after wildfire and can significantly influence the prevalence of sediment bottlenecks. Our results indicate that valley bottom morphology exerts a variety of controls on sediment bottlenecks in burned catchments, directly causing sediment deposition in some locations and influencing occurrence of other structural controls on sediment deposition in other locations. Beyond local controls, several watershed attributes exert a significant influence on the recruitment and transport of sediment and wood. These findings will help refine sediment routing models, assist in identifying the magnitude and location of potential sedimentation risks, and better inform the management of infrastructure and aquatic habitat after wildfire.

(100 pages)

PUBLIC ABSTRACT

Sediment Connectivity in Fluvial Networks Impacted by Wildfire Across Utah

Alec Arditti

Flooding and sedimentation caused by wildfire are among the greatest threats to watersheds, fish populations and reservoirs in the western US. Burned landscapes are at risk for increased runoff and erosion and have the potential to transport sediment that may put downstream resources at risk. The ability of the channel to transport sediment downstream, known as the connectivity, is important for determining where impacts may occur. Sediment bottlenecks are locations within the watershed where local conditions produce a persistent decrease in downstream connectivity of sediment, resulting in increased sediment deposition and potentially a substantial modification of the local channel and floodplain. The primary objective of this research is to evaluate the volume, location, and amount of sediment bottlenecks in watersheds after wildfire. We identified and surveyed 86 sediment bottlenecks associated with 15 wildfires throughout Utah. The mechanisms responsible for these sediment bottlenecks were attributed to either the geometry of the channel and floodplain or physical obstructions, including large in-stream wood, beaver dams, debris flow deposits, and human infrastructure. We measured channel/floodplain geometry and land cover characteristics using GIS, which we then compared to the volume and location of these sediment bottlenecks. Additionally, we drew large wood and debris flow deposits in GIS at each site from aerial imagery, as both often increase considerably after wildfire and can significantly influence the amount of sediment bottlenecks. Our results indicate that the geometry of the channel and floodplain

influences sediment bottlenecks in burned watersheds, directly causing sediment deposition in some locations and influencing occurrence of other physical obstructions on sediment deposition in other locations. Beyond local controls, several watershed attributes exert a significant influence on the recruitment and transport of sediment and wood. These findings will help refine sediment routing models, assist in identifying the magnitude and location of potential sedimentation risks, and better inform the management of infrastructure and aquatic habitat after wildfire.

ACKNOWLEDGMENTS

“It takes a village to raise a child” and it took many collaborators and supporters far and wide to bring this thesis to completion. I must start by acknowledging my advisors Drs. Patrick Belmont and Brendan Murphy who helped guide and refine my research and who were patient and supportive throughout my entire timeline as a graduate student. My abilities as a researcher grew as they pushed me to think critically, develop ideas independently and produce rigorous science. In addition, my committee members Drs. Larissa Yocom and Jon Czuba provided valuable feedback with their specific expertise in wildfire ecology and sediment transport, that helped direct my research and improve my writing. My lab and our greater Pyrogeomorphology Research Collaborative were receptive to answering my questions and sharing suggestions throughout the research process. I would specifically like to thank Dr. Scott David for his help with fighting bugs in my code, Dr. Justin Stout for sharing his extensive knowledge of field methodologies and Sara Wall for helping me acclimate to the post-fire sedimentation world.

I have enormous appreciation for my companions in the field who dug so many holes: Ray Poe, Zach Burgert, Hannah Swernoff, Diane Wagner and Christian Stewart. The post-fire landscape is messy and unforgiving and we battled quicksand, blown alternators, curmudgeonly goats, wild packs of dogs, lightning storms, flat tires, rattlesnakes, flash floods and the most impenetrable sediment deposits you can imagine. I was especially impressed when Ray and Christian took on individual undergraduate research projects which contributed to my research and allowed me to grow as a mentor.

Finally, I would like to thank my friends, family and department who provided the foundation for me to take on this research project. I am incredibly grateful to my parents

and sister who pushed me to follow my love of maps and the outdoors and have supported me since Day 1. I could not have done this without my closest friends, Haley and Kipling, who are always excited to discuss hydrology and forest ecology. Susan Durham and Farooq were vital to my understanding of statistics and random forest models. I would also like to thank the Watershed Sciences Department, whose students, faculty and staff mentally and administratively supported me throughout my journey.

This work would not have been possible without funding from the National Science Foundation, Joint Fire Science Program and Utah Agricultural Experiment Station.

Alec Arditti

CONTENTS

	Page
Abstract.....	iii
Public Abstract.....	v
Acknowledgments.....	vii
List of Tables	xii
List of Figures.....	xiii
1 Introduction.....	1
1.1 Wildfire and Watersheds.....	1
1.2 Sediment Sources and Sinks in Watersheds after Wildfire.....	4
1.3 Objectives.....	7
2 Study Area	9
2.1 Utah Overview	9
2.2 Study Sites.....	10
2.3 Valley Bottom Network	11
3 Methods.....	12
3.1 Sediment Bottlenecks.....	13
3.1.1 Mapping and Measuring of Sediment Bottlenecks.....	13
3.1.2 Development of Explanatory Variables.....	15
3.1.3 Accounting for Explanatory Variable Uncertainty	17
3.1.4 Predicting Volume and Location of Sediment Bottlenecks.....	18
3.1.5 Grain Size Analysis.....	19
3.2 Development of Large Wood and Debris Flow Datasets.....	20
4 Results.....	23

4.1	Sediment Bottlenecks	23
4.1.1	Sediment Bottleneck Dataset	23
4.1.2	Uncertainty in Sediment Bottleneck Mapping.....	24
4.1.3	Causes of Sediment Bottlenecks	25
4.1.5	Prevalence of Sediment Bottlenecks.....	27
4.1.6	Locations of Sediment Bottlenecks	27
4.1.7	Volume of Sediment Bottlenecks	29
4.1.8	Grain Sizes of Sediment Bottlenecks.....	30
4.2	Impacts of Post-fire Debris Dynamics on Sediment Bottlenecks	32
4.2.1	Large Wood Dataset	32
4.2.2	Calibration and Uncertainty in Remote Wood Mapping	33
4.2.3	Density of Large Wood.....	34
4.2.4	Impacts of Large Wood on Sediment Bottlenecks	35
4.2.5	Debris Flow Deposits Dataset.....	37
4.2.6	Impacts of Debris Flows on Sediment Bottlenecks	37
5	Discussion.....	39
5.1	Controls on Sediment Bottlenecks	39
5.1.1	Sediment Bottleneck dataset.....	39
5.1.2	Temporal Aspects of Sediment Bottlenecks.....	40
5.1.3	Causes of Sediment Bottlenecks	41
5.1.4	Sediment Bottleneck Prevalence.....	42
5.1.5	Sediment Bottleneck Presence	43
5.1.6	Sediment Bottleneck Volume	44
5.1.7	Sediment Bottleneck Grain Sizes.....	45
5.1.8	What controls sediment bottlenecks after wildfire?.....	46
5.2	Impacts of Post-fire Debris Flow Deposits and Wood Dynamics on Sediment Bottlenecks.....	47
5.2.1	Wood Dynamics.....	47
5.2.2	Wood and Sediment Bottlenecks	49

5.2.3	Debris Flow Deposits and Sediment Bottlenecks	50
5.2.4	How do post-fire debris flow and wood dynamics influence sediment bottlenecks?.....	50
5.4	Limitations/Uncertainty	52
5.4.1	Sediment Bottleneck Identification.....	52
5.4.2	Development of Explanatory Variables.....	53
5.4.3	Remote Wood Mapping.....	54
5.4.4	Estimation of debris flow delivery volume.....	54
6	Conclusion	55
7	References.....	56
8	Appendices.....	66
	Appendix A. Remote Sediment Bottleneck Sites & Identification.....	67
	Appendix B. Depth Measurement Methods & Volume Calculation	73
	Appendix C. Development of Explanatory Variables	74
	Appendix D. Remote Wood Mapping	77
	Appendix E. Sediment Bottlenecks Results.....	78
	Appendix F. Random Forest Model Development.....	82
	Appendix G. Wood Results	85

LIST OF TABLES

	Page
Table 1 List of predictor variables and response variables tested in random forest model vs response variables.....	16
Table 2 Attributes of study sites, and prevalence of sediment bottlenecks	23
Table 3 Number of sediment bottlenecks at each study site that were field verified, field mapped only, and remote mapped but did not exist (only mapped in aerial imagery)	24
Table A. 1 List of all wildfires in Utah between 2010 and 2018, highlighting which wildfires were chosen as study sites	67
Table A. 2 Aerial Imagery Availability for study sites.....	72
Table C. 1 Attributes of each reach calculated in ArcPy	74
Table D. 1 Desktop measurements and attribution of large wood that were reevaluated in the field.....	77
Table E. 1 Sediment Bottleneck Attributes.....	78
Table E. 2 Sediment Bottleneck misidentification in aerial imagery at each site.....	80
Table G. 1 Volumes and Densities of Large Wood at each Study Site	85
Table G. 2 Properties of measured Wood-Forced Sediment Bottlenecks	86

List of Figures

	Page
Figure 1 Examples of volume, location and prevalence of sediment bottlenecks and wood.....	9
Figure 2 Location of wildfires serving as study sites	11
Figure 3 Diagram of wood mapping and debris flow delivery calculation	22
Figure 4 Examples and distribution of different sediment bottleneck causes	26
Figure 5 Random Forest model results for sediment bottleneck location	29
Figure 6 Random Forest model results for sediment bottleneck volume	30
Figure 7 Sediment bottleneck grain size distributions.....	32
Figure 8 Random Forest model results for wood density.....	35
Figure 9 Random Forest model results for wood-forced sediment bottleneck location...	37
Figure 10 Debris Flow Deposit attributes and impacts to sediment bottlenecks.....	39
Figure A. 1 Examples of identified sediment bottlenecks, including photos corresponding with aerial imagery of the sediment bottleneck	72
Figure B. 1 Diagrams demonstrating how depositional depths were measured.....	73
Figure B. 2 Progression of maps showing how sediment bottleneck volume was calculated	73
Figure C. 1 Channel width power function development and valley bottom width validation.....	76
Figure D. 1 Wood calibration and validation measurements.....	77
Figure E. 1 Pearson correlation coefficients for sediment bottleneck prevalence.....	81
Figure F. 1 Pearson correlation coefficients for variables used in random forest analysis.....	82
Figure F. 2 Example of decision tree created in random forest analysis of sediment bottleneck presence.....	82

Figure F. 3 Original random forest variable importance plot and Boruta selections..... 84

1 INTRODUCTION

1.1 Wildfire and Watersheds

Wildfires have long influenced river and landscape processes in the western United States (Kirchner et al., 2001). For most of the last century, wildfire has occurred at anomalously and artificially low rates due to land use changes and aggressive fire suppression (Marlon et al., 2012; Murphy et al., 2018). More recently however, wildfire activity has been on the rise due to high fuel loading in many western forest ecosystems, as well as climate change, which has created hotter and drier forest conditions (Murphy et al., 2018; Abatzoglou & Williams, 2016; Parks & Abatzoglou, 2020). While the amount of annual burned acreage is still well below that burned prior to European settlement in the western U.S., the threat wildfires pose to infrastructure and artificially fragmented river networks is unprecedented (Duane et al., 2021; Murphy et al., 2018). As climate change continues to desiccate vegetation and raise temperatures, the impacts of wildfires are likely to continue to increase (Abatzoglou et al., 2021; Duane et al., 2021).

Wildfire-induced flooding and sedimentation are among the greatest disturbances to western watersheds (Murphy et al., 2019). While burned forests and structures represent immediate and obvious impacts, wildfires can affect landscapes long after the fire is over through protracted increased runoff and erosion rates. Following a moderate to high severity wildfire, a lack of canopy decreases interception of precipitation and evapotranspiration. Burned soils may become hydrophobic, which inhibits surface water infiltration and leads to increased overland flow (DeBano, 2000). The reduction in root strength of a burned forest diminishes soil stability (Hallema et al., 2017). These

vulnerable soils are eroded by a variety of hillslope processes or runoff-generated debris flows, which can occur even after modest rainfall events in severely burned areas (Staley et al., 2020). While the impacts of climate change on the annual precipitation amounts in the western U.S. is highly uncertain (McKinnon & Deser, 2021), variability is expected to increase, producing longer and more severe droughts. The proportion of precipitation that does fall, is more likely to fall as rain, rather than snow, and rain events have trended towards a shorter duration at a higher intensity (Swain et al., 2018). Furthermore, because of warmer winters, more rain on snow events are also projected, yielding high streamflow events (Musselman et al., 2018). These long-term climatic trends, combined with extensive areas available to burn due to fire suppression, are likely to continue to increase the prevalence and severity of wildfires, and the cascades of post-wildfire hydrologic and sedimentation impacts in the future.

Post-wildfire sedimentation can be devastating to critical infrastructure. Reservoirs are vital in providing drinking and irrigation water to the western U.S. and water budgets are already strained by prolonged drought and warming temperatures (Udall & Overpeck, 2017). Wildfire-induced sediment loading substantially reduces valuable storage capacity of reservoirs (Murphy et al., 2018; Sankey et al., 2017). Sediment can both damage water intakes and make them inoperable, cutting off access to water supplies (Hallema et al., 2019). Accelerated fluvial activity can cause rapid fluctuations in reach-scale incision or deposition. Excavation or inundation of sediment near homes or roads is a public safety hazard and can cause millions of dollars in damages (Valentin & Stormont, 2019). In addition to damaging structures, in conjunction with wood, sediment has the ability to aggravate flooding and erosion when accumulating in front of culverts and bridges

(Schmocker & Weitbrecht, 2013). Even the threat of post-wildfire runoff and debris can substantially devalue homes (Mueller et al., 2018).

While post-wildfire sedimentation poses clear societal and economic risks, the effects on fluvial and riparian habitats have been shown to be both positive and negative. While sediment influxes to river systems have the potential to deposit substantial volumes of fine sediment that degrade geomorphic complexity in the short-term, they can also introduce grain sizes that are beneficial for spawning and cover over longer time scales (Flitcroft et al., 2016; Gillard, 2019; Jager et al., 2021). Sediment deposition, and interactions between sediment and wood have the potential to substantially modify aquatic habitat (Welling et al., 2021). Increased understanding and predictive power of post-wildfire fluvial process are crucial for protecting water resources and mitigating wildfire-watershed risks (Bladon et al., 2014; Murphy et al., 2018; Robinne et al., 2021, Sankey et al., 2017).

Watersheds vary considerably in their ability to convey sediment through their stream network. Watersheds with high downstream connectivity contain few locations prone to accumulate sediment within the river network, but may convey large amounts of sediment to infrastructure further downstream (Wohl et al., 2019). Watersheds with lower downstream connectivity may have numerous locations prone to accumulating large amounts of sediment. We use the phrase ‘sediment bottlenecks’ to refer to locations within the riverscape where local conditions are prone to causing measurable deposition of fluvial sediment. These locations may be hotspots for substantial modification of local channel and valley bottom morphology. Channel dynamics and geometry will also influence where sediment bottlenecks form, potentially impacting infrastructure and

aquatic habitat in these locations. These sediment bottlenecks trap sediment transported through the fluvial network and have the potential to protect downstream resources (Hooke, 2003). The locations and volumes of these sediment bottlenecks is key in predicting downstream risks after wildfire (Murphy et al., 2019).

1.2 Sediment Sources and Sinks in Watersheds after Wildfire

Sediment transport through river networks is an intermittent, discontinuous process, and can be heavily altered by environmental disturbances. For instance, after wildfires in steep terrain, sediment inputs to the fluvial network may increase from hillslopes and debris flows. Enhanced runoff and streamflows can also cause channel erosion, which can contribute to additional sources of sediment. The majority of contemporary post-wildfire sediment yields are unlikely to make it through the fluvial network to a downstream waterbody and are instead deposited within the valley bottom (Fryirs, 2013; Murphy et al., 2019; Rathburn et al., 2013). While the magnitudes of deposition are spatially and temporally variable throughout a river network, locations of persistent deposition due to supply rates far exceeding the transport capacity are defined as sediment bottlenecks (Gran & Czuba, 2017).

The majority of prior sediment connectivity research has focused on utilizing topography and streamflow records to apply sediment transport functions. Schmitt et al. (2016) developed the *Catchment Sediment Connectivity and Delivery* (CASCADE) model, which defined reaches as sources or sinks of sediment. The calculated transport capacity for each reach then determined whether sediment was deposited or transported. Sediment bottlenecks were identified by CASCADE at confluences, particularly where a

smaller tributary entered a larger river and transport capacity abruptly changed. Similarly, Czuba has developed the *Network Sediment Transporter* (NST) model (Pfeiffer et al., 2020), which uses a Lagrangian framework to route sediment based on a stream network with scaled channel and discharge variables, as well as digital elevation model (DEM) derived slope (Czuba, 2018; Czuba et al., 2017; Czuba & Fofoula-Georgiou, 2014; Czuba & Fofoula-Georgiou, 2015). An application of NST to study sediment pulse transport found that aggradation of sediment was most likely to occur in reaches with locally lower slope where transport capacity remains low (Gran & Czuba, 2017). NST has been incorporated as the in-stream routing component into the *Fire-Watershed Assessment Toolkit for Erosion and Routing* (FireWATER), a comprehensive post-wildfire flow and sediment routing framework (Murphy et al., *in review*). When using FireWATER to model sediment transport following the Twitchell Canyon Fire, Murphy et al. (2019) located sediment bottlenecks in areas of the drainage network where the slope locally shallowed.

Few studies have empirically documented sediment bottlenecks or fluvially transported sediment deposits after wildfire. Cannon (2001) mapped debris flow sediment and their prevalence across fires. She determined that fluvially transported debris flow sediment, that is sediment transported through Newtonian flow, was more common than colluvially deposited debris flow sediment in burned drainage basins. Further, these fluvially transported deposits could be formed through bar formation, channel infilling or road obstructions. Nyman et al. (2020) conducted a similar study in Australia, mapping debris flows and tracking their deposition through a singular drainage network. They found that when the valley bottom entered a wider, lower slope domain, fluvial controls

on debris flows deposits increased. Collectively, this research provides insights about potential controls on sediment deposition after wildfire. These studies however, focus more on unsorted alluvial material, instead of fluvially transported and organized sediment (Miller & Juilleret, 2020).

While slope and streamflow serve a primary role in controlling sediment deposition, the dynamics of fluvial networks, especially after wildfire, are more complex. For instance, Fryirs et al. (2013; 2007) identified several types of barriers that impede sediment transport along the channel network. These barriers can be divided into 2 categories: 1) non-structural controls, which is the valley bottom morphology, as well as its relationship to the channel, and 2) structural forcing caused by channel obstructions, such as human structures, beaver dams, debris flow deposits or fluvial wood that present impediments to streamflow (Butler & Malanson, 1995). While slope is considered within NST, other characteristics of the valley bottom, such as its width and lateral connection to the floodplain, have not been explored in their ability to control sediment deposition. In burned watersheds, debris flow deposits and fluvial wood are structural forcing mechanisms that may obstruct or alter flow in channels and floodplains (Benda, Miller, Bigelow, et al., 2003). The Network Dynamics Hypothesis suggested that sediment bottlenecks may frequently occur at tributary junctions, since the sediment or wood outputs of a tributary has the potential to modify the connectivity and morphology of the channel it intersects (Benda et al., 2004).

In addition to increased streamflows and sedimentation, wildfires tend to increase delivery and transport of large wood (≥ 10 cm diameter and 1 m length) in stream networks (Benda et al., 2003; Zelt & Wohl, 2004). Elevated tree mortality contributes to

wood availability, while debris flows, colluvial, and fluvial processes recruit this large wood into the fluvial network (Benda et al., 2003; Wohl, 2020). While there are many parallels between post-wildfire sediment and wood delivery, transport, and deposition, very few studies have documented how and when they differ and the complexities of their interactions (Wohl & Scott, 2017). Sediment trapping caused by large wood has been demonstrated in multiple studies. Welling et al. (2021) showed that wood jams (2 or more pieces) store a disproportionate amount of sediment compared to individual pieces. Channel-spanning logjams of greater structural complexity have been found to be more effective at creating backwater and trapping sediment (Cashman et al., 2021; Livers & Wohl, 2021). The greatest frequency of wood jams is found in 3rd and 4th order streams, which consequentially is also where wood most effectively affects sediment storage (A. Pfeiffer & Wohl, 2018).

1.3 Objectives

R1: What controls sediment bottleneck volume, location and prevalence in drainage networks after wildfire?

This thesis addresses knowledge gaps in empirically identifying sediment bottlenecks in fluvial networks and predicting how and where sediment bottlenecks form in response to large sediment pulses commonly generated after wildfire. We seek to understand which aspects of the underlying valley bottom morphology, local land cover and area draining upstream serve as key controls in the generation of sediment bottlenecks in burned watersheds. We specifically evaluate controls on the volume, location, and prevalence of sediment bottlenecks in fluvial networks after wildfire (*Fig. 1*) that serve as

study sites. We identify factors influencing formation of sediment bottlenecks in burned watersheds, including valley bottom morphology and other structural forcing mechanisms. Independent of formation mechanism, all sediment bottlenecks are evaluated using reach-based metrics, to determine if valley bottom morphology is the principle control on the location and volume of sediment bottlenecks, or if structural forcing creates sediment bottlenecks independently of valley bottom morphology. We examine prevalence of sediment bottlenecks based on the wildfires and watersheds that caused them. We also compare grain size distributions of sediment bottlenecks, relative to each other, nearby reaches and estimated pre-fire values.

R2: How do post-wildfire wood and debris flow dynamics modify the volume, location and prevalence of sediment bottlenecks?

Wood and debris flow deposits influence the volume, location and prevalence of sediment bottlenecks. For example, recruitment of wood and an increase of debris flows alter the riverscape after wildfire by introducing sediment and creating structural forcing. Wood and debris flow deposits can serve as controls on sediment bottlenecks (*R1*), but there has been little research done on the dynamics of wood and debris flows after wildfire and how this may impact sediment routing. We construct large wood and debris flow deposit datasets through field work and novel use of aerial imagery to better understand their influence on the size and prevalence of sediment bottlenecks. We also compare where large wood is deposited within fluvial networks with where sediment bottlenecks occur.

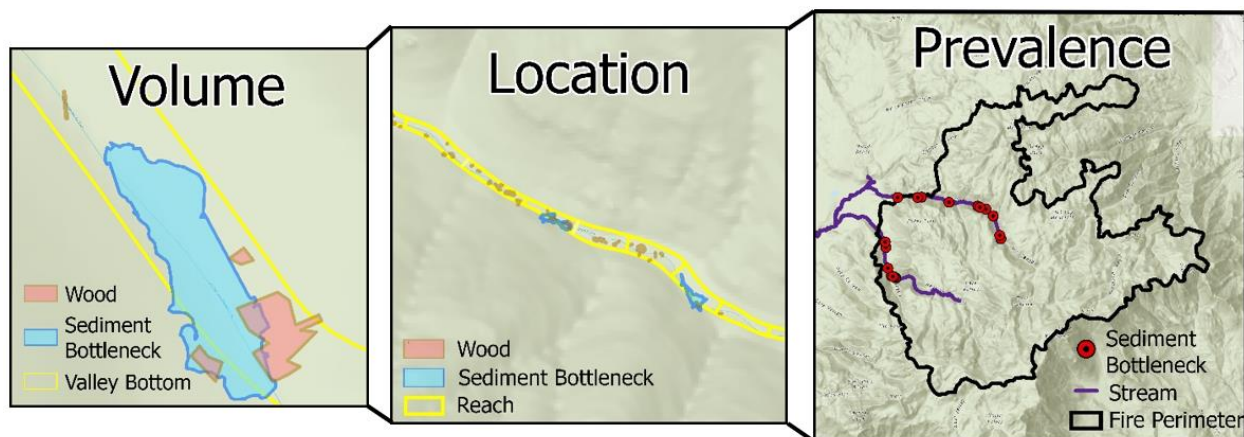


Figure 1 Examples of volume, location and prevalence of sediment bottlenecks and wood. Volume refers to the amount of sediment deposited and large wood within a given reach. Location refers to which stream reaches within river networks contain sediment bottlenecks and large wood. Prevalence refers to the amount of sediment bottlenecks and wood at each study site.

2 Study Area

2.1 Utah Overview

This study focuses on forested regions in Utah, which hosts a diversity of biogeographies, physical geographies, and topographies. Elevation in Utah ranges from 3000-13000 ft across plateau-canyon, basin and range, and steep mountainous topography. Although Utah is the second driest state in the U.S., aridity fluctuates widely, because of these changes in altitude. Higher elevations receive around 50 inches of precipitation a year, and support a variety of forests that cover roughly one third of Utah (Banner et al., 2009). High-elevation mixed conifer forest, mid-elevation ponderosa forests and low-elevation pinyon-juniper and maple-oak forests each display a distinct wildfire regime (Heyerdahl et al., 2011). Many stream networks and the majority of our study sites are fed in the spring by melting snowpack, with summer baseflows punctuated

by high ephemeral flows from thunderstorms and the North American monsoon (Sheppard et al., 2002). However, these flows can be frequently moderated because of Utah's extensive water infrastructure, including upstream dams and water diversions.

2.2 Study Sites

We identified 15 stream networks to serve as study sites within and downstream from recently burned areas representing a diverse set of forest, fire, and geomorphic settings throughout Utah to address our research questions (*Fig. 2*) (*Table 1*). We strategically selected these 15 wildfire perimeters based on their likelihood to produce debris flows, generate wood, and their susceptibility to increase runoff following the burn (*Table A.1*). At the start of the site selection process, we initially considered all Utah wildfires in the Monitoring Trends in Burn Severity (MTBS) database between 2010 and 2018 (n=147). We focused on this temporal range because the resolution of aerial imagery improved considerably (≤ 30 cm) in 2010. In addition, it would be difficult to measure changes to stream networks, for events much earlier or later than this time period. These 147 wildfires were then assessed based on available classified dNBR (differenced normalized burn ratio), DEMs, and pre-fire vegetation cover datasets. Metrics, including % burned at moderate/high severity, % of slope greater than 23 and % conifer were developed from each of these datasets to represent potential for sediment and wood delivery to and transport through fluvial networks after wildfire (Lamb et al., 2013; Staley et al., 2017). Through quantitative analysis of these metrics for each fire, we were able to select study sites with a wide variety of characteristics that we hypothesized to influence the

production of sediment bottlenecks. We examine the correlation of these original study site metrics with bottleneck prevalence in our analysis (section 4.1.4).

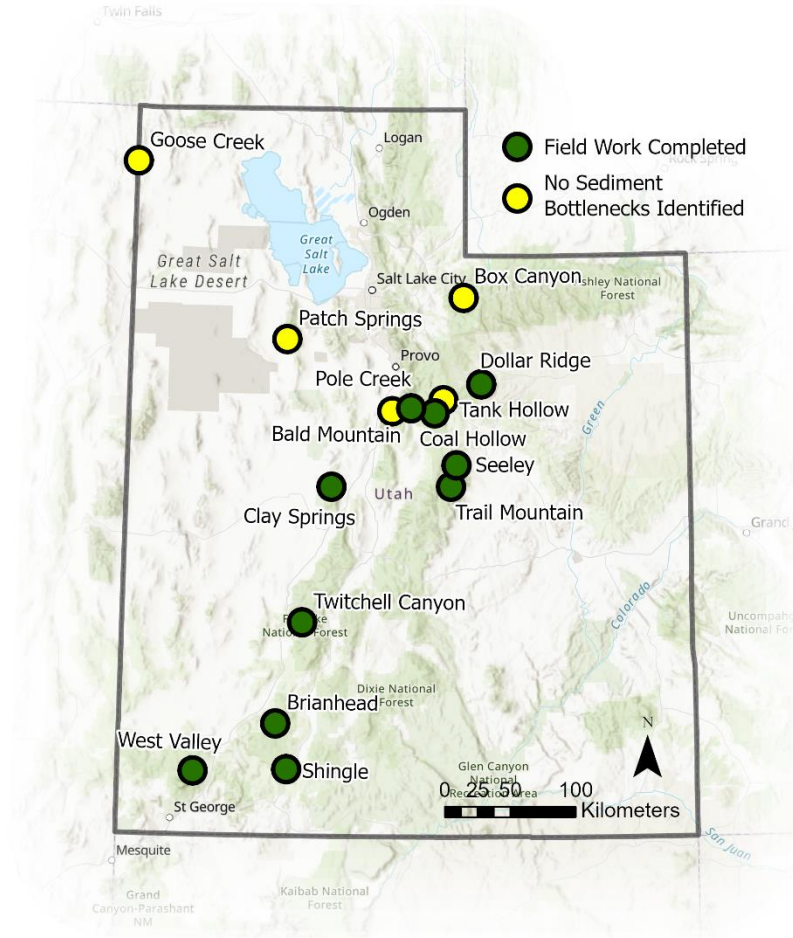


Figure 2 Location of wildfires serving as study sites

2.3 Valley Bottom Network

Within these 15 fire perimeters, we mapped and analyzed sediment and wood within the valley bottom. Valley bottoms were delineated with a minimum drainage area of 5 km² (Staley et al., 2017) using the Fluvial Corridor tool (Murphy et al., 2019; Roux et al.,

2015). Sediment bottlenecks were field mapped within valley bottoms where the majority of the drainage area is burned ($\sim >50\%$), because fluvial wildfire impacts propagate downstream to reaches not within the burn perimeter. We digitized debris flow and wood locations within the valley bottoms of each burn perimeter, where a lack of canopy enabled mapping at a fine scale (*Fig. A.1*). Streams with less than 1 km of longitudinal valley bottom length within the burn perimeter were omitted, to ensure there was adequate data available for analysis.

To identify sediment bottlenecks, debris flow deposits and large wood, high resolution aerial imagery across multiple years was required. We compiled all available imagery with a resolution of 30 cm or less for each site after the fire occurred, through the Utah Geospatial Resource Center (*Table A.2*). Thirty centimeters is the necessary threshold for identifying 20 cm diameter pieces of wood (Wohl, Scott, et al., 2018). Statewide Hexagon proprietary imagery was collected in the summer of 2021, during our first field work season which aided in validation of aerial imagery analysis.

3 Methods

We evaluated landscape controls and debris impacts on sediment bottlenecks through development of field and remote mapped datasets, calculation of reach metrics and statistical models. Error is assessed as necessary for each component of this study.

3.1 Sediment Bottlenecks

3.1.1 Mapping and Measuring of Sediment Bottlenecks

We empirically identified the location of sediment bottlenecks using a combination of sources. Initially, desktop geospatial analysis was used to map probable sediment bottleneck locations using available pre- and post-fire imagery. These locations were then verified in the field. Sediment bottlenecks were identified as large, unvegetated swaths of sediment deposition that spanned the channel and/or valley bottom. Imagery was visually compared before and after the fire and across different years to detect when sediment bottleneck formation occurred and evaluate other temporal aspects.

Field verification took place at all study sites with identified sediment bottlenecks in the summer of 2020. All remotely mapped sediment bottlenecks were visited. While accessing these locations, additional sediment bottlenecks identified in the field were mapped and measured. These sediment bottlenecks were visually verified as areas with fluvial sediment aggradation exceeding or reaching bankfull across the majority of the original channel. Field verification enabled us to identify possible sediment bottlenecks that have been overgrown by vegetation (Kobziar & McBride, 2006; Smith et al., 2009), or that have been eroded or formed after our last available set of imagery. We compared our desktop analysis to field mapped sediment bottlenecks to assess uncertainty of bottleneck identification at each study site. We classified sediment bottlenecks as field-verified (true positives/TP), misidentified in imagery analysis (false positives/FP), and field-discovered (false negatives/FN). We used this classification to assess our abilities in successfully identifying all existing bottlenecks.

We identified factors influencing the formation of sediment bottlenecks as either a change in valley bottom morphology (non-structural controls) and/or structural forcing. When structurally forced, a forcing mechanism was identified (wood jam, debris flow (and other mass wasting), manmade structure, beaver dam, etc.). If there is no obvious structure, mechanism of formation was attributed to non-structural controls. While non-structural controls may have been the underlying cause for structural forcing occurrence, we evaluated this in our statistical analysis through the inclusion of geomorphic predictor variables.

The volume of sediment bottlenecks was calculated using a delineated area of deposition and measured depths across the depositional area. Deposition depths were measured opportunistically using a variety of methods best suited for accuracy and efficiency (*Fig. B.1*). Holes were dug in the deposition in areas of less compacted gravel and sands that were above the water table. We pounded rebar using a rubber mallet and rebar to the point of refusal in areas of submerged sand and fine sediment (Lisle & Hilton, 1992; Welling et al., 2021). Where wood jams provide a structural control, the bed elevation was measured on each side of the jam to determine deposition depths (Andreoli et al., 2007). In areas where the channel has incised below the deposit, we measured depth of the deposit down to the depositional unconformity (Nyman et al., 2020). Depositional unconformities were identified through changes in grain size, presence of soil development and/or gleying, as well as locations of tree buttressing and roots that indicate a stable pre-depositional surface. Using the locations and depths of measurements collected in the field, TINs (Triangulated Irregular Networks) were created of the sediment bottlenecks that allowed us to estimate sediment volumes (e.g., [Wall et](#)

al., 2022) (Fig. B.2). We estimated uncertainty as 30% greater and less than the measured sediment bottleneck volume, using the bounds for volume estimation recommended for debris flow deposits (Santi, 2014).

3.1.2 Development of Explanatory Variables

Geomorphic, local and upstream land cover reach-based metrics informed the statistical models we used to identify controls on sediment bottleneck location and volumes (Table 1). Calculation of each of these metrics for each reach (n=1592) was automated in ArcGIS using Python. Refer to our GitHub repository: USUALmetrics (Table C.1), for all calculations, sources, significance and more detailed descriptions of all metrics. We measured geomorphic metrics using 10 m DEMs. These geomorphic metrics are important for understanding how valley bottom morphology may influence the formation of sediment bottlenecks or conversely facilitate sediment transport through a reach. Local and upstream land cover metrics were developed using available raster datasets, including classified dNBR from the MTBS database (MTBS 2020) and pre-fire existing vegetation type from the LANDFIRE database (LANDFIRE, 2010). Locally measured metrics may help identify reaches with controls on sediment transport from the surrounding hillslopes and riverscape while upstream metrics represent conditions from the land area draining to the reach of interest that may influence upstream generation and transport sediment or wood.

Channel width was a necessary parameter in calculating many of our geomorphic explanatory variables. We developed a power function for channel width based on drainage area to scale channel width through each of our fluvial networks. We mapped 42

reaches across each of our study sites using pre-fire aerial imagery. These reaches were selected to represent a variety of drainage areas in areas with less canopy and higher quality imagery to properly identify the channel perimeter. Our power function produced a curve for channel width $y=1.505x^{0.273}$ where x is in square kilometers and y is in meters ($0.69 R^2$) (Fig. C.1).

Appropriate spatial scaling is necessary to capture the relationship between these metrics and sediment bottlenecks, so we evaluated various reach lengths. We decided to use a 500 m maximum reach length because this most accurately breaks up tributary confluences, which may introduce changes to hydrology and sediment flux (Benda et al., 2004; O'Brien et al., 2019). In addition, this is the length used to parameterize FireWATER (section 3.3), which made our results comparable to the outputs of the model. We delineated our stream networks using the USUAL Watershed Tools (David et al., 2023).

Table 1 List of predictor variables and response variables tested in random forest model vs response variables

	Variable	Comments/Description
Explanatory Variables		
<i>Geomorphic</i>	Reach Slope	Derived from USUAL
	Change in Slope	Finite Difference of Upstream Reach
	Normalized Steepness	Calculated using watershed-specific reference concavities
	Percentile of Normalized Steepness	
	Valley Bottom Width (m)	Derived from Fluvial Corridor Tool
	Change in Valley Bottom Width	Finite Difference of Upstream Reach
	Floodplain to Channel Ratio	
	Stream Power	Calculated using USGS 2 year flows for Utah and slope
	Sinuosity	Manhattan Distance of reach vs Euclidean Distance
	Confinement	Proportion of channel edge abutting valley bottom edge
<i>Local</i>	Topographic Position Index	Position of reach relative to surrounding topography
	Reach Averaged Vegetation Cover	From LANDFIRE Existing Vegetation Type
<i>Contributing Drainage</i>	Reach Averaged Burn Severity	From Monitoring Trends in Burn Severity database
	Upstream Vegetation Cover	From LANDFIRE Existing Vegetation Type
	Upstream Moderate High Severity %	From Monitoring Trends in Burn Severity database
	Upstream Moderate High Severity km ²	From Monitoring Trends in Burn Severity database
	Upstream conifer %	From LANDFIRE Existing Vegetation Type
	Volume of debris flow sediment delivered upstream	From compiled Utah debris flow dataset (Fig. 3)
Response Variables		

Presence/Absence of a Sediment Bottleneck in a reach
Volume of a Sediment Bottleneck in a reach (m ³)
Density of Wood in a reach (m ³ /ha)

3.1.3 Accounting for Explanatory Variable Uncertainty

To measure uncertainty of our reach-based metrics, we evaluated reaches with sediment bottlenecks (79) and extreme values for all reaches (5 greatest and least for each metric for 1608 reaches) for error. The majority of uncertainty we encountered came from the coarse (10 m) resolution of the DEM, which in some cases causes inaccurate watershed delineation and flow accumulation. To fix these issues, we manually delineated watersheds (22 reaches), deleted spur reaches that fell within the valley bottom (4 reaches), and edited the DEM in areas where the filled DEM showed anomalously low slopes, because of culverts, tunnels, past beaver dams or other reaches where the channel elevation was incorrectly identified (20 reaches). In areas with incorrect slopes, we fit the slope of the channel to upstream and downstream elevations to smooth the profile. Finite differencing could not be calculated for upmost reach in each of our fluvial networks because it relies on values from the upstream reach. We generated a stream network using 2.5 km² threshold to calculate finite differencing of slope and valley bottom for each of our upmost reaches (117 reaches).

An accurate valley bottom extent was important for mapping our response variables and calculating many of our explanatory variables. The valley bottom delineated by the Fluvial Corridor Tool was validated by comparing reach-averaged widths to 28 manually mapped sections of valley bottom. Fluvial Corridor had an R² of 0.6 when compared to manually delineated widths (*Fig. C.1*).

3.1.4 Predicting Volume and Location of Sediment Bottlenecks

We used random forest analysis to evaluate factors influencing the volumes and locations of sediment bottlenecks and densities of wood within the fluvial network. Random forests use an ensemble of randomly generated decision trees to relate explanatory and response variables (Cutler et al., 2007). We chose this type of statistical analysis because random forests are non-parametric and work well with data like ours that are not distributed normally and have many possible explanatory variables. We parameterized our random forest models using the reach-based metrics as explanatory variables and the amount/presence of sediment bottlenecks and wood as our response variables. We tested our explanatory variables for multicollinearity by measuring the covariance between each reach-based metric (*Fig. F.1*). We excluded variables that shared high correlation (>0.72) with multiple other explanatory variables.

To measure the influence of reach-based metrics on the volume of sediment and density of wood deposited in a reach we used random forest regression. For the presence of a sediment bottleneck in a reach, which is a categorical variable, we used random forest classification. Because the sediment bottleneck dataset is observational, and our data only indicate presence, we synthesized pseudo-absence data through random sampling to parameterize the random forest model. We selected a number of locations where sediment bottlenecks are absent equal to the number of locations where sediment bottlenecks are present from all watersheds, including those where sediment bottlenecks were not identified (Barbet-Massin et al., 2012; Merow et al., 2013). To ensure a representative distribution, we sampled absences randomly throughout the study domain and ran the random forest 500 times, in a process referred to as down-sampling (Valavi et

al., 2021, 2022). We used a sufficient number of explanatory variables relative to observations (1:10) for each random forest analysis (Austin & Steyerberg, 2015). Random Forest models were fit with the randomForest package (Breiman, 2001) in R (R Core Team, 2013).

We used the Boruta package (Kursa & Rudnicki, 2010) in R (R Core Team, 2013) to obtain a sharp classification of variables into those deemed relevant and those deemed irrelevant (*Fig. F.2*). We then reran our random forest analyses using only the variables deemed relevant. Using our new random forest models, we used variable importance plots based on out-of-bag error to rank variables based on predictive strength, measured as the mean decrease in model accuracy when a given explanatory variable is removed from the model. We evaluated different combinations of the most important variables to produce the most accurate random forest model, using the out of bag error to assess overall accuracy.

3.1.5 Grain Size Analysis

We measured grain size distributions for most sediment bottlenecks by conducting Wolman pebble counts. One hundred surface grain size measurements were taken by randomly selecting sediments and measuring with a gravelometer. We walked downstream in a serpentine pattern from the head to the tail of each sediment bottleneck to minimize the effects of fluvial sorting. We also conducted Wolman pebble counts immediately downstream of each sediment bottleneck. While this is not necessarily a direct proxy for pre-fire grain sizes, it provides a nearby grain size distribution for comparison to the sediment bottleneck.

In addition to comparing these field-measured grain size distributions to one another, we also compared them to a modeled pre-fire grain size following (Snyder et al., 2013). We parameterized this model using the two year recurrence interval (Q2) flows calculated using regional regression equations developed for peak flows in Utah (Kenney et al., 2007).

3.2 Development of Large Wood and Debris Flow Datasets

We characterized wood production and jam formation in fluvial networks after wildfire in order to test how wood dynamics influence sediment bottlenecks. We created wood datasets for seven of our study sites. We digitized all large wood within the valley bottom using the first available aerial imagery after each fire to develop spatial datasets (*Fig. 3*). Large wood has traditionally been defined as dead or downed pieces of wood having a minimum length of 1 m and a minimum diameter of 10 cm (Ruiz-Villanueva et al., 2016; Scott & Wohl, 2018; Wohl & Scott, 2017). We mapped wood at a minimum diameter of 20 cm in order to be successfully mapped from 15 cm aerial imagery. From these spatial datasets of digitized features, we automated volume calculations of large wood in different channel reaches, using ArcPy (*Table D.1*). The volume of individual pieces was calculated as an approximate cylindrical prism, while the volume of wood jams (>2 pieces) was approximated by the dimensions, an estimated height of twice the average wood diameter in the system, and visually estimated porosity (Livers et al., 2020). Features were attributed by location within the valley bottom in relation to the channel to represent proximity to streamflows. The setting of each feature (fluvial, colluvial, in-situ or debris flow) was also recorded, which may indicate each large wood mechanism of

recruitment. The quantity of pieces within each wood jam were counted or visually estimated in jams larger than 10 pieces.

We assess error of our digitized volumes of wood by comparing to field mapped volumes of wood. We mapped wood in the field along 17 100 m longitudinal transects across the valley bottom in July and August of 2021, when 15 cm Hexagon imagery was being collected. While all transects fell within the burn perimeters, we varied transects by burn severity and canopy cover. Wood was mapped using the same methods as described in Wohl et al., 2018, with the exception of our 20 cm diameter threshold. Personnel who digitized wood for the dataset, mapped wood along the transects using the 2021 imagery to gage the error associated with remote mapping (*Fig. D.1*).

Additional field measurements were collected for large wood within sediment bottlenecks that are interacting with and trapping sediment. These measurements help answer how wood modifies volume of sediment bottlenecks. Large wood exhibiting sediment capture had a water level or channel cross section height greater upstream. While the upstream face was completely or partially covered, the downstream face of the large wood feature was exposed. The area of trapped sediment and difference in sediment height was measured in order to calculate volumes (Andreoli et al., 2007). For jams, porosity and fine material was estimated, as these have been shown to be important predictors of sediment trapping ability (Manners et al., 2007; Schalko et al., 2018). We used these volumes of sediment captured by wood to compare to the characteristics of respective wood and wood jams.

We compiled and added to a dataset of digitally identified debris flow deposits across Utah in order to study how debris flow dynamics impact sediment bottlenecks. We used

existing data from Wall et al. (2022) and Murphy et al., (2019) and then used more recently available 2018 and 2021 aerial imagery to digitize remaining debris flow deposits linked to our wildfires. Debris flow perimeters do not account for fluvial erosion that may have occurred at the toe of the debris flow. For digitized debris flow deposits, we estimated volumes using the area-volume relationship Wall et al., (2022) found in their dataset. The amount of sediment delivered to the fluvial network, which served as one of our explanatory variables, was estimated by intersecting the debris flow perimeter with the channel network and using the proportion of the area to calculate the proportional volume (*Fig. 3*).

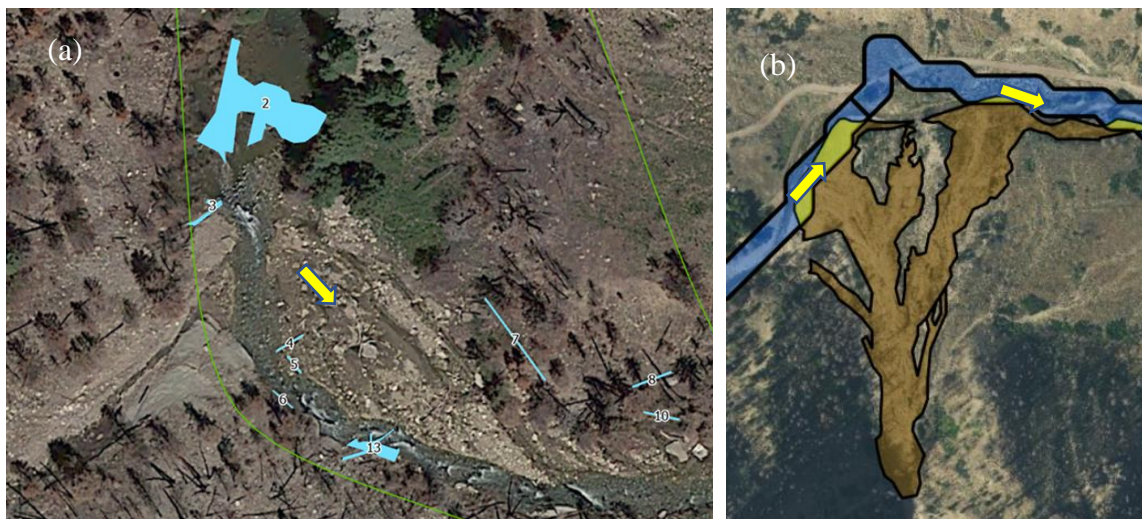


Figure 3 (a) Example of digitized wood features within the valley bottom. The wood features are light blue polygons and rectangles, while the valley bottom is shown with the green line. (b) Example of digitized debris flow and estimated delivery to the stream network. The brown shading represents the debris flow, the blue represents the modelled channel and the yellow represents hypothetical intersection where debris flow delivery occurs. Yellow arrows in both (a) and (b) represent flow direction.

4 Results

4.1 Sediment Bottlenecks

4.1.1 Sediment Bottleneck Dataset

Our sediment bottleneck dataset consists of 86 sediment bottlenecks across 15 study sites encompassing 741 km of stream network (*Table 2*) (*Table E.1*). There were 5 study sites where no sediment bottlenecks were identified. While the Twitchell Canyon fire produced most sediment bottlenecks, the Dollar Ridge fire had the greatest total volume of sediment bottlenecks, even when normalizing each study site by the length of the fluvial network. Sediment bottlenecks exhibited a wide range in volumes: between 3 and 40,000 m³ of sediment. Although this range covers 5 orders of magnitude, the median volume of our sediment bottleneck dataset is only 150 m³.

Table 2 *Attributes of study sites, and prevalence of sediment bottlenecks*

Fire	Year Burned	Fire Extent (sq. km)	Stream Network Length (km)	Stream Network Length Visited (km)	% Burned at Moderate to High Severity	% Slope greater than 23 degrees	% Conifer	# of Bottlenecks	Bottleneck Volume of Sediment (m ³)	Bottleneck Volume of Sediment per length (m ³ /km)
Bald Mountain	2018	85	33	16	58	50	45	0	0	0
Box Canyon	2016	18	8	0	46	37	48	0	0	0
Brian Head	2017	301	70	52	58	16	80	7	1214	17
Clay Springs	2012	435	40	35	23	35	15	9	447	11
Coal Hollow	2018	122	62	51	69	40	68	13	14410	232
Dollar Ridge	2018	283	107	62	48	41	53	8	52269	488
Goose Creek	2018	532	90	0	27	11	34	0	0	0
Patch Springs	2013	120	34	0	36	55	18	0	0	0
Pole Creek	2018	415	121	64	69	40	68	5	13598	112
Seeley	2012	181	33	33	62	61	35	11	4880	148
Shingle	2012	33	14	13	53	24	40	4	2910	208

Tank Hollow	2018	45	21	8	36	44	59	0	0	0
Trail Mountain	2017	74	36	24	54	64	64	1	638	18
Twitchell Canyon	2010	174	56	36	64	51	67	17	14512	259
West Valley	2018	48	15	9	54	42	88	11	2481	165
Total/Average	2016	191	741	406	50	41	52	86	160160	111

4.1.2 Uncertainty in Sediment Bottleneck Mapping

We visited roughly half of the fluvial network through hiking and driving at study sites where sediment bottlenecks were identified in aerial imagery. We quantified confidence in comprehensive geospatial mapping of sediment bottlenecks for each watershed by examining the accuracy of remote mapping (*Table 3*). Fifty-five sediment bottlenecks mapped in aerial imagery were verified in the field, while 31 were newly mapped upon discovery in the field. Eighty-three sediment bottlenecks were mapped in aerial imagery, but were not observed in the field. Remote mapping was overinclusive to not miss any bottlenecks. Discrepancies between sediment bottlenecks observed in aerial imagery and the field may have occurred due to sediment bottleneck formation or deformation in the time between when imagery was collected and when the field was visited. Sediment bottlenecks initially mapped from imagery and verified in the field were on average 7000 m² greater than sediment bottlenecks that were discovered in the field, indicating that larger sediment bottlenecks were more successfully mapped in aerial imagery. This observation increases our certainty that we mapped the major sediment bottlenecks and majority of the sediment volume deposited within the fluvial network at each of our study sites.

Table 3 *Number of sediment bottlenecks at each study site that were field verified, field mapped only, and remote mapped but did not exist (only mapped in aerial imagery)*

Study Site	Remote Mapped Verified ¹	Field Mapped ²	Remote Mapped-not present in field ³
Brian Head	6	1	24
Clay Springs	8	1	5
Coal Hollow	8	5	1
Dollar Ridge	4	4	2
Pole Creek	4	1	7
Seeley	7	4	12
Shingle	3	1	5
Trail Mountain	1	0	2
Twitchell Canyon	11	6	18
West Valley	3	8	7
Total	55	31	83
Average Area (m²)	8011	1264	NA

¹*Sediment bottlenecks that were mapped in aerial imagery and confirmed in the field*

²*Sediment bottlenecks that were not mapped in aerial imagery, but mapped in the field*

³*Sediment bottlenecks that were remote mapped, but were not observed during our field visit*

4.1.3 Causes of Sediment Bottlenecks

The majority of sediment bottlenecks we encountered were formed by structural forcing. We classified four distinct types of structural forcing: debris flow deposits, beaver dams, wood jams and manmade structures (*Fig 4a*). Debris flow deposits and wood jams are two structural forcing mechanisms that can be caused or enhanced by wildfire. The remainder of sediment bottlenecks (24%) where no structural forcing was present were assumed to be caused by attributes of the valley bottom morphology (e.g., local decrease in slope, reduction in confinement) and are referred to hereon as non-structural controls. Woods jams were the most prevalent mechanism of formation for sediment bottlenecks; we identified 39 sediment bottlenecks caused by wood jams (*Fig. 4b*). Debris flow deposits trapped the greatest volume of sediment on average (5955 m³), while wood-forced sediment bottlenecks on average trapped 167 m³ (*Fig. 4c*). Summing total volumes for each mechanism across Utah, indicates debris flow deposits trap more

sediment by magnitude, even though wood-forced sediment bottlenecks are more prevalent (*Fig. 4d*).

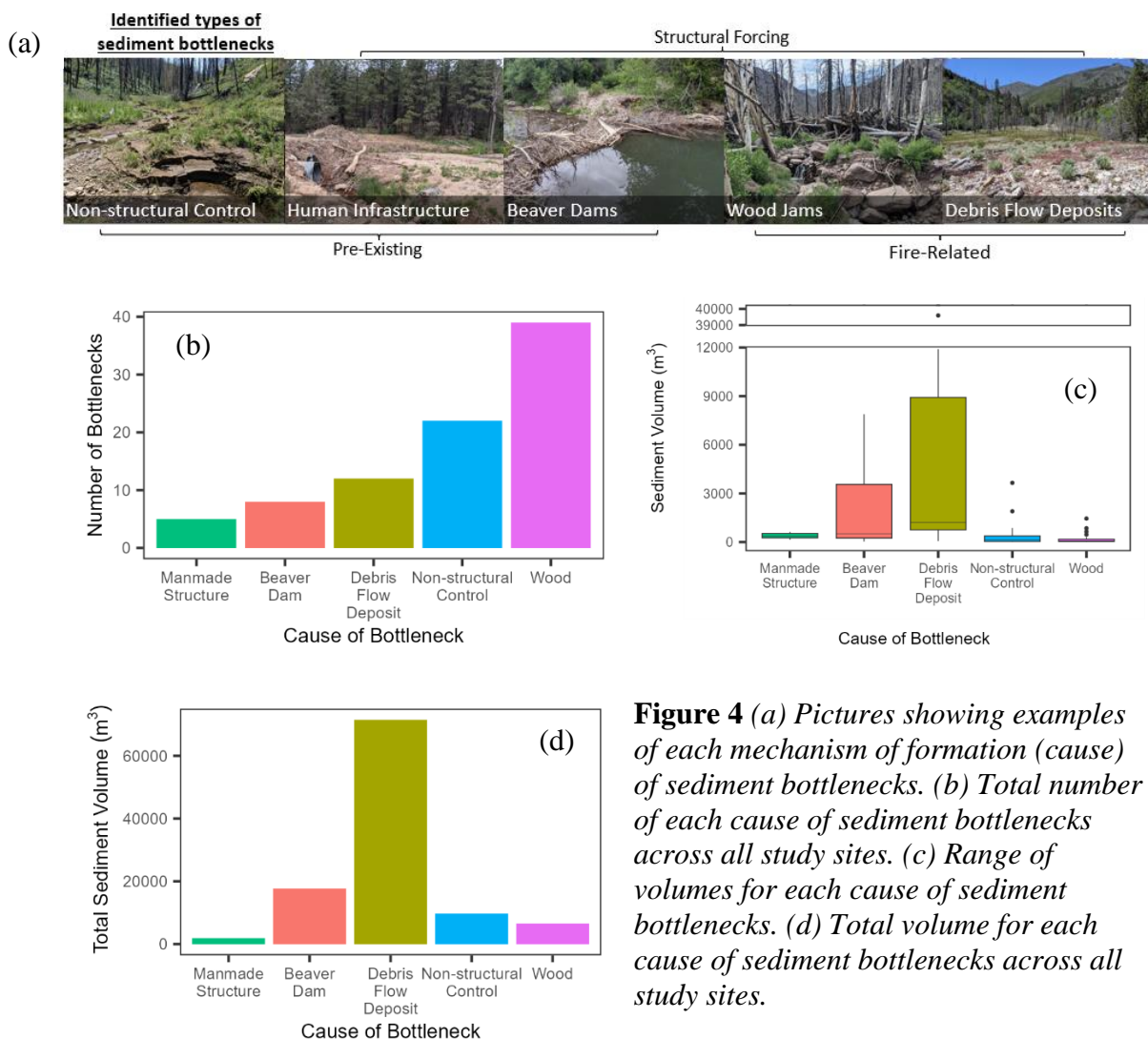


Figure 4 (a) Pictures showing examples of each mechanism of formation (cause) of sediment bottlenecks. (b) Total number of each cause of sediment bottlenecks across all study sites. (c) Range of volumes for each cause of sediment bottlenecks. (d) Total volume for each cause of sediment bottlenecks across all study sites.

4.1.4 Temporal Aspects of Sediment Bottlenecks

Through scanning aerial imagery of our sediment bottlenecks across different years, we were able to determine which bottlenecks formed after fire. We were able to ascertain that 49 of the sediment bottlenecks formed in the first set of imagery following the

occurrence of wildfire and several of these grew larger over time. We could not confirm the presence of 22 of the sediment bottlenecks due to canopy coverage. 15 of our sediment bottlenecks predated the fire, but in most of these cases the sediment deposit grew following the burn. 7 of our wood-forced sediment bottlenecks were not in the first set of imagery, but were in subsequent sets of imagery. We observed one wood-forced sediment bottleneck that was in the first set of imagery but later broke apart.

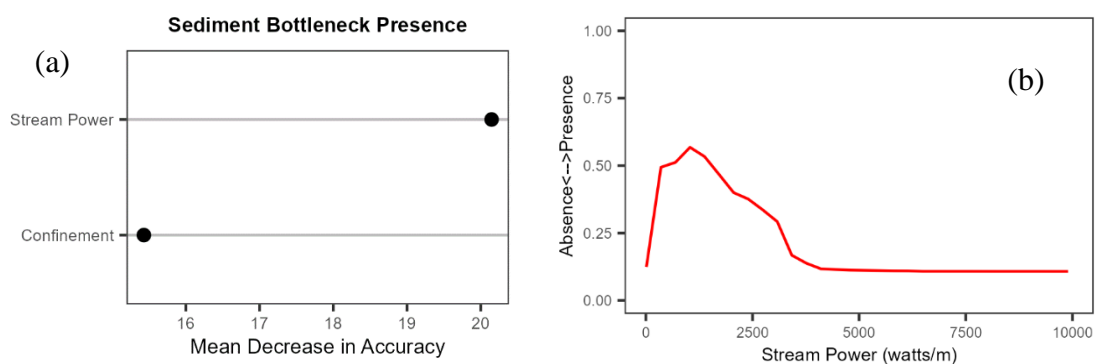
4.1.5 Prevalence of Sediment Bottlenecks

Linear correlation between the original metrics used to select study sites and prevalence of sediment bottlenecks was evaluated by calculating Pearson correlation coefficients (*Fig. E.1*). Sediment bottlenecks were most prevalent in fluvial networks that drained large wildfires where a large percentage of the fire burned at moderate to high severity. The percentage of the fire burned at moderate to high severity exhibited a Pearson correlation coefficient of 0.46 ($p=0.083$) with the amount of sediment bottlenecks at a study site. Percentage of slope greater than 23 degrees and percentage of pre-fire vegetation that was conifer had low correlation coefficients (~ 0.1), but trended positively with sediment bottlenecks amount, volume and density.

4.1.6 Locations of Sediment Bottlenecks

The locations of sediment bottlenecks were primarily influenced by stream power and confinement. After tuning our random forest classification of sediment bottleneck presence/absence ($n=158$), our model explained 36% of the variability with these two explanatory variables (*Fig. 6a*). Sediment bottlenecks typically occurred in locations

where stream power falls within the range of 500 and 1500 watts/m (*Fig. 6b*). Stream power was highest on average for sediment bottlenecks caused by debris flow deposits (1457 watts/m) and lowest for sediment bottlenecks caused by non-structural controls (654 watts/m). We analyzed our confinement values using a weighted generalized additive model ($n=1608$) and in the context of the categorical breaks developed by Fryirs et al., (2016) (*Fig. 6c*). These categorical breaks for confinement can represent the degree to which the channel abuts the valley bottom edge and the ability of the channel to adjust and access the floodplain. Planform controlled (10-50% confined) reaches had the highest probability of producing sediment bottlenecks, and the average confinement values for beaver dams, debris flow deposits and non-structural controls (17%, 35%, 23% respectively) fell into this range. There was a second lesser spike in sediment bottleneck presence in confined reaches (85-100% confined), which was mostly due to wood-forced sediment bottlenecks (*Fig. 6c*). Laterally unconfined (0-10% and margin-controlled reaches (50-85%) were equally likely to produce bottleneck presences and absences, but when a reach is constricted ($100% <$ confined), there is a sharp decline in bottleneck presences.



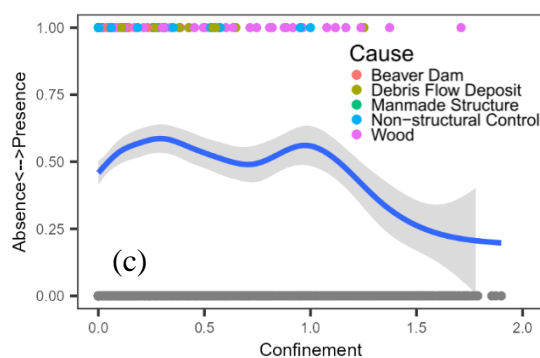


Figure 5 (a) Variable importance plot showing the top variables from the sediment bottleneck presence random forest classification model. (b) Partial dependence plot showing average marginal effect of stream power on the random forest classification model. Blue markers are rug indicators for important data points. (c) Generalized additive model fit of confinement values to presence (1) and absence (0) with sediment bottleneck presences symbolized by mechanism of formation, with the grey band representing the 95% confidence interval.

4.1.7 Volume of Sediment Bottlenecks

We conducted a random forest regression analysis to explore the extent to which our reach-based metrics can explain the volumes of sediment bottlenecks. For our 79 reaches the model was able to explain 44% of variance (*Fig. 7a*). Several reaches contained multiple sediment bottlenecks, in which case volumes were summed. Slope was the strongest explanatory variable for sediment bottleneck volume, throughout all iterations of model tuning (*Fig. 7b*). Lower slopes yielded greater volumes of sediment, with the largest break in volume occurring at 0.05 (*Fig. 7c*). Explanatory variables that represented sediment generation such as square kilometers of moderate/high severity burn draining upstream, volume of debris flow sediment delivered upstream and Upstream Conifer % were also important explanatory variables and trended positively with sediment bottleneck volume. We observed a strong break at 30 km² for contributing area burned at moderate and high severity (*Fig. 7d*). This break matches the threshold at

which debris flow volumes are delivered upstream. No debris flow volumes were delivered in contributing areas of only low severity. The change in slope between subsequent reaches contributed relatively little to model prediction, but its inclusion boosted model accuracy by 4%.

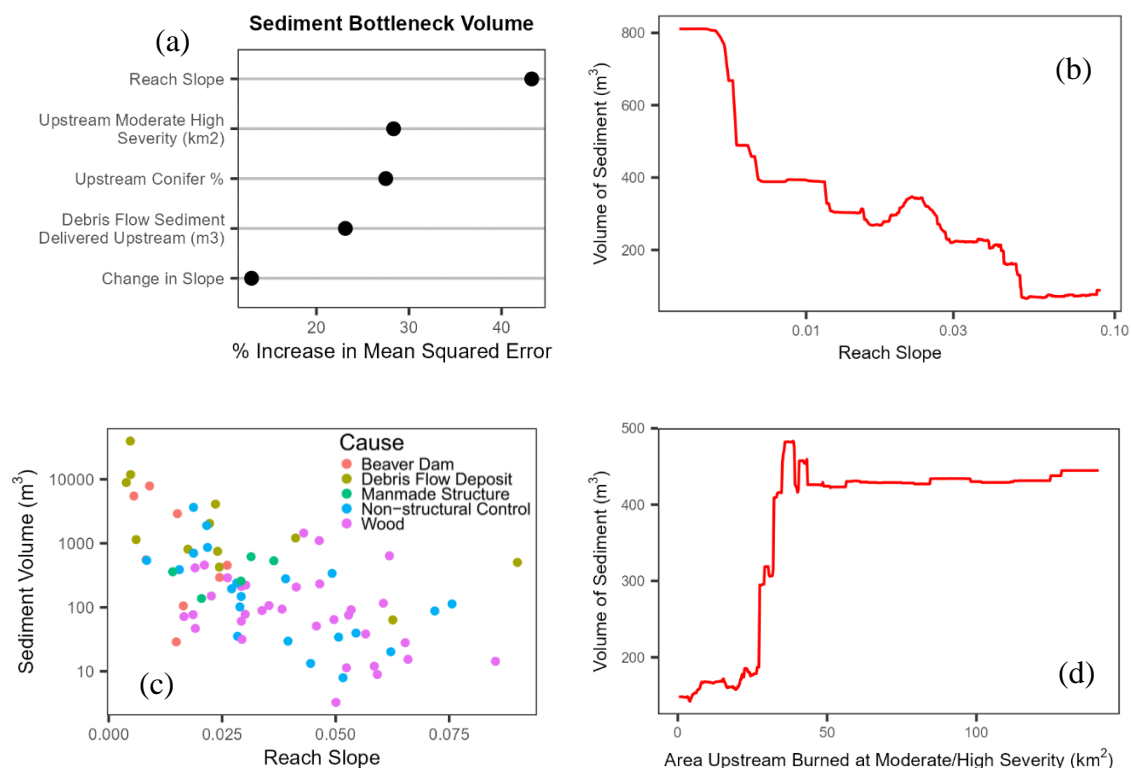
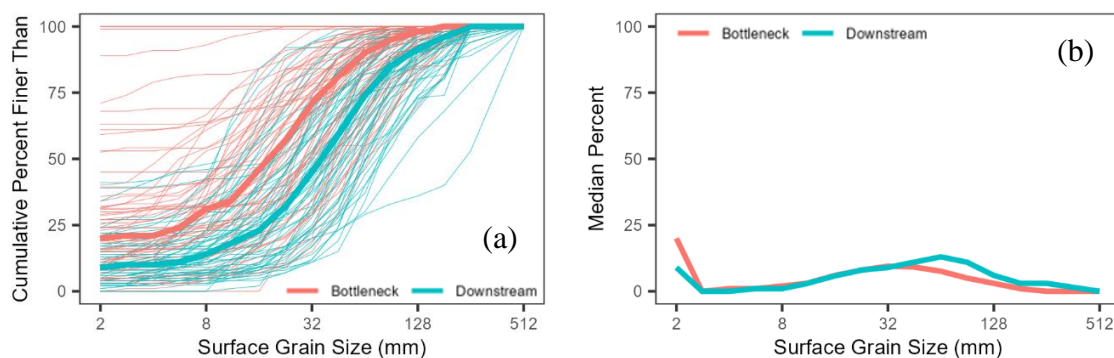


Figure 6 (a) Variable importance plot showing the top variables from the sediment bottleneck volume random forest regression model. (b) Partial dependence plot showing average marginal effect of stream slope on the random forest regression model. (c) Slope vs sediment volume at a log scale, symbolized by structural control (d) Partial dependence plot showing average marginal effect of contributing area (km²) burned at moderate high severity on the regression model.

4.1.8 Grain Sizes of Sediment Bottlenecks

We collected grain size data for 69 of the sediment bottlenecks as well as adjacent downstream reaches. Sediment bottlenecks exhibit a finer grain size distribution than downstream, with the greatest difference in cumulative distribution occurring at 32 mm

(Fig. 8a). When transformed to a probability density function, it is evident that sediment bottlenecks have more fines (2 mm) and less cobbles (64-128 mm) than reference conditions (Fig. 8b). Beaver dams have the finest median grain size 2 (mm), while wood jams have the coarsest D50 value (32 mm) (Fig. 8c). Sediment bottlenecks were coarser for fires that occurred longer ago (Fig. 8d). The median D50 value within the oldest fire (Twitchell Canyon) was 34 mm coarser than the median D50 value from the most recent fires in our dataset that occurred 4 years ago. We also normalized D50 values by modeled pre-fire grain size, but this did not affect our analysis of bottleneck type and age. Comparison of modeled pre-fire grain sizes to our post-fire sediment bottleneck measurements indicates an overall fining of the streambed (Fig. 8e). Only one bottleneck had a D50 value coarser than the modeled pre-fire grain size. Downstream D50 values were more similar to modeled pre-fire D50 values, but were on average still finer.



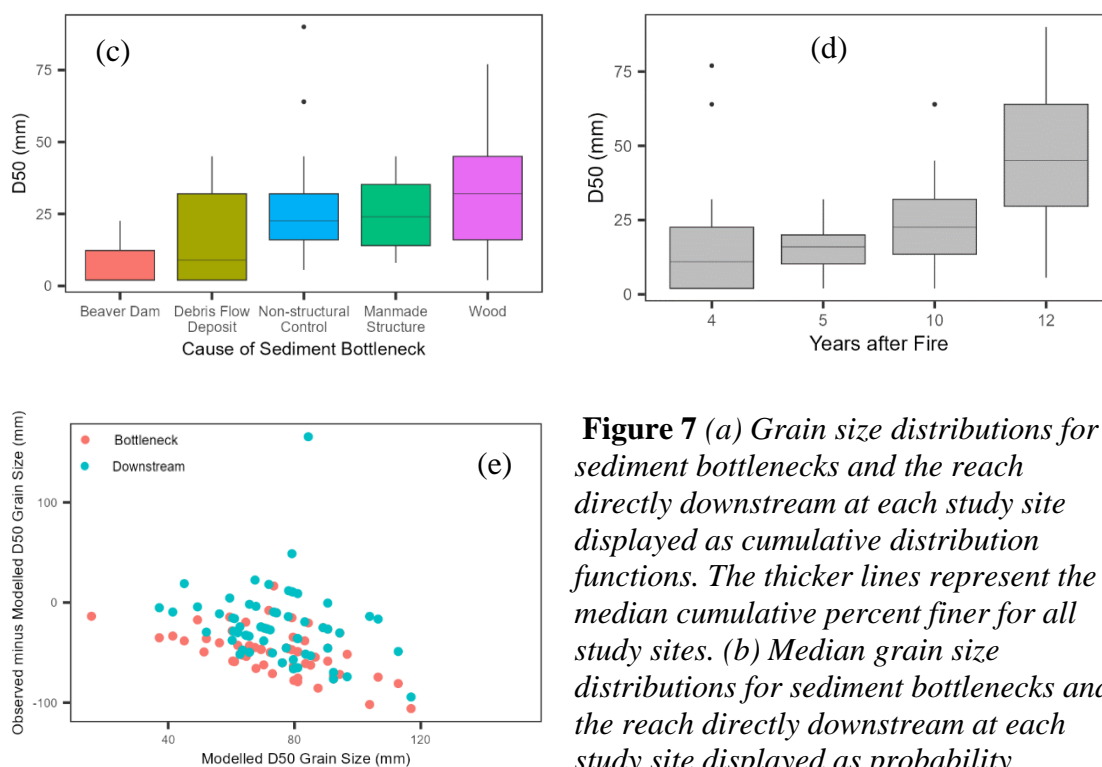


Figure 7 (a) Grain size distributions for sediment bottlenecks and the reach directly downstream at each study site displayed as cumulative distribution functions. The thicker lines represent the median cumulative percent finer for all study sites. (b) Median grain size distributions for sediment bottlenecks and the reach directly downstream at each study site displayed as probability distribution functions. (c) Bottleneck D50 grain size versus sediment bottleneck cause. (d) Bottleneck D50 grain size versus how many years after the fire the grain size measurements were taken. (e) Modeled D50 grain size versus the absolute change between measured bottleneck and downstream D50 grain sizes (representing post-fire conditions) and modeled D50 grain size (representing pre-fire conditions).

4.2 Impacts of Post-fire Debris Dynamics on Sediment Bottlenecks

4.2.1 Large Wood Dataset

Our dataset of large wood is comprised of individual pieces of wood and wood jams across 7 of our study sites, Brian Head, Clay Springs, Dollar Ridge, Seeley, Shingle, Twitchell Canyon, and West Valley fires. Across each of these fires we measured 24,453 pieces of wood, of which 73% were stored in wood jams, rafts and racks. Wood densities

within reaches ranged from 0.12 m³/ha to 742 m³/ha, with 81 of 449 reaches having no wood present. Between fires, average wood density ranged from 2 m³/ha within the Clay Springs fire to 93 m³/ha within the Twitchell Canyon and West Valley fires (*Table G.1*). 63% of the wood was stored in floodplain, while the other 37% intersected the channel in some capacity. Only 5% of features spanned the channel, with wood jams more likely to span the channel than individual pieces. 67% of the wood appeared to have undergone fluvial transport. The average jam size was 26 m³ and average dimensions for individual pieces were a length of 6.5 m, with an average diameter of 37 cm.

4.2.2 Calibration and Uncertainty in Remote Wood Mapping

We evaluated systemic error as well as mapper bias in wood mapping by comparing field mapped transects against remote mapped transects (*Fig. D.1.a/D.1.b*). Three personnel who contributed to development of the wood dataset digitized wood features along the 16 field transects using the 2021 Hexagon imagery. Volumes for two of the transects (#4 and #13) were underestimated, because of shadows diminishing image quality and from dense canopy cover. A third reach (#2) had inflated volume estimates because of many pieces of wood that were just below the 20 cm diameter cutoff were included in jams, increasing the area. When excluding these three transects with low accuracy, two of our mappers achieved a 0.5 R². The third mapper had inflated volumes for all transects, because too many individual pieces were being digitized as wood jams and porosity values were too low. With this knowledge of mapper bias, we recalibrated and edited affected features. Although volumes are marginally accurate, we have confidence that their values relative to each other are sufficiently representative to perform random forest regression.

4.2.3 Density of Large Wood

We used random forest regression to explore attributes that help explain where wood is stored within fluvial networks. Density is a standard metric for determining wood loads and is calculated by dividing wood volume by the area of the valley bottom at the reach scale. Our model was able explain 63% of the variability across 449 reaches (*Fig. 9a*). Upstream vegetation cover and % upstream conifer cover were two of the top variables, indicating that wood density is mainly controlled by the land cover from the contributing upstream area. Aspen-conifer forests, ponderosa pine and riparian areas represent upstream cover classes that increase wood density, while pinyon-juniper forests, grasslands, rangelands and mix conifer watersheds produce a much lower density of wood (*Fig. 9b*). It is important to note that reaches with upstream aspen and conifer cover make up 76% of the data points. Similarly, % upstream conifer trends positively with wood density (*Fig. 9e*). Valley bottom width was also an important variable in predicting wood density and generally displayed a negative relationship (*Fig. 9d*). Wood density was highest in valley bottoms between 30 and 45 m wide and sharply dropped off at 115 m wide (*Fig. 9c*).

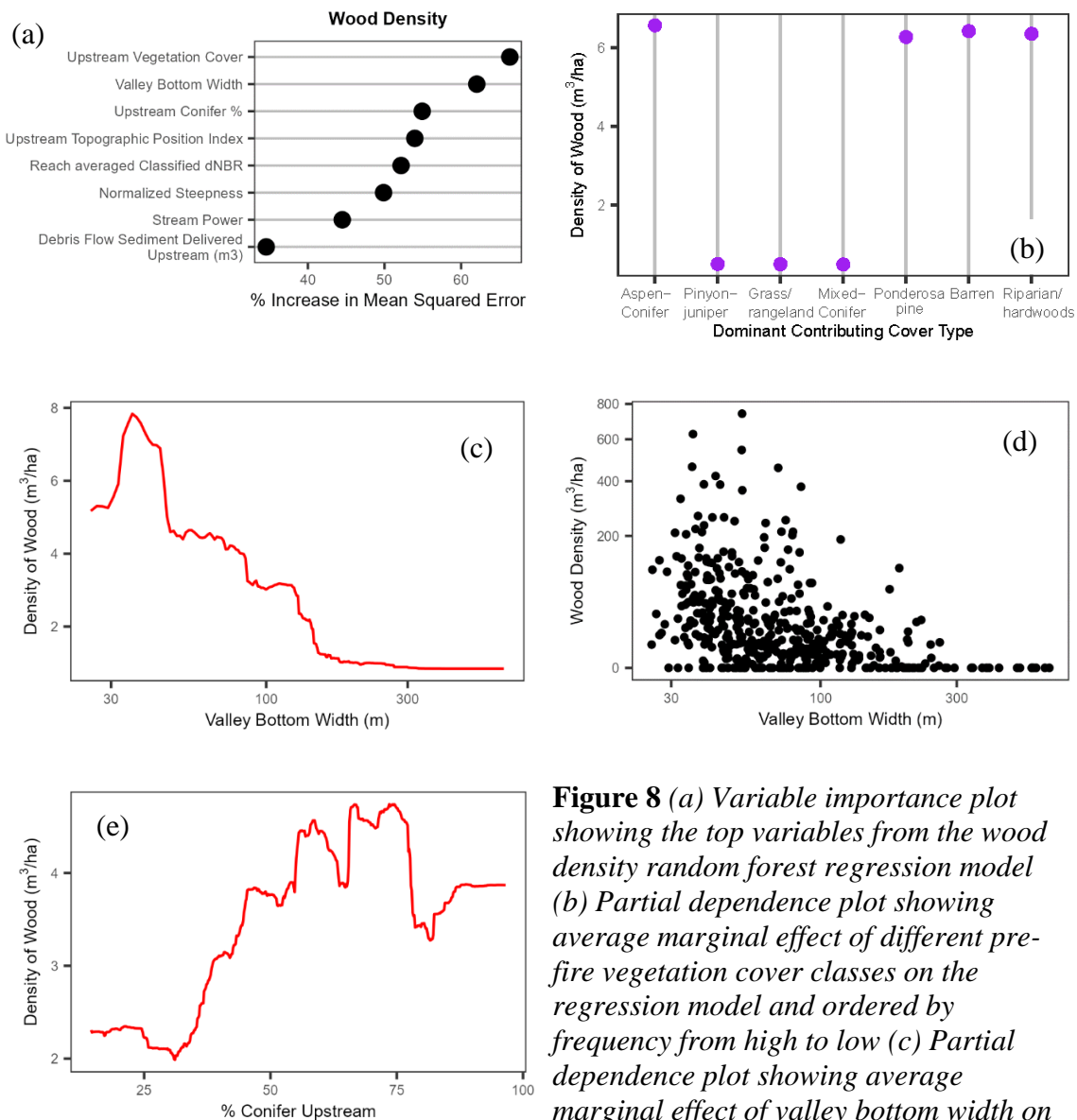


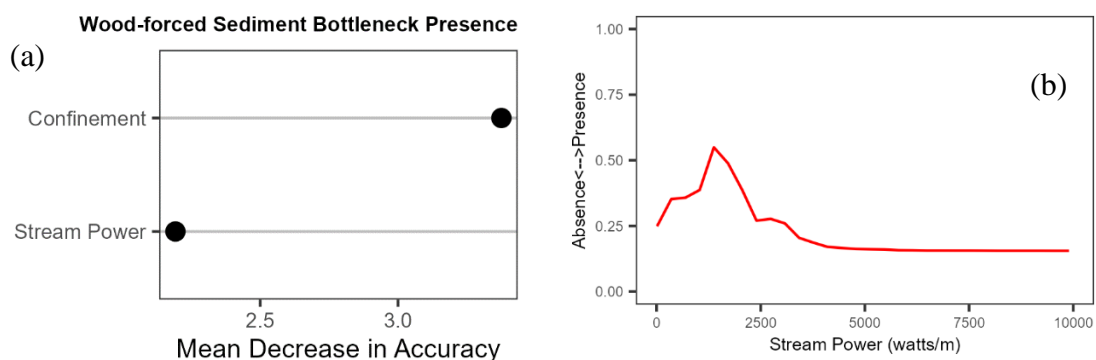
Figure 8 (a) Variable importance plot showing the top variables from the wood density random forest regression model (b) Partial dependence plot showing average marginal effect of different pre-fire vegetation cover classes on the regression model and ordered by frequency from high to low (c) Partial dependence plot showing average marginal effect of valley bottom width on the regression model (d) Valley bottom width vs wood density at a log scale (e) Partial dependence plot showing average marginal effect of % conifer upstream on the regression model

4.2.4 Impacts of Large Wood on Sediment Bottlenecks

Our random forest classification on the presence of only wood-forced sediment bottlenecks again yields stream power and confinement as the most important

explanatory variables (*Fig. 10a*). However, the relative importance of these two variables switches, with confinement now as the most important variable. Sediment bottlenecks caused by wood are most likely to occur in areas with a confinement value of 0.85, which is typically the threshold at which a valley bottom is considered to transition from margin controlled to confined (O'Brien et al., 2019) (*Fig. 10b*). Stream power values at which wood-forced sediment bottlenecks occur are similar to the range observed for all sediment bottlenecks (*Fig. 10c*).

Our measurements of wood and respective sediment volumes showed that the volume of wood generally scales proportionally with sediment volume. The large wood particulate storage index (LWPSI), which represents the volume ratio of wood to sediment (Pfeiffer & Wohl, 2018), varies between wood jams of different volumes (*Table G.2*). All wood-forced sediment bottlenecks were caused by wood jams occurring in reaches where the individual piece length was between half and 3 times the channel width. We only observed two sites where in-channel wood jams did not span the whole channel, and these sites trapped smaller than average volumes of sediment.



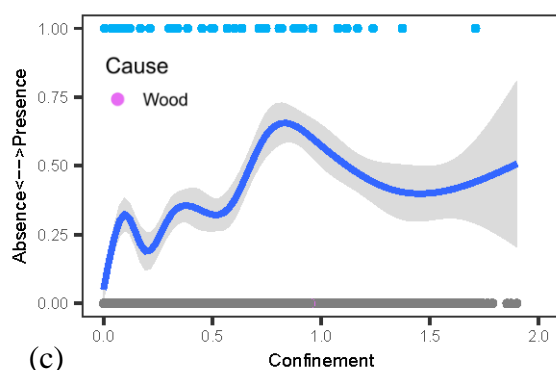


Figure 9 (a) Variable importance plot showing the top variables from the wood sediment bottleneck presence random forest classification model. (b) Partial dependence plot showing average marginal effect of stream power on the random forest classification model. Blue markers are rug indicators for important data points. (c) Generalized additive model fit of confinement values to presence (1) and absence (0) of wood-forced sediment bottlenecks, with the grey band representing the 95% confidence interval.

4.2.5 Debris Flow Deposits Dataset

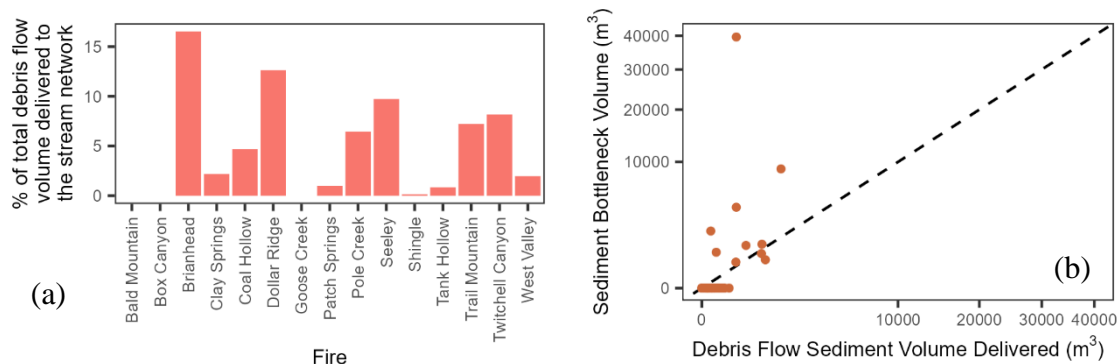
We used the debris flow deposit dataset we compiled for each fire to understand how debris flow dynamics impact sediment bottlenecks. Our dataset consists of 947 debris flow deposits which total 1.3 million m^3 of sediment. Debris flow deposits ranged in size from 8 to 42,785 m^3 , with the median size being 582 m^3 . Only 208 reaches out of 1608 had debris flow sediment delivered to the stream channel. The volume of sediment delivered to the channel was 43,915 m^3 or 3.4% of the total debris flow deposit volume (Fig. 11a). While Dollar Ridge had the most debris flow deposit sediment (57482 m^3), Brian Head delivered the greatest proportion to the stream network (17%).

4.2.6 Impacts of Debris Flows on Sediment Bottlenecks

We evaluated debris flow impacts on sediment bottlenecks through sediment contribution as well as channel blockage. Debris flow deposits trapped more sediment than other structural forcing mechanisms, but were also frequently the main source of

sediment in watersheds after wildfire. Total sediment bottleneck volume correlated positively with total debris flow deposit sediment at the reach scale. Most sediment bottlenecks caused by debris flow deposits trapped more fluvial sediment than the debris flow itself delivered to the channel (*Fig. 11b*). However, most of our study sites delivered more debris flow sediment in total than the amount of fluvial sediment trapped behind debris fans (*Fig. 11c*). The exceptions were Twitchell Canyon and West Valley fires, which each experienced an extremely large debris flow deposit in a narrow valley bottom, resulting in sediment accumulating five meters deep upstream of the fan.

We were curious which basins would produce debris flow deposits that would cause sediment bottlenecks to form. We considered the Network Dynamics Hypothesis (Benda et al., 2004) in our analysis, which considers the influence of tributary confluences. We found a significant difference between basins using the product of distal tributary area and slope (Rice, 2017) (*Fig. 11d*). Basins with a greater magnitude of impact, represented by this variable, were more likely to produce debris flow deposits that attenuated sediment.



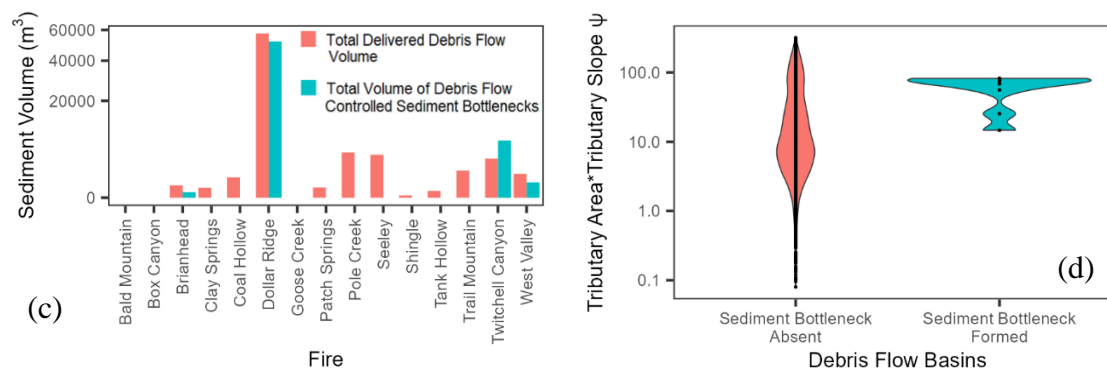


Figure 10 (a) Percent of total debris flow deposit volume delivered to the stream network across all fires (b) Volume of sediment delivered to the stream network by debris flow deposit versus sediment bottleneck volume caused by that debris flow deposit, with the dashed line representing a 1:1 ratio (c) Total debris flow deposit volume delivered to the stream network versus total sediment bottleneck volume caused by debris flow (d) Violin plots of debris flow deposit forced sediment bottlenecks versus Ψ , a variable developed by (Rice, 2017) that represents the product of the debris flow basin area and its slope

5 Discussion

5.1 Controls on Sediment Bottlenecks

5.1.1 Sediment Bottleneck dataset

Our sediment bottleneck dataset is the most extensive empirically mapped fluvial deposit dataset after wildfire that we are aware of. It is one of the few studies conducted on sediment connectivity after wildfire that compares multiple watersheds. In addition, our study is on greater scale than the majority of other studies focused on sediment connectivity after wildfire. The largest watersheds in our sample pool approach 2000 km² while most other studies focus on areas less than 15 km² (González-Romero et al., 2021; Nyman et al., 2020; Rengers et al., 2021; Wilson et al., 2021). Our dataset was able to be so extensive because of initial mapping through aerial imagery. The combination of recent higher resolution aerial imagery and a lack of canopy following wildfire allowed

us to identify locations of many sediment bottlenecks remotely before visiting them for measurement.

5.1.2 Temporal Aspects of Sediment Bottlenecks

In evaluating the temporal aspects of our sediment bottlenecks, our findings suggest that sediment bottlenecks and the wood jams and debris flow deposits that caused them originated due to wildfire, but were not necessarily static over time. We found that majority of our sediment bottlenecks occurred in the first set of imagery following wildfire, leading us to believe that fire caused many of our sediment bottlenecks to form. In addition, many debris flow deposits and wood jams that caused sediment bottlenecks appeared immediately after fire. However, a few debris flow deposits were redeposited and therefore can subsequently deliver additional sediment to the stream network and fortify debris flow deposit-forced sediment bottlenecks. Esposito et al., (2023) found that 27% of their 113 post-fire debris flow deposits have secondary deposition events, with one catchment experiencing up to 4 events. We also observed new wood jams formed in latter sets of imagery demonstrating the lingering impacts of wildfire. While trees may perish immediately during the wildfire, roots take several years to decay and there may be a lag in recruitment to the fluvial network (De Graff, 2018; Iskin & Wohl, 2021).

We mapped our sediment bottlenecks at a single point in time, with 3-12 years having passed since the watershed burned. In aerial imagery we noted that some sediment bottlenecks grew or shrank in size. We hypothesize that all of our sediment bottlenecks were in different phases of their lifespan. Several of our sediment bottlenecks were still aggrading, or had caused the channel to avulse, while others had begun to incise as part

of the cut and fill cycles that occur following disturbance (K. A. Fryirs & Brierley, 2013). While we only observed one sediment bottleneck that formed and deformed within our sets of aerial imagery, it is possible that sediment bottlenecks within our study sites existed between sets of aerial imagery. Wood jams and beaver dams can be more susceptible to failure (Macfarlane et al., 2017; Wohl & Scamardo, 2021), while reaches above tributary confluences or with amenable valley bottom morphology can store sediment for decades (Gran & Czuba, 2017). More continuous monitoring of sediment bottleneck sites over longer timespans is needed to fully understand the evolution and longevity of sediment bottlenecks after wildfire.

5.1.3 Causes of Sediment Bottlenecks

The majority of sediment bottlenecks we mapped in post-fire fluvial networks were caused by structural controls. Features such as beaver dams, debris flow deposits, manmade structures and wood jams established local base level controls and/or physically obstructed sediment. Wood jams were the most common type of structural control, but because they were mostly located in steeper, more confined upstream reaches, they also trapped the least sediment on average. Debris flow deposits exerted the greatest impact on the volume of sediment bottlenecks. Many of these debris flow deposits redeposited on top of existing debris fans, supporting that these tributary junctions exert long-standing controls on the bed elevation of the fluvial network. We also observed beaver dams and wood jams trapping sediment above tributary junctions. Macfarlane et al., (2017) developed the BRAT model to predict the capacity of stream reaches to support beaver dams across Utah. Sediment bottlenecks caused by beaver

dams corresponded with locations where the BRAT model predicted “frequent” beaver dams (the second highest tier) to occur. Areas within our stream networks with “pervasive” beaver dams were observed at our study sites to have such a high density of beaver dams, that sediment wasn’t being transported into them. There were several man-made structures that caused sediment bottlenecks to form including culverts, bridge piers and an old retaining wall. More frequently however, we observed instances of man-made structures being washed out, or damaged.

5.1.4 Sediment Bottleneck Prevalence

All of our original predictor variables for our study sites trended positively with the prevalence of sediment bottlenecks, but % moderate/high burn severity clearly showed the strongest linear correlation. Moderate/high burn severity is a key variable in explaining sediment generation and debris flow likelihood after wildfire (Cannon et al., 2010; Staley et al., 2017), which are the sources for the production of sediment bottlenecks. At sites burned less severely, such as Box Canyon and Tank Hollow we observed less rilling and debris flow deposits and largely unimpacted channels. We hypothesized % of slope greater than 23° to be an important variable in predicting debris flow generation and therefore prevalence, but we observed only a weak correlation. We suspect the relationship between slope and sediment bottlenecks is more complex than a linear function. Extremely steep study sites such as Patch Springs and Trail Mountain generated debris flow deposits, but almost all sediment was exported out of their watersheds because of consistently high longitudinal connectivity. Flatter sites such as Goose Creek and Brian Head lacked sediment delivery to the channel network. Much of

the fluvial network in Brian Head was buffered from high severity fire by upland meadows created by the underlying volcanic lithology (Wilson et al., 2021). Conifer cover, which we initially chose as a surrogate for wood generation and therefore wood forced sediment bottlenecks also did not correlate as strongly as we expected. This is likely because conifer cover includes more arid forest types such as pinyon-juniper and mixed conifer we observed to burn at a lower severity. Although these arid environments have higher runoff-ratios and erosion in general, post-disturbance runoff ratios in these areas are less affected than in wetter environments (Goeking & Tarboton, 2022; Van der Sant et al., 2018).

5.1.5 Sediment Bottleneck Presence

Valley bottom morphologic explanatory variables were the strongest indicators of locations where a sediment bottleneck would occur within the fluvial network. Stream power between 500 watts/m and 1500 watts/m appears to be the strongest predictor of a sediment bottleneck being present in a reach. Stream power values lower than this range likely weren't able to fluvially transport sediment into the reach and higher stream power reaches likely transported sediment through or eroded local base level controls. Stream power has been shown to be the strongest predictor of where sediment transport and deposition will occur in many studies (D'Haen et al., 2013; Kuo & Brierley, 2013; Rengers et al., 2021; Taylor & Kite, 2006). Confinement also controls in which reaches sediment bottlenecks will occur. Planform controlled reaches were most likely to host sediment bottlenecks, except those caused by wood, which were mainly present in confined reaches. Sediment bottlenecks were not located in reaches that were constricted

(where the channel abuts both sides of the valley bottom), because confinement tends to increase transport capacity (Montgomery & Buffington, 1997). Conversely, laterally unconfined reaches also had decreased likelihood of sediment bottlenecks, likely because these reaches have lower lateral and longitudinal connectivity of sediment.

5.1.6 Sediment Bottleneck Volume

Reach slope was the strongest predictor of sediment bottleneck volume, and is therefore the primary control on the amount of fluvial sediment that deposits in a reach. Lower sediment transport capacity in low slope reaches tends to cause deposition in locations with high sediment supply. A smaller scale study (6 km²) focused on debris flow sediment in southern California had similar findings (Rengers et al., 2021). They found that sediment yield correlated with slope, while sediment deposition was inversely correlated. The remaining significant explanatory variables: contributing area of moderate/high burn severity, volume of debris flow deposit sediment delivered upstream, and % conifer, link the amount of sediment generated in the watershed to the amount of sediment that will be deposited downstream. Wall et al., (2022) showed that contributing area at moderate/high burn severity and soil organic matter can be used to calculate debris flow deposit volume, suggesting that these explanatory variables can signal excess sediment generation in these reaches.

We find these controls on sediment bottleneck volume similar to inputs used in sediment transport models. Slope is the primary determinant for sediment transport in the CASCADE and NST models within each individual reach (J. Czuba, 2018; Schmitt et al., 2016). Shear stress or unit stream power would more accurately represent sediment

transport, however the channel dimensions needed for these calculations cannot reliably be extracted from DEMs (Keck et al., 2022; Macfarlane et al., 2017).

In the FireWATER model, which specifically predicts post-wildfire sediment dynamics, debris flows are used as sediment inputs and sediment is routed based on reach slope. Discharge, in addition to slope is included in stream power, which is the primary control on sediment bottleneck location. These debris flow inputs and discharge are scaled using burn severity, which impacts the sediment generation and hydrology. While there is no acknowledgement of wood, culverts or beaver dams into the FireWATER model, the model adjusts slope based on debris flow inputs, which can have the largest influence on sediment connectivity (Murphy et. al, 2024). Our results support the process used to model sediment transport in fluvial networks after wildfire.

5.1.7 Sediment Bottleneck Grain Sizes

The grain size distributions we attained through field measurements and modeling indicate that sediment bottlenecks have geomorphically distinct grain sizes from reference reaches and pre-fire grain size. Specifically, our findings suggest that there is an influx of fine sediment after wildfire and a decrease in cobbles on the bed surface. Cobbles provide interstitial space for macroinvertebrates important in fish diets, while fine sediments fill these spaces and increase embeddedness (Jones et al., 2012). Nevertheless, sediment bottlenecks diversify stream reaches and networks through differing grain size distributions upstream and downstream of the sediment bottleneck (Flitcroft et al., 2016; Jager et al., 2021). In addition, the structural controls that cause

sediment bottlenecks can provide habitat through the pools, cover and spatial heterogeneity they create (N. Bouwes et al., 2011; Seixas et al., 2020; Wohl et al., 2022).

Beaver dams were found to be the most effective sediment bottleneck cause, as they trap the finest grained sediment moving through the fluvial system. Beaver dams have been shown in other studies to increase resiliency to wildfire and to decrease connectivity (Fairfax & Whittle, 2020; Wohl et al., 2017), because of their ability to force backwaters. If valley bottom morphology allows, introducing beaver to fluvial networks can prepare watersheds for the catastrophic sedimentation and enhanced connectivity following wildfire.

The median grain size in sediment bottlenecks correlated positively with the years since fire, suggesting that sediment bottlenecks coarsen over time. Fine sediments are stored within sediment bottlenecks within the fluvial network after wildfire and then are remobilized over time as the channel profile adjusts. In older fires we observed armoring, consistent with Murphy et al. (2019). Two of our sites experienced severe summer thunderstorms while visiting and we noted substantial pockets of fines following each event. We hypothesize that shorter duration summer thunderstorms can deliver fine sediment to the fluvial network, while sustained spring runoff will clear the network of existing fine sediment. This would suggest that surface grain size distributions might fluctuate throughout the year, which is a potential avenue for future research.

5.1.8 What controls sediment bottlenecks after wildfire?

Overall, we see that sediment bottleneck prevalence is associated with higher severity fire. Without significantly increased sediment generation, it is unlikely sediment

bottlenecks will form. Our findings indicate that while many sediment bottlenecks in burned watersheds are caused by structural controls, valley bottom morphology is the primary determinant of where sediment deposition will occur. Specifically, we identify stream power between 500 and 1500 watts/m as the leading control on the locations of sediment bottlenecks. Lower stream power was more important in predicting sediment bottlenecks without structural controls, while structurally controlled bottlenecks occurred in a wider range of stream power values. Confinement was a secondary predictor of sediment bottleneck occurrence, with wood forced sediment bottlenecks likely to occur in confined reaches and all other types likely to occur in planform-controlled reaches. These locations scale in volume with slope and upstream sediment generation. Sediment bottlenecks host finer sediment than surrounding reaches and pre-fire conditions that likely will coarsen over time as sediment moves through the system.

5.2 Impacts of Post-fire Debris Flow Deposits and Wood Dynamics on Sediment Bottlenecks

5.2.1 Wood Dynamics

We find that large in-stream wood metrics for our dataset corroborate existing literature on wood loads after wildfire. Our wood densities fall within a similar range compared to other studies, based on their forest types, aridity and burned condition (Iskin & Wohl, 2021; Welling et al., 2021; Wohl, 2020). 73% of wood was stored in jams, supporting the aggregational nature of channels impacted by disturbance (Wohl & Scamardo, 2021). Additionally, most of our wood was found in the floodplain, which was

found in other studies to be caused by increased in-situ recruitment following wildfire (Wohl, Cadol, et al., 2018).

Factors controlling where sediment and wood are stored within fluvial networks were shown to differ through our random forest analysis. Variables that represent wood generation including cover type and % conifer upstream were found to be most significant in predicting wood density, which parallels key variables for predicting sediment bottleneck volume. This relationship corroborates existing literature supporting increasing wood loads with increasing forest primary productivity (Iskin & Wohl, 2021; Wohl, 2020). Density of wood was also influenced by valley bottom width. Wood density was highest in valley bottoms between 8 and 16 m wide, with density sharply dropping off at 32 m wide. Eight meters is slightly greater than the average individual piece length we measured. Valley bottoms greater than 32 meters may represent wet meadows at higher elevations or a transition to lower elevation and more arid basins. Elevated recruitment and transport following wildfire may also explain why narrower valley bottoms housed more wood (Wohl, Cadol, et al., 2018). Initial spikes in tree mortality drive in situ and colluvial recruitment to the floodplain (Iskin & Wohl, 2021), however downstream where the valley bottom and channel width become wider, fluvial transport capacity of large wood increases, especially with higher flows after wildfire (Wohl & Scott, 2017). We do not know the extent to which our spatial patterns of wood were caused by wildfire, as this is the first fluvial large wood dataset within Utah and we do not have baseline measurements.

5.2.2 Wood and Sediment Bottlenecks

We analyzed specifically where wood-forced sediment bottlenecks occur within the fluvial network. In narrowing the presence of sediment bottlenecks to only those caused by wood in our random forest classification, we observed a switch in the importance of confinement and stream power. This observation demonstrates the importance of the controls on wood in predicting where wood is able to trap sediment. Stream power is still an important control, but the range shifts slightly up from the original random forest classification to reflect the steeper slopes present in confined headwater reaches. [Wohl et al., \(2022\)](#) found reaches in a burned catchment in Colorado with a greater floodplain to channel ratio promote sediment trapping wood jams. This contradicts our findings that wood jams trapping sediment occurred in reaches that were more confined. However, their study focused on retention instead of creation of wood jams and the resolution of our studies was also different (40 km² vs 1000 km²). The majority of our wood-forced sediment bottlenecks occurred at the scale of their study (40 km²), suggesting that their entire study area may be confined relative to reaches downstream. Many of our wood jams and their respective sediment volumes were larger than we found in the literature (Welling et al., 2021; Wohl et al., 2022). However, our observed density of wood features trapping sediment was decreased compared to nearby reference reaches and the literature. This suggests that similar amounts of sediment trapped by wood may be present in burned and unburned fluvial systems or at least that there is no evidence of significant differences in sediment storage.

5.2.3 Debris Flow Deposits and Sediment Bottlenecks

Our results show that debris flow deposits create the largest sediment bottlenecks, often trapping more sediment than is actually contained within the debris flow deposit itself. The impacts of confluences are amplified following disturbance, because tributary junctions have elevated base level controls caused by debris flow deposits (Benda et al., 2004). The most geomorphically significant confluences are those that produce the greatest morphologic effects and those that are likely to produce sediment bottlenecks. In a wildfire context, this depends on the debris flow deposit volume generated by a tributary and the ability of that debris flow deposit to block the channel (Finnegan et al., 2019). These concepts can be represented by ψ (product of tributary basin area and distal tributary slope) which differentiates which debris flow deposits will cause sediment bottlenecks in our dataset (Rice, 1998; Rice, 2017). However, most watersheds with debris flow deposits deliver more sediment than they trap, because there are many debris flow deposits that do not cause sediment bottlenecks. This suggests that debris flow deposits are more important in generating sediment than forming sediment bottlenecks.

5.2.4 How do post-fire debris flow and wood dynamics influence sediment bottlenecks?

Our field observations clearly showed that post-fire debris flow and wood dynamics are increased following wildfire, and they are the greatest contributors to the presence and volume of sediment bottlenecks. However, there is little evidence in our results that post-fire wood jams and debris flow deposits increase the volume of sediment stored compared to the pre-fire watershed. Large wood recruitment to the stream channel increases, but elevated flows dislodge existing jams and allow for increased fluvial

transport. While wood jams may attain larger sizes than in pre-fire fluvial networks, they may occur at lower densities in the channel and many may occur within the floodplain (Wohl, Cadol, et al., 2018). Large jams in the channel exhibit similar LWPSI's to smaller jams and those in unburned environments and so although they trap greater volumes of sediment we cannot say whether wood traps more sediment than in pre-fire conditions (Pfeiffer & Wohl, 2018). Certain debris flow deposits can cause large breaks in sediment connectivity, and can trap more sediment than they generate. Overall though, debris flows are greater generators of sediment and their presence leads to a net increase in sediment being transported versus stored.

Locations of wood and debris flow deposit forced sediment bottlenecks after wildfire rely heavily on where they are generated within watersheds. Sediment bottlenecks caused by wood jams are found in more confined reaches with high wood generation, because that is where wood is most likely to be stored. Sediment trapped by wood, like other types of sediment bottlenecks, still depends on stream power, but is more heavily influenced by the domain in which wood can be functional. Functional is a term developed by Vaz et al., (2013) to describe large wood that interacts with the stream channel and modifies hydraulics and sediment transport. We found wood to be most functional in our headwaters (5-10 km²), where it was a frequent control on sediment. Debris flow deposits can create sediment bottlenecks from basins that have a high magnitude of delivery to the channel. This means that greater volumes of debris flow deposits in proximity to the channel will form sediment bottlenecks.

5.4 Limitations/Uncertainty

We caution that there are limitations from deriving our sediment, wood and debris flow deposit datasets from aerial imagery and our explanatory variables from DEMs and other remotely sensed data. While high resolution raster datasets of aerial imagery and topography are recent advancements that have improved remote modelling and mapping capabilities of landscapes, there is still uncertainty surrounding these datasets. We recognize that our interpretation of fluvial geomorphology and comparison of watersheds from remotely sourced data is imperfect and requires calibration. We discuss the uncertainty and quality control associated with linking the desktop to the landscape for each of our datasets and derivation of our explanatory variables below.

5.4.1 Sediment Bottleneck Identification

Sediment bottleneck identification was confounded by areas of scour and debris flow deposits present in post-fire environments which can also display in aerial imagery as unvegetated swaths of sediment. Initial field visits compensated for difficulties in differentiation through overmapping of remotely mapped sediment bottlenecks. Through subsequent field visits, the number of sediment bottlenecks discovered decreased, signaling successful calibration of mapping sediment bottlenecks in aerial imagery (*Table E.2*). Another challenge was that recent imagery was not available for all sites and sediment bottlenecks may have formed or dissipated in the time since the imagery was acquired. We were more successful in mapping larger sediment bottlenecks, which are more easily identified in remotely sensed data, less likely to be covered by riparian vegetation, and may have greater longevity. Understanding how long the life of a

sediment bottleneck is and how sediment transport dynamics within sediment bottlenecks change over time is critical for our understanding of connectivity and is a promising area of future research.

5.4.2 Development of Explanatory Variables

Our explanatory variables were limited by the resolution of the digital elevation models and the accuracy of the tools we used. One of our largest potential sources of error was our estimation of channel width. Bankfull widths can vary widely over relatively short distances along the channel and this variation is not represented in our power function between channel width and drainage area. We considered using existing channel width power functions (Beechie & Imaki, 2014; Wilkerson et al., 2014), but because Utah watersheds are more arid than the rest of the U.S. and artificial water withdrawals are common, these models tend to overestimate channel widths at larger drainage areas. Our delineation of valley bottoms was most accurate in confined or constricted reaches, but introduction of alluvial fans, roads and artificial embankments made determining valley bottom extent more difficult (*Fig. C.1*). While alternatives, such as VBET (Gilbert et al., 2016) exist, we recommend manual editing of any valley bottom delineation tool. Uncertainty in other variables was increased by the error and resolution of our 10m DEM. For example, delineation of our stream network and valley bottom each had an error of up to 5 meters, which could greatly influence our calculation of confinement or floodplain to channel ratio. Our validation and correction of these explanatory variables gives us confidence that our analysis minimized uncertainty.

5.4.3 Remote Wood Mapping

Our validation of remote wood mapping highlights the difficulties associated with deriving accurate volumes of wood from aerial imagery. Other attempts to map wood have been to validate retention of pieces or have used higher resolution over a smaller scale with less variability (Wohl et al., 2018). While our validation shows that we cannot expect to obtain exact volumes and densities of wood, it shows promise in identifying general trends of wood deposition in publicly available imagery in areas with less canopy (*Fig. D.1*). Our calibration of mapping highlights the importance digitizing individual pieces when possible to avoid the remote estimation of porosity for jams. We find systemic error stemming from unburned riparian canopy, shadows and many pieces near the threshold of consideration. We were able to identify roughly 70% of pieces, slightly less than Wohl et al., (2018), but we found that our digitization overestimated area and therefore volume of wood features.

5.4.4 Estimation of debris flow delivery volume

There are two important caveats to our calculation of debris flows delivery. One is that debris flows likely delivered a great deal of sediment to the channel upon occurrence and with increased flows, which is not represented in the aerial imagery. Wall et al., (2022) estimated on average 29% of the debris flow deposit volumes to have been eroded between the time of delivery and mapping. The second caveat is that the debris flow deposit areas may not incorporate channel dynamics over time because we are using the pre-fire channel to estimate delivery. Many of the debris flow deposit perimeters don't extend into areas of the channel that may have eroded before mapping. In some cases, the

channel laterally adjusted due to the impacts of the debris flow deposits, which is not incorporated into our delivery estimates. Erosion of debris flow deposits over time and channel adjustment in response to debris flow deposits should be a focus of future research.

6 Conclusion

We evaluate wildfire impacted watersheds across Utah for their ability to produce sediment bottlenecks, to determine where they occur and the respective volume and grain sizes of each. Our unique dataset consists of 86 sediment bottlenecks within and downstream of 15 wildfires, that were mapped using a combination of aerial imagery and field verification. Our findings indicate that while many sediment bottlenecks in burned watersheds are caused by structural forcing, valley bottom morphology is the primary determinant of where sediment deposition will occur. Specifically, we identify stream power as the leading control on the locations of sediment bottlenecks in post-fire fluvial networks, with increasing volume occurring through greater storage provided by flatter slopes and greater sediment generation sourced from debris flows and higher burn severity. The grain sizes of these sediment bottlenecks are finer than surrounding reaches and pre-fire conditions. However, the grain size will likely will coarsen over time as sediment moves through the system.

We also consider the dynamics of post-fire structural forcing caused by debris flow deposits and wood in modifying sediment bottleneck prevalence. Wood jams were the most common cause for sediment bottlenecks, while debris flow deposits present (dis)connectivity of the greatest magnitude. Wood jams were more effective at trapping

sediment in confined headwater catchments, while debris flow deposits deposited from large steep basins were able to block flatter main-stem reaches. Because dynamics of debris flows and wood increase after wildfire and large volumes of sediment can be trapped by these mechanisms, our exploration of these variables suggests that they mediate the amplified sedimentation that occurs in burned watersheds.

Watersheds will inevitably be impacted by wildfires as climate continues to become hotter and drier in the western U.S. Knowing where to expect aggradation of post-fire sediment in river systems will be critical information for watershed managers and researchers. Our research offers insights as to which watersheds are highly connected and will enable efficient sediment transport to downstream reservoirs, infrastructure of concern and aquatic habitat. These findings support existing post-fire sediment transport models, but suggest that structural controls introduce variance to their assumptions. Valley bottom morphology is the most important consideration for in-stream sediment transport after wildfire, however protection of water resources and mitigation of wildfire-watershed risks could be improved through knowledge of structural controls present within a watershed.

7 References

- Abatzoglou, J. T., Juang, C. S., Williams, A. P., Kolden, C. A., & Westerling, A. L. (2021). Increasing Synchronous Fire Danger in Forests of the Western United States. *Geophysical Research Letters*, *48*(2), e2020GL091377. <https://doi.org/10.1029/2020GL091377>
- Abatzoglou, J. T., & Williams, A. P. (2016). Impact of anthropogenic climate change on wildfire across western US forests. *Proceedings of the National Academy of Sciences*, *113*(42), 11770–11775. <https://doi.org/10.1073/pnas.1607171113>
- Andreoli, A., Comiti, F., & Lenzi, M. A. (2007). Characteristics, distribution and geomorphic role of large woody debris in a mountain stream of the Chilean

- Andes. *Earth Surface Processes and Landforms*, 32(11), 1675–1692.
<https://doi.org/10.1002/esp.1593>
- Austin, P. C., & Steyerberg, E. W. (2015). The number of subjects per variable required in linear regression analyses. *Journal of Clinical Epidemiology*, 68(6), 627–636.
<https://doi.org/10.1016/j.jclinepi.2014.12.014>
- Banner, R., Baldwin, B., & McGinty, E. (2009). *Rangeland Resources of Utah*.
<https://www.semanticscholar.org/paper/Rangeland-Resources-of-Utah-Banner-Baldwin/a041376d3564415734aa21a47978f077603f6905>
- Barbet-Massin, M., Jiguet, F., Albert, C. H., & Thuiller, W. (2012). Selecting pseudo-absences for species distribution models: How, where and how many?: *How to use pseudo-absences in niche modelling? Methods in Ecology and Evolution*, 3(2), 327–338. <https://doi.org/10.1111/j.2041-210X.2011.00172.x>
- Beechie, T., & Imaki, H. (2014). Predicting natural channel patterns based on landscape and geomorphic controls in the Columbia River basin, USA: Predicting Channel Patterns in the Columbia Basin. *Water Resources Research*, 50(1), 39–57.
<https://doi.org/10.1002/2013WR013629>
- Benda, L., Miller, D., Bigelow, P., & Andras, K. (2003). Effects of post-wildfire erosion on channel environments, Boise River, Idaho. *Forest Ecology and Management*, 178(1), 105–119. [https://doi.org/10.1016/S0378-1127\(03\)00056-2](https://doi.org/10.1016/S0378-1127(03)00056-2)
- Benda, L., Miller, D., Sias, J., Martin, D., Bilby, R., & Veldhuisen, C. (2003). *Wood Recruitment Processes and Wood Budgeting*.
<https://www.semanticscholar.org/paper/Wood-Recruitment-Processes-and-Wood-Budgeting-Benda-Miller/55275095d3c04a23f9e4f47ea1e6bb96387482fd>
- Benda, L., Poff, N. L., Miller, D., Dunne, T., Reeves, G., Pess, G., & Pollock, M. (2004). The Network Dynamics Hypothesis: How Channel Networks Structure Riverine Habitats. *BioScience*, 54(5), 413–427. [https://doi.org/10.1641/0006-3568\(2004\)054\[0413:TNDHHC\]2.0.CO;2](https://doi.org/10.1641/0006-3568(2004)054[0413:TNDHHC]2.0.CO;2)
- Breiman, L. (2001). Random Forests. *Machine Learning*, 45(1), 5–32.
<https://doi.org/10.1023/A:1010933404324>
- Butler, D. R., & Malanson, G. P. (1995). Sedimentation rates and patterns in beaver ponds in a mountain environment. *Geomorphology*, 13(1), 255–269.
[https://doi.org/10.1016/0169-555X\(95\)00031-Y](https://doi.org/10.1016/0169-555X(95)00031-Y)
- Cannon, S. H. (2001). Debris-flow generation from recently burned watersheds. *Environmental and Engineering Geoscience*, 7(4), 321–341.
<https://doi.org/10.2113/gseegeosci.7.4.321>
- Cannon, S. H., Gartner, J. E., Rupert, M. G., Michael, J. A., Rea, A. H., & Parrett, C. (2010). Predicting the probability and volume of postwildfire debris flows in the intermountain western United States. *Geological Society of America Bulletin*, 122(1–2), 127144. <https://doi.org/10.1130/B26459.1>
- Cashman, M. J., Harvey, G. L., & Wharton, G. (n.d.). Structural complexity influences the ecosystem engineering effects of instream large wood. *Earth Surface Processes and Landforms*, n/a(n/a). <https://doi.org/10.1002/esp.5145>
- Cutler, D. R., Edwards Jr., T. C., Beard, K. H., Cutler, A., Hess, K. T., Gibson, J., & Lawler, J. J. (2007). Random Forests for Classification in Ecology. *Ecology*, 88(11), 2783–2792. <https://doi.org/10.1890/07-0539.1>

- Czuba, J. (2018). A Lagrangian framework for exploring complexities of mixed-size sediment transport in gravel-bedded river networks. *Geomorphology*, 321, 146–152. <https://doi.org/10.1016/j.geomorph.2018.08.031>
- Czuba, J. A., & Fofoula-Georgiou, E. (2014). A network-based framework for identifying potential synchronizations and amplifications of sediment delivery in river basins. *Water Resources Research*, 50(5), 3826–3851. <https://doi.org/10.1002/2013WR014227>
- Czuba, J. A., & Fofoula-Georgiou, E. (2015). Dynamic connectivity in a fluvial network for identifying hotspots of geomorphic change. *Water Resources Research*, 51(3), 1401–1421. <https://doi.org/10.1002/2014WR016139>
- Czuba, J. A., Fofoula-Georgiou, E., Gran, K. B., Belmont, P., & Wilcock, P. R. (2017). Interplay between spatially explicit sediment sourcing, hierarchical river-network structure, and in-channel bed material sediment transport and storage dynamics. *Journal of Geophysical Research: Earth Surface*, 122(5), 1090–1120. <https://doi.org/10.1002/2016JF003965>
- David, S. R., Murphy, B. P., Czuba, J. A., Ahammad, M., & Belmont, P. (2023). USUAL Watershed Tools: A new geospatial toolkit for hydro-geomorphic delineation. *Environmental Modelling & Software*, 159, 105576. <https://doi.org/10.1016/j.envsoft.2022.105576>
- De Graff, J. V. (2018). A rationale for effective post-fire debris flow mitigation within forested terrain. *Geoenvironmental Disasters*, 5(1), 7. <https://doi.org/10.1186/s40677-018-0099-z>
- DeBano, L. F. (2000). The role of fire and soil heating on water repellency in wildland environments: A review. *Journal of Hydrology*, 231–232, 195–206. [https://doi.org/10.1016/S0022-1694\(00\)00194-3](https://doi.org/10.1016/S0022-1694(00)00194-3)
- D’Haen, K., Dusar, B., Verstraeten, G., Degryse, P., & De Brue, H. (2013). A sediment fingerprinting approach to understand the geomorphic coupling in an eastern Mediterranean mountainous river catchment. *Geomorphology*, 197, 64–75. <https://doi.org/10.1016/j.geomorph.2013.04.038>
- Duane, A., Castellnou, M., & Brotons, L. (2021). Towards a comprehensive look at global drivers of novel extreme wildfire events. *Climatic Change*, 165(3), 43. <https://doi.org/10.1007/s10584-021-03066-4>
- Esposito, G., Gariano, S. L., Masi, R., Alfano, S., & Giannatiempo, G. (2023). Rainfall conditions leading to runoff-initiated post-fire debris flows in Campania, Southern Italy. *Geomorphology*, 423, 108557. <https://doi.org/10.1016/j.geomorph.2022.108557>
- Fairfax, E., & Whittle, A. (2020). Smokey the Beaver: Beaver-dammed riparian corridors stay green during wildfire throughout the western United States. *Ecological Applications*, 30(8). <https://doi.org/10.1002/eap.2225>
- Finnegan, N. J., Broudy, K. N., Nereson, A. L., Roering, J. J., Handwerker, A. L., & Bennett, G. (2019). River channel width controls blocking by slow-moving landslides in California’s Franciscan mélange. *Earth Surface Dynamics*, 7(3), 879–894. <https://doi.org/10.5194/esurf-7-879-2019>
- Flitcroft, R. L., Falke, J. A., Reeves, G. H., Hessburg, P. F., McNyset, K. M., & Benda, L. E. (2016). Wildfire may increase habitat quality for spring Chinook salmon in

- the Wenatchee River subbasin, WA, USA. *Forest Ecology and Management*, 359, 126–140. <https://doi.org/10.1016/j.foreco.2015.09.049>
- Fryirs, K. (2013). (Dis)Connectivity in catchment sediment cascades: A fresh look at the sediment delivery problem. *Earth Surface Processes and Landforms*, 38(1), 30–46. <https://doi.org/10.1002/esp.3242>
- Fryirs, K. A., & Brierley, G. J. (2013). *Geomorphic analysis of river systems: An approach to reading the landscape*. Wiley.
- Fryirs, K. A., Brierley, G. J., Preston, N. J., & Kasai, M. (2007). Buffers, barriers and blankets: The (dis)connectivity of catchment-scale sediment cascades. *CATENA*, 70(1), 49–67. <https://doi.org/10.1016/j.catena.2006.07.007>
- Gilbert, J. T., Macfarlane, W. W., & Wheaton, J. M. (2016). The Valley Bottom Extraction Tool (V-BET): A GIS tool for delineating valley bottoms across entire drainage networks. *Computers & Geosciences*, 97, 1–14. <https://doi.org/10.1016/j.cageo.2016.07.014>
- Gillard, N. (2019). Wildfire in the West: An Initial Analysis of Wildfire Impacts on Hydrology and Riverbed Grain Size in Relation to Salmonid Habitat. *All Graduate Theses and Dissertations*. <https://doi.org/10.26076/2e5e-8238>
- Goeking, S. A., & Tarboton, D. G. (2022). Variable Streamflow Response to Forest Disturbance in the Western US: A Large-Sample Hydrology Approach. *Water Resources Research*, 58(6). <https://doi.org/10.1029/2021WR031575>
- González-Romero, J., López-Vicente, M., Gómez-Sánchez, E., Peña-Molina, E., Galletero, P., Plaza-Alvarez, P., Moya, D., De las Heras, J., & Lucas-Borja, M. E. (2021). Post-fire management effects on sediment (dis)connectivity in Mediterranean forest ecosystems: Channel and catchment response. *Earth Surface Processes and Landforms*, 46(13), 2710–2727. <https://doi.org/10.1002/esp.5202>
- Gran, K. B., & Czuba, J. A. (2017). Sediment pulse evolution and the role of network structure. *Geomorphology*, 277, 17–30. <https://doi.org/10.1016/j.geomorph.2015.12.015>
- Hallema, D., Kinoshita, A. M., Martin, D. A., Robinne, F.-N., Galleguillos, M., McNulty, S., Sun, G., Singh, K. K., Mordecai, R. S., & Moore, P. F. (2019). Fire, forest and city water supplies. *Unasylva*, 70(251), 58–66.
- Hallema, D. W., Sun, G., Bladon, K. D., Norman, S. P., Caldwell, P. V., Liu, Y., & McNulty, S. G. (2017). Regional patterns of postwildfire streamflow response in the Western United States: The importance of scale-specific connectivity. *Hydrological Processes*, 3(1), 1–17. <https://doi.org/10.1002/hyp.11208>
- Heyerdahl, E. K., Brown, P. M., Kitchen, S. G., & Weber, M. H. (2011). Multicentury fire and forest histories at 19 sites in Utah and eastern Nevada. *Gen. Tech. Rep. RMRS-GTR-261WWW*. Fort Collins, CO: U.S. Department of Agriculture, Forest Service, Rocky Mountain Research Station. 192 p., 261. <https://doi.org/10.2737/RMRS-GTR-261>
- Hooke, J. (2003). Coarse sediment connectivity in river channel systems: A conceptual framework and methodology. *Geomorphology*, 56(1), 79–94. [https://doi.org/10.1016/S0169-555X\(03\)00047-3](https://doi.org/10.1016/S0169-555X(03)00047-3)
- Iskin, E., & Wohl. (2021). Wildfire and the patterns of floodplain large wood on the Merced River, Yosemite National Park, California, USA. *Geomorphology*, 107805. <https://doi.org/10.1016/j.geomorph.2021.107805>

- Jager, H. I., Long, J. W., Malison, R. L., Murphy, B. P., Rust, A., Silva, L. G. M., Sollmann, R., Steel, Z. L., Bowen, M. D., Dunham, J. B., Ebersole, J. L., & Flitcroft, R. L. (n.d.). Resilience of terrestrial and aquatic fauna to historical and future wildfire regimes in western North America. *Ecology and Evolution*, n/a(n/a). <https://doi.org/10.1002/ece3.8026>
- Jager, H. I., Long, J. W., Malison, R. L., Murphy, B. P., Rust, A., Silva, L. G. M., Sollmann, R., Steel, Z. L., Bowen, M. D., Dunham, J. B., Ebersole, J. L., & Flitcroft, R. L. (2021). Resilience of terrestrial and aquatic fauna to historical and future wildfire regimes in western North America. *Ecology and Evolution*, 11(18), 12259–12284. <https://doi.org/10.1002/ece3.8026>
- Jones, J. I., Murphy, J. F., Collins, A. L., Sear, D. A., Naden, P. S., & Armitage, P. D. (2012). THE IMPACT OF FINE SEDIMENT ON MACRO-INVERTEBRATES: FINE SEDIMENT AND MACRO-INVERTEBRATES. *River Research and Applications*, 28(8), 1055–1071. <https://doi.org/10.1002/rra.1516>
- Keck, J., Istanbuluoglu, E., Lundquist, J., Bandaragoda, C., Jaeger, K., Mauger, G., & Horner-Devine, A. (2022). How Does Precipitation Variability Control Bedload Response Across a Mountainous Channel Network in a Maritime Climate? *Water Resources Research*, 58(8). <https://doi.org/10.1029/2021WR030358>
- Kenney, T. A., Wilkowske, C. D., & Wright, S. J. (2007). *Methods for estimating magnitude and frequency of peak flows for natural streams in Utah* (No. 2007–5158). U.S. Geological Survey. <https://doi.org/10.3133/sir20075158>
- Kirby, E., & Whipple, K. (2001). Quantifying differential rock-uplift rates via stream profile analysis. *Geology*, 29(5), 415–418. [https://doi.org/10.1130/0091-7613\(2001\)029<0415:QDRURV>2.0.CO;2](https://doi.org/10.1130/0091-7613(2001)029<0415:QDRURV>2.0.CO;2)
- Kirchner, J., Finkel, R., Riebe, C., Granger, D., & Clayton, J. (2001). Mountain erosion over 10 yr, 10 k.y., and 10 m.y. Time scales. *Geology*, 29(7), 591–594. [https://doi.org/10.1130/0091-7613\(2001\)029%3C0591:MEOYKY%3E2.0.CO;2](https://doi.org/10.1130/0091-7613(2001)029%3C0591:MEOYKY%3E2.0.CO;2)
- Kobziar, L. N., & McBride, J. R. (2006). Wildfire burn patterns and riparian vegetation response along two northern Sierra Nevada streams. *Forest Ecology and Management*, 222(1–3), 254–265. <https://doi.org/10.1016/j.foreco.2005.10.024>
- Kuo, C.-W., & Brierley, G. J. (2013). The influence of landscape configuration upon patterns of sediment storage in a highly connected river system. *Geomorphology*, 180–181, 255–266. <https://doi.org/10.1016/j.geomorph.2012.10.015>
- Kursa, M. B., & Rudnicki, W. R. (2010). Feature Selection with the Boruta Package. *Journal of Statistical Software*, 36, 1–13. <https://doi.org/10.18637/jss.v036.i11>
- Lamb, M. P., Levina, M., DiBiase, R. A., & Fuller, B. M. (2013). Sediment storage by vegetation in steep bedrock landscapes: Theory, experiments, and implications for postfire sediment yield: SEDIMENT STORAGE IN BEDROCK LANDSCAPES. *Journal of Geophysical Research: Earth Surface*, 118(2), 1147–1160. <https://doi.org/10.1002/jgrf.20058>
- LANDFIRE, 2016, Existing Vegetation Type Layer, LANDFIRE 2.0.0, U.S. Department of the Interior, Geological Survey, and U.S. Department of Agriculture. Accessed 28 October 2021 at <http://www.landfire/viewer>.
- Lisle, T. E., & Hilton, S. (1992). The Volume of Fine Sediment in Pools: An Index of Sediment Supply in Gravel-Bed Streams1. *JAWRA Journal of the American*

- Water Resources Association*, 28(2), 371–383. <https://doi.org/10.1111/j.1752-1688.1992.tb04003.x>
- Livers, B., Lininger, K. B., Kramer, N., & Sendrowski, A. (2020). Porosity problems: Comparing and reviewing methods for estimating porosity and volume of wood jams in the field. *Earth Surface Processes and Landforms*, 45(13), 3336–3353. <https://doi.org/10.1002/esp.4969>
- Livers, B., & Wohl, E. (2021). All Logjams Are Not Created Equal. *Journal of Geophysical Research: Earth Surface*, 126(8), e2021JF006076. <https://doi.org/10.1029/2021JF006076>
- Macfarlane, W. W., Wheaton, J. M., Bouwes, N., Jensen, M. L., Gilbert, J. T., Hough-Snee, N., & Shvik, J. A. (2017). Modeling the capacity of riverscapes to support beaver dams. *Geomorphology*, 277, 72–99. <https://doi.org/10.1016/j.geomorph.2015.11.019>
- Manners, R. B., Doyle, M. W., & Small, M. J. (2007). Structure and hydraulics of natural woody debris jams. *Water Resources Research*, 43(6). <https://doi.org/10.1029/2006WR004910>
- Marlon, J. R., Bartlein, P. J., Gavin, D. G., Long, C. J., Anderson, R. S., Briles, C. E., Brown, K. J., Colombaroli, D., Hallett, D. J., Power, M. J., Scharf, E. A., & Walsh, M. K. (2012). Long-term perspective on wildfires in the western USA. *Proceedings of the National Academy of Sciences*, 109(9), E535–E543. <https://doi.org/10.1073/pnas.1112839109>
- McKinnon, K. A., & Deser, C. (2021). The Inherent Uncertainty of Precipitation Variability, Trends, and Extremes due to Internal Variability, with Implications for Western U.S. Water Resources. *Journal of Climate*, 34(24), 9605–9622. <https://doi.org/10.1175/JCLI-D-21-0251.1>
- Merow, C., Smith, M. J., & Silander Jr, J. A. (2013). A practical guide to MaxEnt for modeling species' distributions: What it does, and why inputs and settings matter. *Ecography*, 36(10), 1058–1069. <https://doi.org/10.1111/j.1600-0587.2013.07872.x>
- Miller, B. A., & Juilleret, J. (2020). The colluvium and alluvium problem: Historical review and current state of definitions. *Earth-Science Reviews*, 209, 103316. <https://doi.org/10.1016/j.earscirev.2020.103316>
- Montgomery, D. R., & Buffington, J. M. (1997). Channel-reach morphology in mountain drainage basins. *Geological Society of America Bulletin*, 109(5), 596–611. [https://doi.org/10.1130/0016-7606\(1997\)109<0596:CRMIMD>2.3.CO;2](https://doi.org/10.1130/0016-7606(1997)109<0596:CRMIMD>2.3.CO;2)
- MTBS Data Access: Fire Level Geospatial Data. (2017, July - last revised). MTBS Project (USDA Forest Service/U.S. Geological Survey). Available online: <http://mtbs.gov/direct-download> [2017, July12].
- Mueller, J. M., Lima, R. E., Springer, A. E., & Schiefer, E. (2018). Using Matching Methods to Estimate Impacts of Wildfire and Postwildfire Flooding on House Prices. *Water Resources Research*, 54(9), 6189–6201. <https://doi.org/10.1029/2017WR022195>
- Murphy, B. P., Czuba, J. A., & Belmont, P. (2019). Post-wildfire sediment cascades: A modeling framework linking debris flow generation and network-scale sediment routing. *Earth Surface Processes and Landforms*, 44(11), 2126–2140. <https://doi.org/10.1002/esp.4635>

- Murphy, B. P., Yocom, L. L., & Belmont, P. (2018). Beyond the 1984 Perspective: Narrow Focus on Modern Wildfire Trends Underestimates Future Risks to Water Security. *Earth's Future*, 6(11), 1492–1497. <https://doi.org/10.1029/2018EF001006>
- Musselman, K. N., Lehner, F., Ikeda, K., Clark, M. P., Prein, A. F., Liu, C., Barlage, M., & Rasmussen, R. (2018). Projected increases and shifts in rain-on-snow flood risk over western North America. *Nature Climate Change*, 8(9), 808–812. <https://doi.org/10.1038/s41558-018-0236-4>
- N. Bouwes, J. Moberg, N. Weber, B. Bouwes, S. Bennett, C. Beasley, C.E. Jordan, P. Nelle, M. Polino, S. Rentmeester, B. Semmens, C. Volk, M.B. Ward, & J. White. (2011). *Scientific Protocol for Salmonid Habitat Surveys within the Columbia Habitat Monitoring Program*. <https://doi.org/10.13140/RG.2.1.4609.6886>
- Nyman, P., Box, W. A. C., Stout, J. C., Sheridan, G. J., Keesstra, S. D., Lane, P. N. J., & Langhans, C. (2020). Debris-flow-dominated sediment transport through a channel network after wildfire. *Earth Surface Processes and Landforms*, 45(5), 1155–1167. <https://doi.org/10.1002/esp.4785>
- O'Brien, G. R., Wheaton, J. M., Fryirs, K., Macfarlane, W. W., Brierley, G., Whitehead, K., Gilbert, J., & Volk, C. (2019). Mapping valley bottom confinement at the network scale. *Earth Surface Processes and Landforms*, 44(9), 1828–1845. <https://doi.org/10.1002/esp.4615>
- Parks, S. A., & Abatzoglou, J. T. (2020). Warmer and Drier Fire Seasons Contribute to Increases in Area Burned at High Severity in Western US Forests From 1985 to 2017. *Geophysical Research Letters*, 47(22), e2020GL089858. <https://doi.org/10.1029/2020GL089858>
- Pfeiffer, A. M., Barnhart, K. R., Czuba, J. A., & Hutton, E. W. h. (2020). NetworkSedimentTransporter: A Landlab component for bed material transport through river networks. *Journal of Open Source Software*, 5(53), 2341. <https://doi.org/10.21105/joss.02341>
- Pfeiffer, A., & Wohl, E. (2018). Where Does Wood Most Effectively Enhance Storage? Network-Scale Distribution of Sediment and Organic Matter Stored by Instream Wood. *Geophysical Research Letters*, 45(1), 194–200. <https://doi.org/10.1002/2017GL076057>
- R Core Team (2023). R: A language and environment for statistical computing. R Foundation for Statistical Computing, Vienna, Austria. URL <https://www.R-project.org/>.
- Rathburn, S. L., Rubin, Z. K., & Wohl, E. E. (2013). Evaluating channel response to an extreme sedimentation event in the context of historical range of variability: Upper Colorado River, USA. *Earth Surface Processes and Landforms*, 38(4), 391–406. <https://doi.org/10.1002/esp.3329>
- Rengers, F. K., McGuire, L. A., Kean, J. W., Staley, D. M., Dobre, M., Robichaud, P. R., & Swetnam, T. (2021). Movement of Sediment Through a Burned Landscape: Sediment Volume Observations and Model Comparisons in the San Gabriel Mountains, California, USA. *Journal of Geophysical Research: Earth Surface*, 126(7). <https://doi.org/10.1029/2020JF006053>
- Rice, S. (1998). Which tributaries disrupt downstream fining along gravel-bed rivers? *Geomorphology*, 22(1), 39–56. [https://doi.org/10.1016/S0169-555X\(97\)00052-4](https://doi.org/10.1016/S0169-555X(97)00052-4)

- Rice, S. P. (2017). Tributary connectivity, confluence aggradation and network biodiversity. *Geomorphology*, 277, 6–16.
<https://doi.org/10.1016/j.geomorph.2016.03.027>
- Robinne, F.-N., Hallema, D. W., Bladon, K. D., Flannigan, M. D., Boisramé, G., Bréthaut, C. M., Doerr, S. H., Baldassarre, G. D., Gallagher, L. A., Hohner, A. K., Khan, S. J., Kinoshita, A. M., Mordecai, R., Nunes, J. P., Nyman, P., Santín, C., Sheridan, G., Stoof, C. R., Thompson, M. P., ... Wei, Y. (2021). Scientists' warning on extreme wildfire risks to water supply. *Hydrological Processes*, 35(5), e14086. <https://doi.org/10.1002/hyp.14086>
- Roux, C., Alber, A., Bertrand, M., Vaudor, L., & Piégay, H. (2015). “FluvialCorridor”: A new ArcGIS toolbox package for multiscale riverscape exploration. *Geomorphology*, 242, 29–37. <https://doi.org/10.1016/j.geomorph.2014.04.018>
- Ruiz-Villanueva, V., Piégay, H., Gurnell, A. M., Marston, R. A., & Stoffel, M. (2016). Recent advances quantifying the large wood dynamics in river basins: New methods and remaining challenges. *Reviews of Geophysics*, 54(3), 611–652. <https://doi.org/10.1002/2015RG000514>
- Sankey, J. B., Kreitler, J., Hawbaker, T. J., McVay, J. L., Miller, M. E., Mueller, E. R., Vaillant, N. M., Lowe, S. E., & Sankey, T. T. (2017). Climate, wildfire, and erosion ensemble foretells more sediment in western USA watersheds. *Geophysical Research Letters*, 44(17), 8884–8892. <https://doi.org/10.1002/2017GL073979>
- Santi, P. M. (2014). Precision and Accuracy in Debris-Flow Volume Measurement. *Environmental & Engineering Geoscience*, 20(4), 349–359. <https://doi.org/10.2113/gseegeosci.20.4.349>
- Schalko, I., Schmocker, L., Weitbrecht, V., & Boes, R. M. (2018). Backwater Rise due to Large Wood Accumulations. *Journal of Hydraulic Engineering*, 144(9), 04018056. [https://doi.org/10.1061/\(ASCE\)HY.1943-7900.0001501](https://doi.org/10.1061/(ASCE)HY.1943-7900.0001501)
- Schmitt, R. J. P., Bizzi, S., & Castelletti, A. (2016). Tracking multiple sediment cascades at the river network scale identifies controls and emerging patterns of sediment connectivity. *Water Resources Research*, 52(5), 3941–3965. <https://doi.org/10.1002/2015WR018097>
- Schmocker, L., & Weitbrecht, V. (2013). Driftwood: Risk Analysis and Engineering Measures. *Journal of Hydraulic Engineering*, 139(7), 683–695. [https://doi.org/10.1061/\(ASCE\)HY.1943-7900.0000728](https://doi.org/10.1061/(ASCE)HY.1943-7900.0000728)
- Scott, D. N., & Wohl, E. E. (2018). Natural and Anthropogenic Controls on Wood Loads in River Corridors of the Rocky, Cascade, and Olympic Mountains, USA. *Water Resources Research*, 54(10), 7893–7909. <https://doi.org/10.1029/2018WR022754>
- Seixas, G. B., Veldhuisen, C. N., & Olis, M. (2020). Wood controls on pool spacing, step characteristics and sediment storage in headwater streams of the northwestern Cascade Mountains. *Geomorphology*, 348, 106898. <https://doi.org/10.1016/j.geomorph.2019.106898>
- Sheppard, P. R., Comrie, A. C., Packin, G. D., Angersbach, K., & Hughes, M. K. (2002). The climate of the US Southwest. *Climate Research*, 21(3), 219–238. <https://doi.org/10.3354/cr021219>
- Smith, D. M., Finch, D. M., Gunning, C., Jemison, R., & Kelly, J. F. (2009). Post-Wildfire Recovery of Riparian Vegetation during a Period of Water Scarcity in

- the Southwestern USA. *Fire Ecology*, 5(1), 38–55.
<https://doi.org/10.4996/fireecology.0501038>
- Snyder, N. P., Nesheim, A. O., Wilkins, B. C., & Edmonds, D. A. (2013). Predicting grain size in gravel-bedded rivers using digital elevation models: Application to three Maine watersheds. *Geological Society of America Bulletin*, 125(1–2), 148–163. <https://doi.org/10.1130/B30694.1>
- Staley, D., Kean, J., & Rengers, F. (2020). The recurrence interval of post-fire debris-flow generating rainfall in the southwestern United States. *Geomorphology*, 370, 107392. <https://doi.org/10.1016/j.geomorph.2020.107392>
- Staley, D. M., Negri, J. A., Kean, J. W., Laber, J. L., Tillery, A. C., & Youberg, A. M. (2017). Prediction of spatially explicit rainfall intensity–duration thresholds for post-fire debris-flow generation in the western United States. *Geomorphology*, 278, 149–162. <https://doi.org/10.1016/j.geomorph.2016.10.019>
- Swain, D. L., Langenbrunner, B., Neelin, J. D., & Hall, A. (2018). Increasing precipitation volatility in twenty-first-century California. *Nature Climate Change*, 8(5), 427–433. <https://doi.org/10.1038/s41558-018-0140-y>
- Taylor, S. B., & Kite, J. S. (2006). Comparative geomorphic analysis of surficial deposits at three central Appalachian watersheds: Implications for controls on sediment-transport efficiency. *Geomorphology*, 78(1), 22–43.
<https://doi.org/10.1016/j.geomorph.2006.01.032>
- Udall, B., & Overpeck, J. (2017). The twenty-first century Colorado River hot drought and implications for the future. *Water Resources Research*, 53(3), 2404–2418.
<https://doi.org/10.1002/2016WR019638>
- Valavi, R., Elith, J., Lahoz-Monfort, J. J., & Guillera-Aroita, G. (2021). Modelling species presence-only data with random forests. *Ecography*, 44(12), 1731–1742.
<https://doi.org/10.1111/ecog.05615>
- Valavi, R., Guillera-Aroita, G., Lahoz-Monfort, J. J., & Elith, J. (2022). Predictive performance of presence-only species distribution models: A benchmark study with reproducible code. *Ecological Monographs*, 92(1).
<https://doi.org/10.1002/ecm.1486>
- Valentin, V., & Stormont, J. (2019). *Evaluating Post-Wildfire Flood Impacts on Transportation Infrastructure for Mitigation Planning*.
<https://trid.trb.org/view/1676607>
- Van der Sant, R. E., Nyman, P., Noske, P. J., Langhans, C., Lane, P. N. J., & Sheridan, G. J. (2018). Quantifying relations between surface runoff and aridity after wildfire: Relations between surface runoff and aridity after wildfire. *Earth Surface Processes and Landforms*, 43(10), 2033–2044.
<https://doi.org/10.1002/esp.4370>
- Vaz, P. G., Merten, E. C., Warren, D. R., Robinson, C. T., Pinto, P., & Rego, F. C. (2013). Which stream wood becomes functional following wildfires? *Ecological Engineering*, 54, 82–89. <https://doi.org/10.1016/j.ecoleng.2013.01.009>
- Wall, S., Murphy, B. P., Belmont, P., & Yocom, L. (2022). Predicting post-fire debris flow grain sizes and depositional volumes in the Intermountain West, USA. *Earth Surface Processes and Landforms*, esp.5480. <https://doi.org/10.1002/esp.5480>
- Weiss, A. (2001). *Topographic Position and Landforms Analysis* [Poster Presentation]. ESRI Users Conference, San Diego, CA. chrome-

- extension://efaidnbmnnnibpcajpcglclefindmkaj/http://www.jennessent.com/downloads/tpi-poster-tnc_18x22.pdf
- Welling, R. T., Wilcox, A. C., & Dixon, J. L. (2021). Large wood and sediment storage in a mixed bedrock-alluvial stream, western Montana, USA. *Geomorphology*, 384, 107703. <https://doi.org/10.1016/j.geomorph.2021.107703>
- Wilkerson, G. V., Kandel, D. R., Perg, L. A., Dietrich, W. E., Wilcock, P. R., & Whiles, M. R. (2014). Continental-scale relationship between bankfull width and drainage area for single-thread alluvial channels: BANKFULL WIDTH AND DRAINAGE AREA RELATIONSHIP. *Water Resources Research*, 50(2), 919–936. <https://doi.org/10.1002/2013WR013916>
- Wilson, C., Kampf, S. K., Ryan, S., Covino, T., MacDonald, L. H., & Gleason, H. (2021). Connectivity of post-fire runoff and sediment from nested hillslopes and watersheds. *Hydrological Processes*, 35(1). <https://doi.org/10.1002/hyp.13975>
- Wohl, E. (2020). Wood process domains and wood loads on floodplains. *Earth Surface Processes and Landforms*, 45(1), 144–156. <https://doi.org/10.1002/esp.4771>
- Wohl, E., Brierley, G., Cadol, D., Coulthard, T. J., Covino, T., Fryirs, K. A., Grant, G., Hilton, R. G., Lane, S. N., Magilligan, F. J., Meitzen, K. M., Passalacqua, P., Poepl, R. E., Rathburn, S. L., & Sklar, L. S. (2019). Connectivity as an emergent property of geomorphic systems. *Earth Surface Processes and Landforms*, 44(1), 4–26. <https://doi.org/10.1002/esp.4434>
- Wohl, E., Cadol, D., Pfeiffer, A., Jackson, K., & Laurel, D. (2018). Distribution of Large Wood Within River Corridors in Relation to Flow Regime in the Semiarid Western US. *Water Resources Research*, 54(3), 1890–1904. <https://doi.org/10.1002/2017WR022009>
- Wohl, E., Marshall, A. E., Scamardo, J., White, D., & Morrison, R. R. (2022). Biogeomorphic influences on river corridor resilience to wildfire disturbances in a mountain stream of the Southern Rockies, USA. *Science of The Total Environment*, 820, 153321. <https://doi.org/10.1016/j.scitotenv.2022.153321>
- Wohl, E., Rathburn, S., Chignell, S., Garrett, K., Laurel, D., Livers, B., Patton, A., Records, R., Richards, M., Schook, D. M., Sutfin, N. A., & Wegener, P. (2017). Mapping longitudinal stream connectivity in the North St. Vrain Creek watershed of Colorado. *Geomorphology*, 277, 171–181. <https://doi.org/10.1016/j.geomorph.2016.05.004>
- Wohl, E., & Scamardo, J. E. (2021). The resilience of logjams to floods. *Hydrological Processes*, 35(1). <https://doi.org/10.1002/hyp.13970>
- Wohl, E., & Scott, D. N. (2017). Wood and sediment storage and dynamics in river corridors. *Earth Surface Processes and Landforms*, 42(1), 5–23. <https://doi.org/10.1002/esp.3909>
- Wohl, E., Scott, D. N., & Lininger, K. B. (2018). Spatial Distribution of Channel and Floodplain Large Wood in Forested River Corridors of the Northern Rockies. *Water Resources Research*, 54(10), 7879–7892. <https://doi.org/10.1029/2018WR022750>
- Zelt, R. B., & Wohl, E. E. (2004). Channel and woody debris characteristics in adjacent burned and unburned watersheds a decade after wildfire, Park County, Wyoming. *Geomorphology*, 57(3), 217–233. [https://doi.org/10.1016/S0169-555X\(03\)00104-1](https://doi.org/10.1016/S0169-555X(03)00104-1)

8 Appendices

Appendix A. Remote Sediment Bottleneck Sites & Identification

Table A. 1 List of all wildfires in Utah between 2010 and 2018, with wildfires selected as study sites highlighted in yellow

Fire Name	% Burned at Moderate/High Severity	% of slope greater than 23°	% Conifer	Burn Classification	Slope Classification	Wood Classification	Wall et al., 2023 fire?	Acres
NORTH MOORE	86	7	7	High Severity	Shallow	Less LW	No	1341
SAND LEDGES	73	2	4	High Severity	Shallow	Less LW	No	3242
DOTS	71	24	11	High Severity	Shallow	Less LW	No	10265
LOST LAKE	69	8	44	High Severity	Shallow	Less LW	No	2062
BLIND CANYON	68	9	39	High Severity	Shallow	Less LW	Yes	2443
LOWER EBBS	64	25	11	High Severity	Shallow	Less LW	No	5338
AUGUSTI	62	36	37	High Severity	Shallow	Less LW	No	1291
LITTLE PINE	61	37	13	High Severity	Shallow	Less LW	No	2107
222	60	29	12	High Severity	Shallow	Less LW	No	1657
BIG POLE	60	35	8	High Severity	Shallow	Less LW	No	41579
SHEEP	60	22	16	High Severity	Shallow	Less LW	No	3039
WILDFLOWER	58	43	15	High Severity	Shallow	Less LW	No	1708
WHITE ROCK	57	4	4	High Severity	Shallow	Less LW	No	5603
PINYON	57	21	4	High Severity	Shallow	Less LW	No	5659
LAKE FORK	56	49	42	High Severity	Shallow	Less LW	Yes	2331
FLY CANYON	55	41	15	High Severity	Shallow	Less LW	No	2673
BROKEN RIDGE	55	6	13	High Severity	Shallow	Less LW	No	5441
HORSE	53	20	38	High Severity	Shallow	Less LW	No	1858
MACHINE GUN	53	18	7	High Severity	Shallow	Less LW	No	4076
SHINGLE	53	24	40	High Severity	Shallow	Less LW	Yes	8122
PLAYGROUND	53	5	4	High Severity	Shallow	Less LW	No	3110
SHEEP CREEK	52	30	7	High Severity	Shallow	Less LW	No	1083
FAUST	51	37	11	High Severity	Shallow	Less LW	No	22155
MILL FLAT	79	49	67	High Severity	Shallow	LW	No	12708
COOPER SPRING	77	11	68	High Severity	Shallow	LW	No	1523
COAL HOLLOW	69	40	68	High Severity	Shallow	LW	Yes	30239
HORSE VALLEY	64	6	63	High Severity	Shallow	LW	No	2563
HILL TOP	63	9	61	High Severity	Shallow	LW	No	1784
SOLOMON BASIN WFM	63	17	58	High Severity	Shallow	LW	No	1940
RAT HOLE	63	24	51	High Severity	Shallow	LW	No	3118
BRIANHEAD	58	16	80	High Severity	Shallow	LW	Yes	74276
WEST VALLEY	54	42	88	High Severity	Shallow	LW	Yes	11914
CHURCH CAMP	54	42	58	High Severity	Shallow	LW	No	7016
LEVAN	74	54	12	High Severity	Steep	Less LW	No	4356

TUNNEL HOLLOW	66	74	14	High Severity	Steep	Less LW	No	1504
LION PEAK	65	59	7	High Severity	Steep	Less LW	No	1171
RED LEDGES	64	57	23	High Severity	Steep	Less LW	No	1732
SADDLE	63	64	35	High Severity	Steep	Less LW	No	2365
SEELEY	62	61	35	High Severity	Steep	Less LW	Yes	44626
JOCKS CANYON	60	50	4	High Severity	Steep	Less LW	No	1612
BALD MOUNTAIN	58	50	45	High Severity	Steep	Less LW	No	21016
SAWMILL	58	51	8	High Severity	Steep	Less LW	No	1494
COFFEE POT	52	50	4	High Severity	Steep	Less LW	No	2031
BEAR TRAP	68	80	71	High Severity	Steep	LW	No	9215
TWITCHELL CANYON	64	51	67	High Severity	Steep	LW	Yes	42956
TRAIL MOUNTAIN	54	64	64	High Severity	Steep	LW	Yes	18342
QUAIL	54	84	67	High Severity	Steep	LW	No	2040
AMOS CANYON WFM	51	60	75	High Severity	Steep	LW	No	1333
WHITE VALLEY	49	24	0	Low Severity	Shallow	Less LW	No	1701
MILE MARKER 166	48	0	1	Low Severity	Shallow	Less LW	No	2546
BROAD MOUTH	46	34	1	Low Severity	Shallow	Less LW	No	21009
POLE CREEK	46	39	39	Low Severity	Shallow	Less LW	No	102426
SAWMILL CANYON	46	33	35	Low Severity	Shallow	Less LW	No	7696
BOX CANYON	46	37	48	Low Severity	Shallow	Less LW	No	4479
HICKS CREEK	44	37	38	Low Severity	Shallow	Less LW	No	1471
PONY	42	3	6	Low Severity	Shallow	Less LW	No	1036
ROCKPORT	41	15	8	Low Severity	Shallow	Less LW	No	2018
STATE	40	38	8	Low Severity	Shallow	Less LW	No	31011
BENDER MOUNTAIN	38	20	42	Low Severity	Shallow	Less LW	No	3797
ROUNDBOUT	38	1	12	Low Severity	Shallow	Less LW	No	2527
GORING	37	16	2	Low Severity	Shallow	Less LW	No	14538
BOX CREEK	37	9	35	Low Severity	Shallow	Less LW	No	1552
ROUGH CANYON	36	49	9	Low Severity	Shallow	Less LW	No	3986
NEW HARMONY	33	1	11	Low Severity	Shallow	Less LW	No	1895
PETERSON HOLLOW	32	20	44	Low Severity	Shallow	Less LW	No	1381
RATTLESNAKEPASS	30	1	0	Low Severity	Shallow	Less LW	No	1454
RAFT RIVER	28	4	41	Low Severity	Shallow	Less LW	No	1302
GOOSE CREEK	27	11	34	Low Severity	Shallow	Less LW	No	131432
BLACK	27	45	32	Low Severity	Shallow	Less LW	No	1771
WOLF DEN	26	13	17	Low Severity	Shallow	Less LW	No	19419
CEDAR MOUNTAIN ONE	25	45	32	Low Severity	Shallow	Less LW	No	13226
WEST GOVERNMENT CREEK	25	24	23	Low Severity	Shallow	Less LW	No	4412
A R	25	2	0	Low Severity	Shallow	Less LW	No	1809
CLAY SPRINGS	23	35	15	Low Severity	Shallow	Less LW	Yes	107391

WHITE ROCKS 1	22	3	2	Low Severity	Shallow	Less LW	No	9719
BLACK MOUNTAIN	21	1	4	Low Severity	Shallow	Less LW	No	4603
PORCUPINE	20	15	35	Low Severity	Shallow	Less LW	No	2492
SE CEDAR	19	1	2	Low Severity	Shallow	Less LW	No	1367
RHYOLITE	19	22	3	Low Severity	Shallow	Less LW	No	4109
WOOD HOLLOW	15	6	16	Low Severity	Shallow	Less LW	No	46763
DAVIS	15	5	2	Low Severity	Shallow	Less LW	No	35071
JERICO	14	4	6	Low Severity	Shallow	Less LW	No	2230
DUMP	14	46	5	Low Severity	Shallow	Less LW	No	5676
NORTH EDEN	14	7	1	Low Severity	Shallow	Less LW	No	14398
BABOON	13	5	4	Low Severity	Shallow	Less LW	No	20453
SHIVWITS	13	47	9	Low Severity	Shallow	Less LW	No	5299
IBAPAH	12	0	0	Low Severity	Shallow	Less LW	No	1573
BARN	11	15	6	Low Severity	Shallow	Less LW	No	1415
TRIBAL	11	0	0	Low Severity	Shallow	Less LW	No	1925
MACK SHAFT	10	0	0	Low Severity	Shallow	Less LW	No	2562
DUTCH MOUNTAIN	9	13	0	Low Severity	Shallow	Less LW	No	1409
ANACONDA	9	1	2	Low Severity	Shallow	Less LW	No	1142
ROUGH HAUL	7	1	0	Low Severity	Shallow	Less LW	No	5373
OPHIR CREEK	7	0	0	Low Severity	Shallow	Less LW	No	1589
TAYLOR MOUNTAIN ROAD	7	3	2	Low Severity	Shallow	Less LW	No	2965
RED BUTTE	6	2	4	Low Severity	Shallow	Less LW	No	1978
HANSEL POINT	6	10	22	Low Severity	Shallow	Less LW	No	4492
PUDDLE	6	0	0	Low Severity	Shallow	Less LW	No	1920
ELLERBECK	6	35	4	Low Severity	Shallow	Less LW	No	3717
PEPLIN	6	1	0	Low Severity	Shallow	Less LW	No	7097
HAG 1	6	9	0	Low Severity	Shallow	Less LW	No	2070
LAKESIDE	5	23	1	Low Severity	Shallow	Less LW	No	16165
LOCOMOTIVE	5	0	0	Low Severity	Shallow	Less LW	No	6124
DESERET	4	2	0	Low Severity	Shallow	Less LW	No	2239
CEDAR MOUNTAIN	4	24	4	Low Severity	Shallow	Less LW	No	21388
WEST MOUNTAIN	4	44	11	Low Severity	Shallow	Less LW	No	2504
DALLAS CANYON	4	14	5	Low Severity	Shallow	Less LW	No	43386
POLE CREEK	4	14	40	Low Severity	Shallow	Less LW	Yes	2137
HANSEL VALLEY	4	1	1	Low Severity	Shallow	Less LW	No	2967
LONG CANYON	3	3	4	Low Severity	Shallow	Less LW	No	4450
MAPLECANYON	3	42	20	Low Severity	Shallow	Less LW	No	5008
IRON HILL	3	44	2	Low Severity	Shallow	Less LW	No	1638
WRANGLER	2	2	1	Low Severity	Shallow	Less LW	No	8505
LONG RIDGE	2	50	13	Low Severity	Shallow	Less LW	No	6500
COTTONWOOD TRAIL	2	0	0	Low Severity	Shallow	Less LW	No	1279
BUTTE	1	13	0	Low Severity	Shallow	Less LW	No	2204

73	0	1	3	Low Severity	Shallow	Less LW	No	1549
CHAPARRAL	0	39	5	Low Severity	Shallow	Less LW	No	1745
WESTSAHARA	0	0	0	Low Severity	Shallow	Less LW	No	1127
WEST ANTELOPE	0	20	0	Low Severity	Shallow	Less LW	No	15483
CEDAR	0	0	0	Low Severity	Shallow	Less LW	No	1323
CARRINGTON ISLAND	0	2	0	Low Severity	Shallow	Less LW	No	1444
SKULL VALLEY	0	0	0	Low Severity	Shallow	Less LW	No	1365
LIGHT SAGE	0	0	0	Low Severity	Shallow	Less LW	No	11159
LINCOLN BEACH	0	41	4	Low Severity	Shallow	Less LW	No	2298
LITTLE VALLEY	0	11	25	Low Severity	Shallow	Less LW	No	2431
STREAM	0	0	0	Low Severity	Shallow	Less LW	No	8107
CEDAR HILLS	0	0	3	Low Severity	Shallow	Less LW	No	5159
SALLY	0	12	0	Low Severity	Shallow	Less LW	No	10840
WILDCAT	0	0	5	Low Severity	Shallow	Less LW	No	13100
KELTON	0	0	0	Low Severity	Shallow	Less LW	No	4226
SHAW SPRINGS	0	0	0	Low Severity	Shallow	Less LW	No	2455
LAKESIDE	0	35	3	Low Severity	Shallow	Less LW	No	10609
HORSE VALLEY	0	1	3	Low Severity	Shallow	Less LW	No	1190
GLENANNA	0	26	5	Low Severity	Shallow	Less LW	No	3418
GREASE	0	0	0	Low Severity	Shallow	Less LW	No	1531
WEST TWIN PEAK	0	6	0	Low Severity	Shallow	Less LW	No	16155
HURRICANE ASSIST 02	0	21	2	Low Severity	Shallow	Less LW	No	1971
QUAIL	0	8	1	Low Severity	Shallow	Less LW	No	1952
RESERVE	0	16	8	Low Severity	Shallow	Less LW	No	1809
OMG	0	42	6	Low Severity	Shallow	Less LW	No	3250
THIRTY TWO	0	0	0	Low Severity	Shallow	Less LW	No	2852
ANTELOPE	0	20	5	Low Severity	Shallow	Less LW	No	1114
COTTONWOOD	0	5	0	Low Severity	Shallow	Less LW	No	5515
GOOSENEST	0	15	7	Low Severity	Shallow	Less LW	No	1195
DOLLAR RIDGE	48	41	53	Low Severity	Shallow	LW	Yes	69817
BRIDGE	47	14	76	Low Severity	Shallow	LW	No	5067
RIGGS	44	31	88	Low Severity	Shallow	LW	No	2331
COVE CREEK	43	30	78	Low Severity	Shallow	LW	No	2438
WILLOW PATCH	39	14	74	Low Severity	Shallow	LW	No	4592
SOLITUDE	39	32	56	Low Severity	Shallow	LW	No	1899
BRIGGS	36	38	57	Low Severity	Shallow	LW	No	6805
MURDOCK	36	32	87	Low Severity	Shallow	LW	No	5169
TANK HOLLOW	36	44	59	Low Severity	Shallow	LW	Yes	11003
LAKE CREEK	33	3	79	Low Severity	Shallow	LW	No	1336
BLACK MOUNTAIN	13	17	67	Low Severity	Shallow	LW	No	5431
MILLVILLE	36	82	16	Low Severity	Steep	Less LW	No	2934
PATCH SPRINGS	36	55	18	Low Severity	Steep	Less LW	No	29562

CHOKER CHERRY	33	51	23	Low Severity	Steep	Less LW	No	1790
BLACK MOUNTAIN	11	61	5	Low Severity	Steep	Less LW	No	1381
SHANTY CANYON	0	50	0	Low Severity	Steep	Less LW	No	1306





Figure A. 1 Examples of identified sediment bottlenecks, including photos corresponding with aerial imagery of the sediment bottleneck (highlighted in yellow). From top to bottom: Twitchell Canyon, Seeley and Pole Creek Fires.

Table A. 2 Aerial Imagery Availability for study sites. Each year (1-5) denotes a different year with available high-resolution aerial imagery. Hexagon and Google refer to imagery provider. Partial refers to incomplete coverage of aerial imagery at a study site on a given year.

Fire	Fire Year	Year 1	Year 2	Year 3	Year 4	Year 5
Patch Springs	2013	Google 2015	Google 2017	Hexagon 2018	Hexagon 2021	
Goose Creek	2018	Hexagon 2018	Hexagon 2021			
Box Canyon	2016	Google 2017	Hexagon 2018	Hexagon 2021		
Pole Creek	2018	Google 2019 (partial)	Google 2020 (partial)	Hexagon 2021		
Clay Springs	2012	Google 2014	Hexagon 2018	Google 2019	Hexagon 2021	
Dollar Ridge	2018	Hexagon 2018	Google 2019	Hexagon 2021		
Tank Hollow	2017	Google 2019	Hexagon 2021			
Seeley	2012	Google 2013	Google 2015	Hexagon 2018	Hexagon 2021	
Bald Mountain	2018	Google 2019 (partial)	Google 2020 (partial)	Hexagon 2021		
Shingle	2012	Google 2013	Google 2015	Hexagon 2018	Google 2019	Hexagon 2021
Trail Mountain	2018	Hexagon 2018	Hexagon 2021			
Twitchell Canyon	2010	Google 2011	Google 2014	Hexagon 2018	Hexagon 2021	
Brianhead	2017	Hexagon 2018	Google 2019	Hexagon 2021		
Coal Hollow	2018	Google 2019	Hexagon 2021			
West Valley	2018	Hexagon 2018	Google 2019 (partial)	Hexagon 2021		

Appendix B. Depth Measurement Methods & Volume Calculation

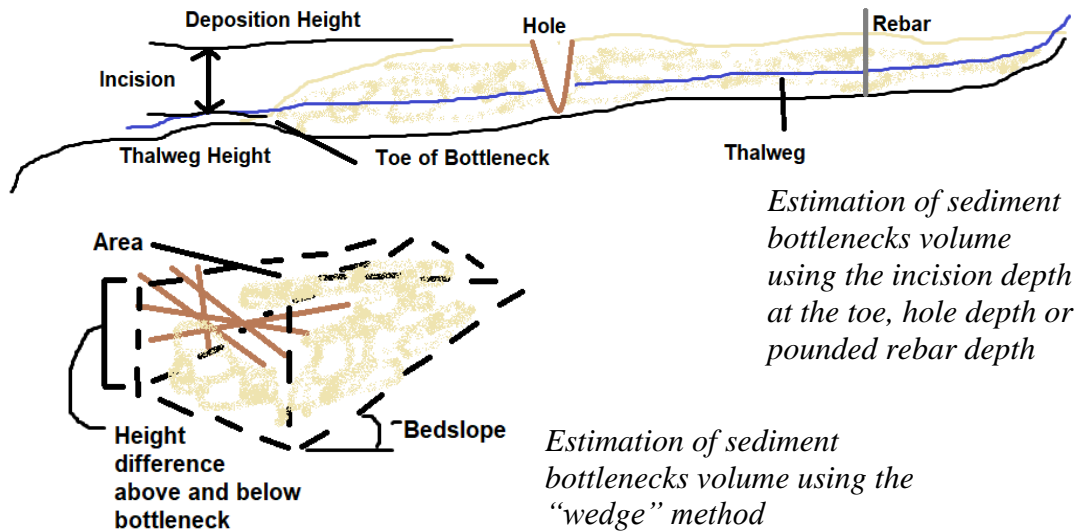


Figure B. 1 Diagrams demonstrating how depositional depths were measured

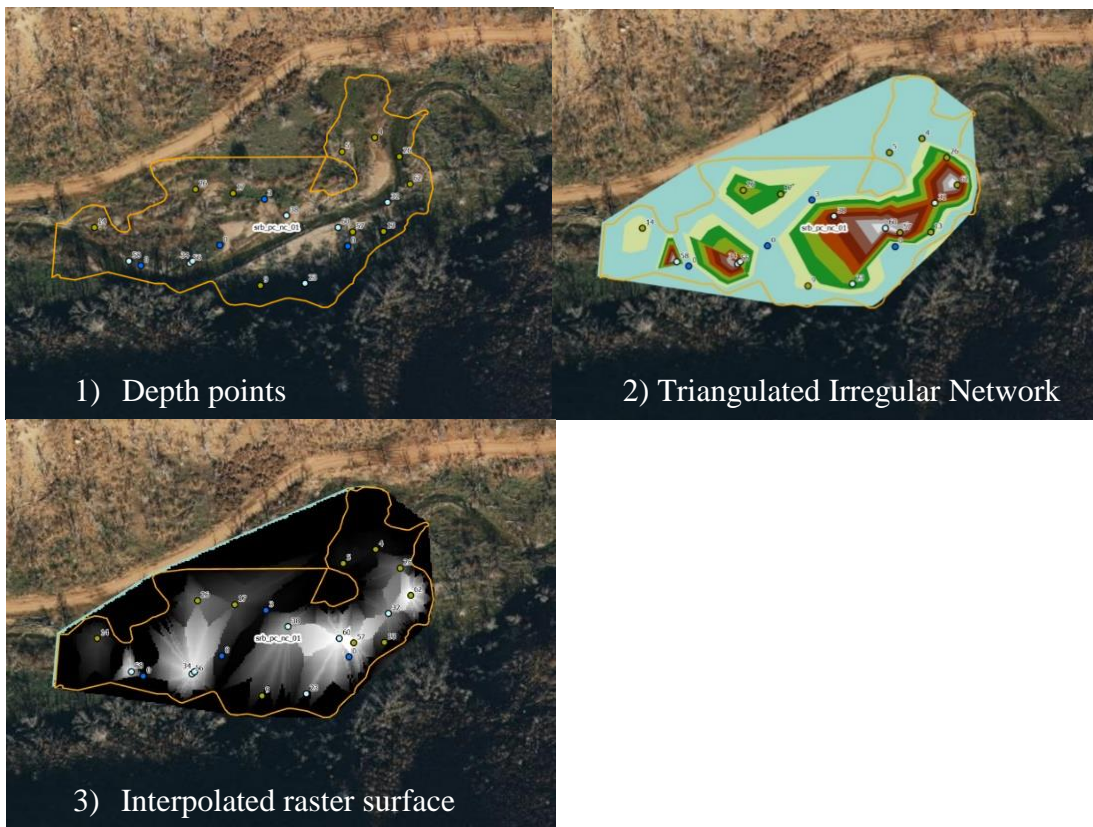


Figure B. 2 Progression of maps showing how sediment bottleneck volume was calculated

Appendix C. Development of Explanatory Variables

Table C. 1 Attributes of each reach calculated in ArcPy

Variable	GIS Alias	Calculation	Implications	Source
Predictor Variables				
Reach Slope	Slope	$\frac{Rise}{Run}$	Channel gradient is a key predictor of sediment transport	
Change in Slope	S-change	$\frac{Downstream\ Slope - Upstream\ Slope}{Downstream\ Slope}$	Changes to flatter slopes decrease stream power	
Normalized Steepness	NormSteep	Slope normalized by drainage area $k_{sn} = \frac{s}{A-\theta_{ref}}$	This will help pick out locally shallower slopes	(Kirby & Whipple, 2001)
Normalized Steepness Percentile		Ranked normalized steepness values for each watershed and calculated the percentile	This will help make normalized steepness more comparable across all watersheds	
Valley Bottom Width (m)	VB_width	Width of the floodplain	Greater width means there is more room for the channel has to move around and to store sediment	Valley bottom derived using the Fluvial Corridor Tool (Roux et al., 2015)
Change in Valley Bottom Width	VB_Change	$\frac{Downstream - Upstream\ Floodplain\ Width}{Downstream\ Floodplain\ Width}$	Changes to wider reaches means there may be more room to store sediment and there may be an increase in transport capacity	
Floodplain to Channel Ratio	fpchanrat	$\frac{Floodplain\ Width}{Channel\ Width}$	This variable was shown to be one of the greatest predictors of logjams resilience.	(Wohl & Scamardo, 2021)
Sinuosity	Sinuosity	$\frac{Euclidean\ Distance\ between\ Ends\ of\ Reach}{Length\ of\ Reach}$	If there are many bends in the channel, this decreases velocity. Also, wood and sediment may keep traveling straight.	
Confinement	Confine	% of the channel abutting the floodplain edge: one side is 100%, both sides is 200%	This is another measure of how much the floodplain edge restricts the channel. Greater confinement means the channel has less room to meander and transport capacity can be increased.	(O'Brien et al., 2019)
Topographic Position Index	TPI	Relative position of cell to moving window of adjacent cells	This metric is similar to confinement. The value represents how inset the stream network is compared to the nearby topography	(Weiss, 2001)
Stream Power	StreamPow	$Slope \times Upstream\ Drainage\ Area$ Density of water and gravity are assumed to be constants. We assume our discharge scales proportionally with drainage area.	Stream power directly represents the energy of the channel and the transport capacity of the reach to transport sediment. Unit stream power would be more accurate, but it was difficult to get accurate channel widths	
Local Cover	Cover	LANDFIRE vegetation type from remote sensing within the reach	This is the categorical cover type. The idea is forested areas may act differently than shrublands for example.	The EVT (existing vegetation type raster) from the 2008 LANDFIRE dataset was used (LANDFIRE, 2008)
Reach Averaged dNBR	Burn	Averaged burn severity in the reach	Areas that are more highly burned may move sediment through or may more effectively trap sediment	Classified dNBR from the MTBS (monitoring trends in burn severity) database (MTBS, 2020)
Reach Averaged Cover	Cover_Shld	Majority of upstream cover draining to a reach	This is the categorical cover type. The idea is forested areas may act differently than shrublands for example.	The EVT (existing vegetation type raster) from the 2008 LANDFIRE dataset was used (LANDFIRE, 2008)
Upstream Moderate High Severity %	Mod_High	% of upstream area that is moderately or highly burned	This helps predict likelihood of sediment generation and debris flows.	Classified dNBR from the MTBS (monitoring trends in burn severity) database (MTBS, 2020)
Upstream Moderate High km ²	mh_sqm	Volume of wood present within each reach	This helps predict volume of sediment generation as scaled by upstream area.	Classified dNBR from the MTBS (monitoring trends in burn severity) database (MTBS, 2020)

Upstream conifer %	Conifer	% of upstream area that has conifer cover	Conifer cover is more likely to contribute to high severity fire and greater large wood recruitment	The EVT (existing vegetation type raster) from the 2008 LANDFIRE dataset was used (LANDFIRE, 2008)
Average Topographic Position Index upstream	TPI_up	Relative position of cell to moving window of adjacent cells	The upstream topography relative to the stream network influences sediment delivery and storage	(Weiss, 2001)
Volume of debris flow sediment delivered upstream	df_vol_up	Volume of debris flows deposited into the stream channel in the upstream draining area	Debris flows can be the largest sources of sediment and wood into the stream network	
Channel Width	ChanWidth	Power function developed in Figure C.1.a	A wider channel means a greater transport capacity	
Response Variables				
Sediment Bottleneck Location	srb	Number of sediment bottlenecks in each reach. Presence or absence of a sediment bottleneck in a reach is then given by 0 or 1		A point bottleneck location representing each sediment bottleneck polygon
Sediment Bottleneck Volume (m ³)	srb_vol	The total volume of sediment in each reach		Field-measured sediment bottleneck volumes
Wood Volume (m ³)	lw_volume	Volume of wood present within each reach		Remote mapped wood dataset
Wood Density (m ³ /ha)	lw_density	Total volume of wood divided by the valley bottom area of each reach		Remote mapped wood dataset
Grain Size	D50	Modelled D50 grain size, calculated using 2 yr regression equations for Utah and the Snyder model		(Kenney et al., 2007; Snyder et al., 2013)
Sediment Transport	Sed_Trans	Debris flow volume of sediment minus the sediment bottleneck volume in the upstream draining area. A simplified sediment budget calculation for how much sediment is passing through a reach.		
Categorization Variables				
Type of Bottleneck	Cause	Sediment deposition classified cause: non-structural control, wood, debris flows, beaver dam, manmade structure		
Category of Bottleneck	srb_vbm_sf	Sediment deposition classified cause: non-structurally or structurally controlled		
Fire	Fire_name	Wildfire reach is in/downstream of		
Location in Watershed	Wtshd	Within the burned zone, within 50% of the drainage area burned, within less than 50% of the drainage area burned		
Visit	Visit	Reaches were classified as: Yes- visited in the field Site- not visited, but included in analysis No-not included in analysis		
Wood	Wood	Yes means wood was mapped in this reach and is included in wood analysis. No means wood was not		
Error	Error	Errors in metric calculation were manually fixed for this reach		

Available as a shapefile at <https://github.com/aarditti/USUALmetrics/blob/main/README.md>

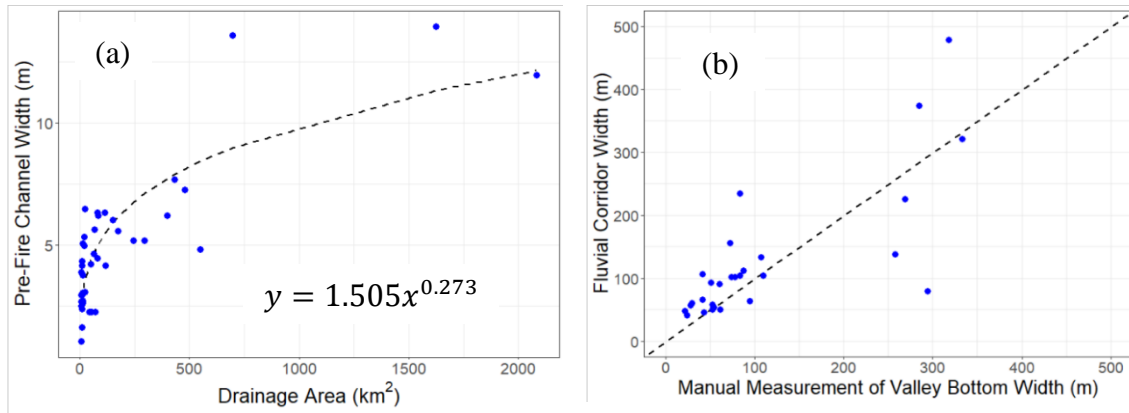


Figure C. 1 (a) The points show manually delineated channel widths from aerial imagery versus drainage area. The dashed line represents a power function we developed to interpolate channel width in other locations. (b) Width of a manually delineated reach of a valley bottom compared to the width of the valley bottom delineated by the Fluvial Corridor Tool. The perfect fit of the fluvial corridor delineation to the manual delineation is shown by the dashed 1:1 line.

Appendix D. Remote Wood Mapping

Table D. 1 Desktop measurements and attribution of large wood that will be reevaluated in the field

ID	Quantity	Location	Obscured	Setting	Burn Level	Volume
eg: LW- SEE- 004	# (estimated >10)	Channel Floodplain Channel and Floodplain Channel-spanning	None Some Many	Fluvial Bank Debris Flow	Unburned Partially Burned Burned	In cubic meters

For volume calculations, see

https://github.com/aarditti/USUALmetrics/blob/main/Wood_Volume_Calcs.py

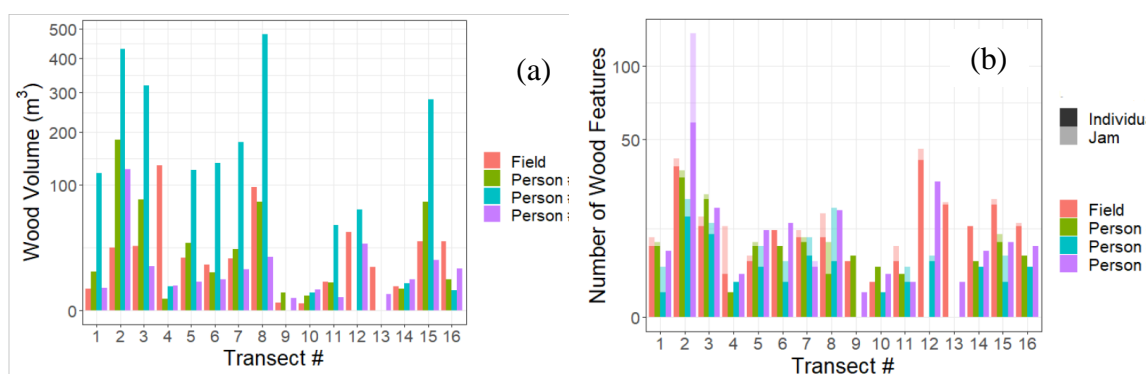


Figure D. 1 (a) Total volumes measured at each transect in the field and by each remote mapper. (b) Total individual pieces and wood jams measured at each transect in the field and by each remote mapper. Individuals are solid, while jams are transparent. Jams are stacked on top of individuals, i.e. the height of the column refers to the total number of features.

Appendix E. Sediment Bottlenecks Results

Table E. 1 *Sediment Bottleneck Attributes*

ID	Fire	Cause	Area (m ²)	Volume (m ³)	Latitude	Longitude
srb_tc_rc_02	Twitchell Canyon	Non-structural Control	2091	339.121075	38.53326622	-112.3988357
srb_tc_rc_01	Twitchell Canyon	Non-structural Control	585	87.6980929	38.53022882	-112.4054159
srb_tc_fc_03	Twitchell Canyon	Non-structural Control	25339	3651.667507	38.55049483	-112.4450921
srb_tc_sc_01	Twitchell Canyon	Non-structural Control	1373	101.341577	38.56770436	-112.4671654
srb_wv_mc_04	West Valley	Wood	69	12.74424719	37.44776264	-113.4058693
srb_wv_mc_06	West Valley	Wood	392	72.68402081	37.44862456	-113.408601
srb_tc_fc_01	Twitchell Canyon	Manmade Structure	2257	359.4300482	38.56269117	-112.4316967
srb_tc_fc_02	Twitchell Canyon	Debris Flow Deposit	10297	2047.26276	38.53884176	-112.449383
srb_tc_sc_02	Twitchell Canyon	Non-structural Control	2573	147.8728998	38.56920147	-112.4651783
srb_tc_sc_03	Twitchell Canyon	Wood	84	12.01336537	38.4987581	-112.4942861
srb_tc_sc_05	Twitchell Canyon	Wood	1305	87.67798158	38.55045129	-112.4797817
srb_tc_sc_08	Twitchell Canyon	Wood	5635	1446.341417	38.55938538	-112.4760428
srb_wv_mc_05	West Valley	Wood	426	30.25833326	37.44831195	-113.4079522
srb_wv_mc_01	West Valley	Wood	76	491.1470437	37.43963123	-113.4005783
srb_wv_mc_02	West Valley	Wood	326	27.98778655	37.44060787	-113.4008846
srb_wv_mc_03	West Valley	Wood	642	106.43985	37.44592397	-113.4032049
srb_wv_mc_09	West Valley	Wood	354	58.25158701	37.45112157	-113.4281401
srb_wv_mc_10	West Valley	Wood	1753	33.4228117	37.45111844	-113.4295571
srb_wv_rc_02	West Valley	Wood	3617	253.567073	37.43721451	-113.4405045
srb_wv_rc_03	West Valley	Wood	232	848.8697821	37.43872949	-113.4406951
srb_tc_sc_07	Twitchell Canyon	Wood	3753	144.3109068	38.55222169	-112.4785816
srb_wv_mc_07	West Valley	Manmade Structure	194	532.8054905	37.45101142	-113.4364051
srb_cs_oc_03	Clay Springs	Wood	1046	11.33309526	39.35468064	-112.2151841
srb_cs_oc_02	Clay Springs	Non-structural Control	218	34.14203942	39.35669142	-112.2331978
srb_cs_oc_01	Clay Springs	Non-structural Control	3677	13.27137727	39.35691436	-112.2441926
srb_cs_cs_02	Clay Springs	Non-structural Control	956	279.3279176	39.30214042	-112.346187
srb_cs_cs_01	Clay Springs	Non-structural Control	95	29.5803081	39.30103758	-112.3509182
srb_cs_dc_02	Clay Springs	Wood	101	8.919167853	39.31538455	-112.2469259
srb_cs_dc_01	Clay Springs	Wood	351	15.38959237	39.31681455	-112.2403384
srb_cs_wcr_01	Clay Springs	Non-structural Control	1067	20.20531493	39.29499181	-112.2809949
srb_cs_wc_01	Clay Springs	Non-structural Control	993	35.21350549	39.43254784	-112.1273282
srb_se_lf_06	Seeley	Wood	1567	279.5478605	39.50656903	-111.1765176
srb_tm_mc_01	Trail Mountain	Wood	1478	638.2274843	39.42318187	-111.1280485
srb_se_lf_05	Seeley	Wood	1780	132.8029527	39.50480076	-111.1723644

srb_se_lf_04	Seeley	Wood	1014	457.5323231	39.51180223	-111.1876944
srb_se_lf_03	Seeley	Wood	1793	150.0569084	39.52119827	-111.2012276
srb_se_lf_02	Seeley	Wood	1075	222.224362	39.52344445	-111.2048401
srb_se_lf_01	Seeley	Wood	1040	212.0120931	39.52685031	-111.209788
srb_ch_cc_05	Coal Hollow	Wood	6715	71.55628512	39.93519464	-111.2040548
srb_pc_nc_01	Pole Creek	Non-structural Control	59	862.2664999	39.8577684	-111.6107296
srb_pc_bc_01	Pole Creek	Wood	333	3.263196516	39.94246252	-111.5325693
srb_ch_cc_04	Coal Hollow	Non-structural Control	294	39.55593288	39.89487681	-111.2720579
srb_ch_cc_02	Coal Hollow	Wood	302	18.8468779	39.92101524	-111.2460196
srb_ch_cc_01	Coal Hollow	Non-structural Control	471	19.48802444	39.91957022	-111.2477116
srb_ch_df_01	Coal Hollow	Non-structural Control	561	7.934759113	39.94377437	-111.3574981
srb_ch_cc_03	Coal Hollow	Wood	2086	75.39359457	39.89118927	-111.2772096
srb_wv_rc_01	West Valley	Debris Flow Deposit	185	503.7605749	37.4288467	-113.4370842
srb_dr_bc_01	Dollar Ridge	Debris Flow Deposit	22527	1209.830764	40.11629045	-110.9375537
srb_dr_sr_05	Dollar Ridge	Debris Flow Deposit	1987	8920.701558	40.12692747	-110.8647959
srb_dr_tc_01	Dollar Ridge	Wood	132170	207.401616	40.07939113	-110.8457515
srb_dr_bc_02	Dollar Ridge	Wood	653	14.32510162	40.12258318	-110.9299913
srb_dr_sr_01	Dollar Ridge	Debris Flow Deposit	11085	39597.96512	40.12972638	-110.8890707
srb_tc_fc_09	Twitchell Canyon	Beaver Dam	1246	105.3019865	38.5714649	-112.4253118
srb_tc_fc_08	Twitchell Canyon	Non-structural Control	730	701.7377552	38.55634866	-112.4389696
srb_bh_tm_03	Brianhead	Non-structural Control	4806	240.3406794	37.86619499	-112.5407945
srb_bh_tm_02	Brianhead	Wood	1138	89.05557813	37.86373852	-112.5497501
srb_bh_lc_01	Brianhead	Non-structural Control	839	194.2976348	37.8802536	-112.6594785
srb_bh_cc_01	Brianhead	Debris Flow Deposit	1901	63.55229533	37.76136087	-112.7972402
srb_sh_sc_04	Shingle	Manmade Structure	2732	137.2792915	37.44147126	-112.5717655
srb_sh_sc_03	Shingle	Manmade Structure	9809	256.5276313	37.43273906	-112.5755178
srb_sh_sc_02	Shingle	Manmade Structure	1095	618.0671418	37.42647531	-112.5802617
srb_sh_sc_01	Shingle	Non-structural Control	462	1897.934148	37.42426566	-112.5819878
srb_bh_dc_01	Brianhead	Non-structural Control	1705	112.8485231	37.68619424	-112.7017155
srb_bh_hc_01	Brianhead	Wood	5530	60.66748952	37.73831073	-112.6308539
srb_tc_fc_07	Twitchell Canyon	Beaver Dam	255	293.0786441	38.48809565	-112.4469958
srb_tc_fc_06	Twitchell Canyon	Debris Flow Deposit	17892	807.8659656	38.52845588	-112.4532764
srb_tc_fc_05	Twitchell Canyon	Wood	444	76.71504969	38.52501741	-112.4550127
srb_tc_fc_04	Twitchell Canyon	Debris Flow Deposit	278	4102.67907	38.5172123	-112.4577786
srb_se_nw_01	Seeley	Wood	6588	50.89728889	39.53123186	-111.1499204
srb_se_hc_03	Seeley	Beaver Dam	402	28.80636556	39.55061434	-111.1693771
srb_se_hc_02	Seeley	Beaver Dam	2932	2911.525495	39.53138078	-111.1554893
srb_se_lf_07	Seeley	Wood	2615	46.7952856	39.50318012	-111.168146
srb_se_hc_01	Seeley	Non-structural Control	733	387.8427509	39.46480247	-111.1478045
srb_bh_tm_01	Brianhead	Beaver Dam	43182	453.5903064	37.86815059	-112.5151926
srb_pc_lf_01	Pole Creek	Wood	3066	289.404393	39.94694689	-111.4303904
srb_pc_sf_01	Pole Creek	Debris Flow Deposit	5382	11891.71129	39.99567648	-111.4990768
srb_ch_sc_03	Coal Hollow	Non-structural Control	589	541.1610698	39.97372261	-111.3399947

srb_pc_tc_01	Pole Creek	Beaver Dam	593	552.3035558	39.93487232	-111.5453068
srb_ch_mc_03	Coal Hollow	Wood	324	31.5060542	39.95938681	-111.3090255
srb_ch_mc_02	Coal Hollow	Wood	15364	93.79186172	39.95140229	-111.3100399
srb_ch_mc_01	Coal Hollow	Wood	26272	64.25700414	39.91963292	-111.3115378
srb_ch_sc_02	Coal Hollow	Beaver Dam	1375	7884.060702	39.9576345	-111.3032149
srb_ch_sc_01	Coal Hollow	Beaver Dam	2468	5485.078149	39.97531975	-111.3457809
srb_ch_cl_06	Coal Hollow	Wood	4797	77.75109248	39.93494207	-111.2076857
srb_dr_tc_04	Dollar Ridge	Debris Flow Deposit	40004	425.7910885	40.07100544	-110.8588212
srb_dr_tc_03	Dollar Ridge	Debris Flow Deposit	10858	749.5659722	40.09073474	-110.8293081
srb_dr_sr_04	Dollar Ridge	Debris Flow Deposit		1143.711634	40.12266358	-110.7753518

Table E. 2 *Sediment Bottleneck misidentification in aerial imagery at each site sorted by date of visit*

Fire	Date First Visited	# of Sediment Bottlenecks only Identified in the Field
West Valley	6/16/21	8
Twitchell Canyon	6/29/21	6
Coal Hollow	7/6/21	5
Clay Springs	7/20/21	1
Seeley	7/26/21	4
Trail Mountain	7/27/21	0
Pole Creek	8/9/21	1
Dollar Ridge	9/11/21	4
Bald Mountain	5/26/2022	0
Shingle	6/17/22	1
Brianhead	6/18/22	1

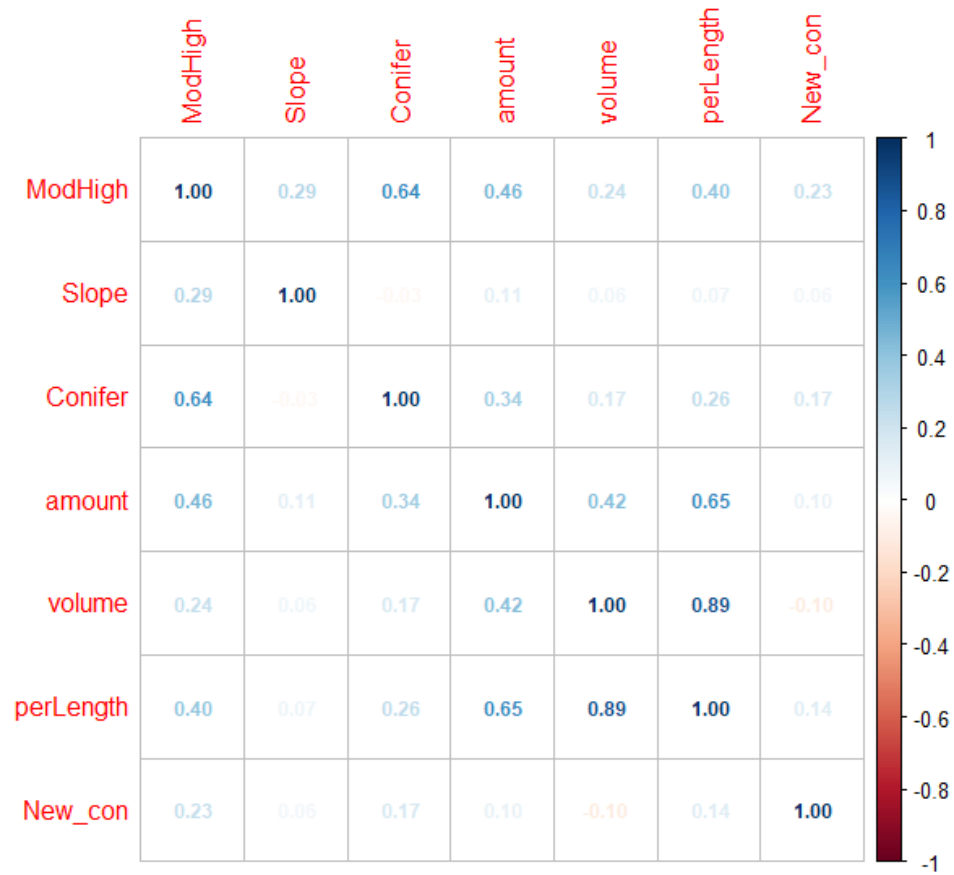


Figure E. 1 *Pearson correlation coefficients for sediment bottleneck prevalence*

Appendix F. Random Forest Model Development

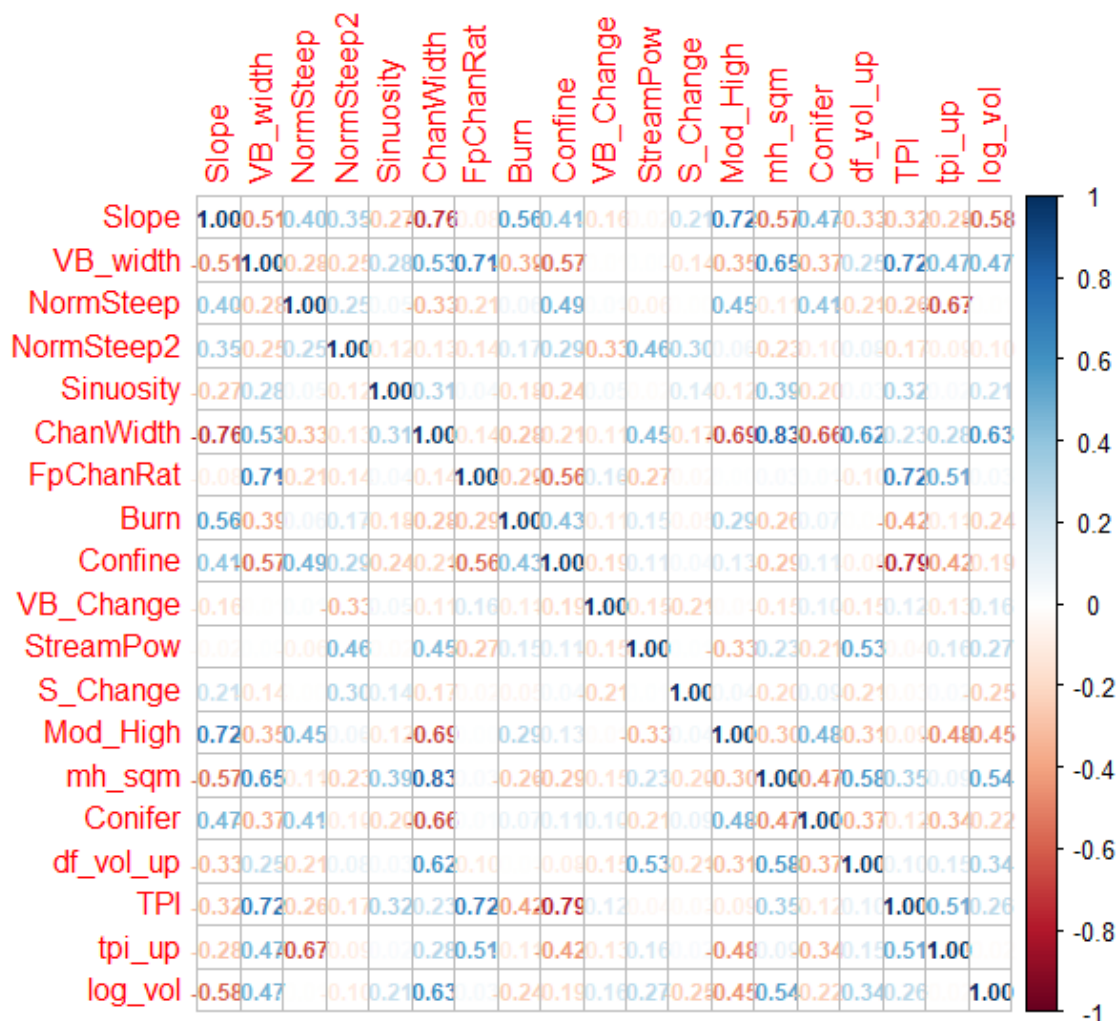


Figure F. 1 Pearson correlation coefficients for variables used in random forest analysis

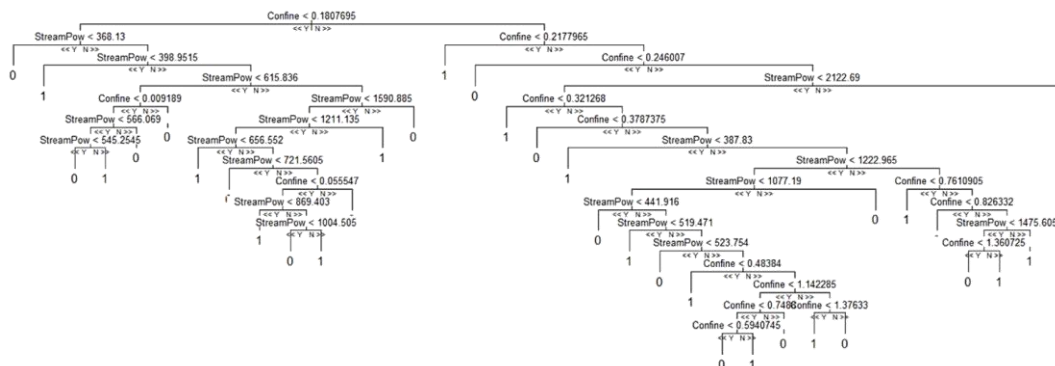
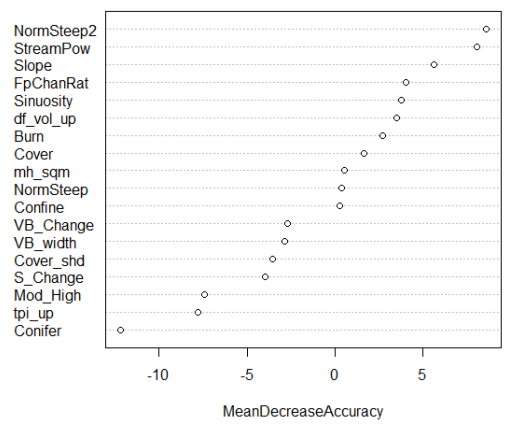
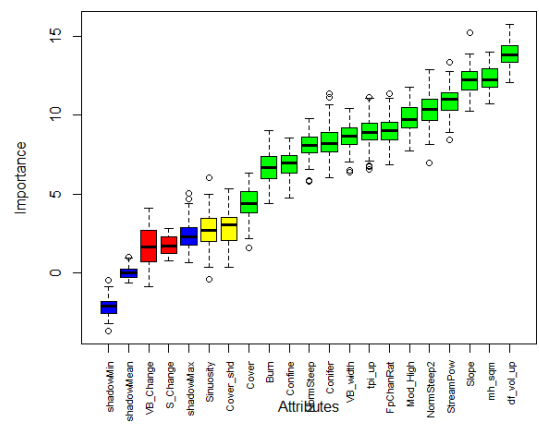


Figure F. 2 Example of decision tree created in random forest analysis of sediment bottleneck presence

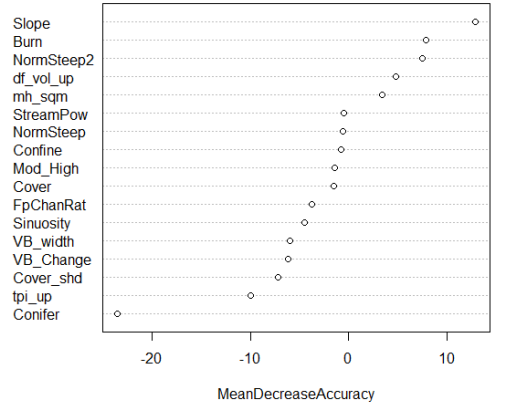
(a) rf.srb_presence



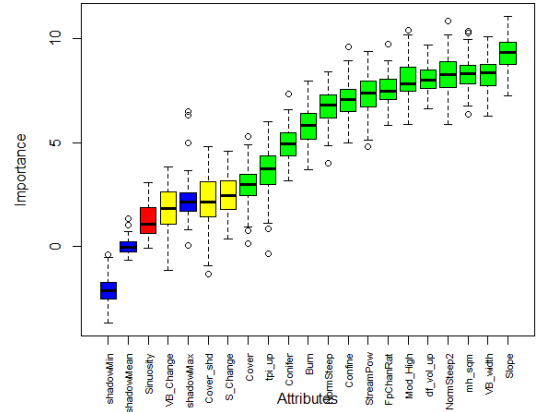
(b)



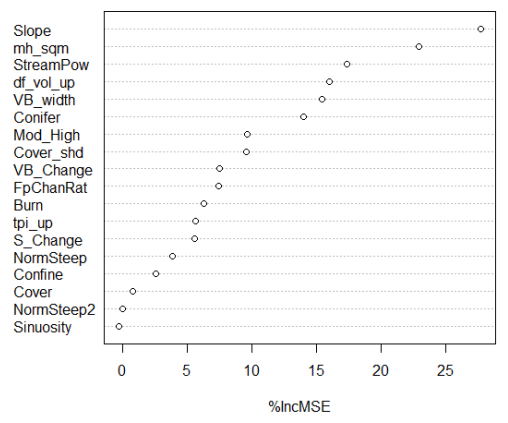
(c) rf.srb_wood_presence



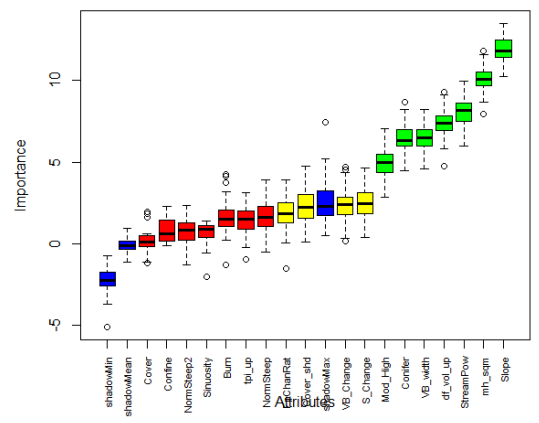
(d)



(e) rf.srb_volume



(f)



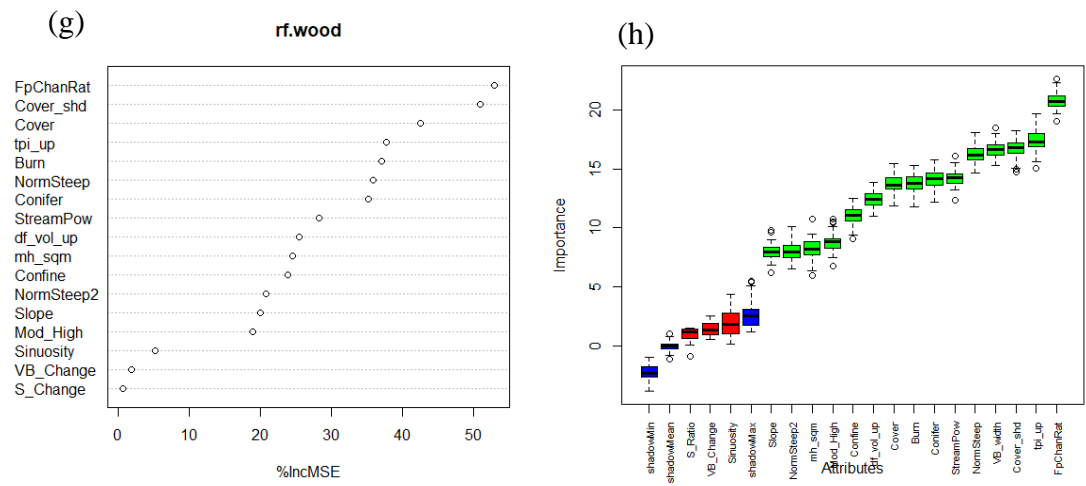


Figure F. 3 Original random forest variable importance plot and Boruta selections for (a/b) sediment bottleneck presence (c/d) wood-forced sediment bottleneck presence (e/f) sediment bottleneck volume (g/h) wood density

Appendix G. Wood Results

Table G. 1 *Volumes and Densities of Large Wood at each Study Site*

Fire	Stream Network Length (km)	% Conifer	Large Wood Volume (m³)	Large Wood Density (m³/ha)	% of wood stored in jams	Wood Volume per length (m³/km)	Wood-Forced Sediment Bottleneck volume (m³)	Sediment volume per length (m³/km)	% of Sediment Volume Captured by Large Wood
Bald Mountain	33	45	NA	NA	NA	NA	0	0	NA
Box Canyon	8	48	NA	NA	NA	NA	0	0	NA
Brian Head	70	80	5705	41	85%	81	150	2	12.36%
Clay Springs	40	15	535	2	88%	13	36	1	8.05%
Coal Hollow	62	68	NA	NA	NA	NA	433	7	3.00%
Dollar Ridge	107	53	8472	16	73%	79	222	2	0.42%
Goose Creek	90	34	NA	NA	NA	NA	0	0	NA
Patch Springs	34	18	NA	NA	NA	NA	0	0	NA
Pole Creek	121	68	NA	NA	NA	NA	293	2	2.15%
Seeley	33	35	13585	80	93%	412	1552	47	31.80%
Shingle	14	40	121	7	0%	9	0	0	0.00%
Tank Hollow	21	59	NA	NA	NA	NA	0	0	NA
Trail Mountain	36	64	NA	NA	NA	NA	638	18	100.00%
Twitchell Canyon	56	67	17787	94	76%	318	1767	32	12.18%
West Valley	15	88	2820	93	84%	188	1444	96	58.20%
<i>Total/Average</i>	741	52	49024	48	71%	157	6535	14	22.82%

Table G. 2 *Properties of measured Wood-Forced Sediment Bottlenecks*

ID	Quantity	Fine		Length (m)	Diameter (cm)	DS Height (cm)	US Height (cm)	Wood Volume (m ³)	Sediment Volume (m ³)	LWPSI
		Material	Porosity							
srb_bh_hc_01	0	100	20	5	100	60	0	2	61	25.3
srb_bh_tm_02	12	60	70	16	510	160	120	39	89	2.3
srb_ch_cc_02	9	12	60	5.7	310	190	140	13	19	1.4
srb_ch_cc_03	8	152	70	5.8	160	130	0	4	75	20.8
srb_ch_cc_05	20	18	30	10.7	270	110	65	22	72	3.2
srb_ch_cl_06	11	60	40	13	100	90	10	7*	78	11.1
srb_ch_mc_01	17	50	30	7	200	300	130	29	64	2.2
srb_ch_mc_02	30	30	30	11	200	300	2	46*	94	2.0
srb_ch_mc_03	40	50	50	21	1000	400	3	420	32	0.1
srb_cs_dc_01	1	0	1	5	20	100	0	1	15	15.4
srb_cs_dc_02	1	0	1	5	35	90	0	2*	9	5.7
srb_cs_oc_03	5	10	70	5	200	90		3	11	4.2
srb_dr_bc_02	28	5	45	14	500	220	1	85	14	0.2
srb_dr_tc_01	55	20	40	26	1000	110	1	172*	207	1.2
srb_pc_bc_01	3	14	40	6.8	135	90	0	5	3	0.7
srb_pc_lf_01	30	30	60	17	630	150	1	64	289	4.5
srb_se_lf_01	200	5	50	15	1500	100	0	113	212	1.9
srb_se_lf_02	150	3	70	12	2000	120	10	86	222	2.6
srb_se_lf_03	200	3	80	20	2000	100	0	80	150	1.9
srb_se_lf_04	100	3	70	12	1500	190	10	103	458	4.5
srb_se_lf_05	500	3	50	15	3000	150	0	338	133	0.4
srb_se_lf_06	300	10	40	17.2	3200	210	60	694	280	0.4
srb_se_lf_07	45	10	20	17.2	780	210	150	225	47	0.2
srb_se_nw_01	1	0	1	9	70	40	0	3	51	20.2
srb_tc_sc_03	7	3	50	5	800	140	0	28	12	0.4
srb_tc_sc_05	50	3	30	6	1000	140	0	59	88	1.5
srb_tc_sc_07	40	2	50	15	1000	155	0	116	144	1.2
srb_tc_sc_08	150	3	60	25	3500	550	0	1925*	1446	0.8

* indicates that subsequent smaller wood jams or individual pieces were found upstream and potentially contributed to the volume of sediment captured. All wood measurements are of the primary controlling downstream wood jam/piece.